Université catholique de Louvain
Louvain Drug Research Institute

Targeted nanomedicines to stimulate the differentiation of oligodendrocyte progenitor cells in the scope of multiple sclerosis

Yasmine Labrak

Thèse présentée en vue de l'obtention du grade de docteur en Sciences biomédicales et pharmaceutiques

Director: Professor Anne des Rieux
Co-Director : Professor Giulio Muccioli

2022

REMERCIEMENTS

J'aimerais commencer par remercier mes deux promoteurs de thèse les Professeurs Anne des Rieux et Giulio Muccioli.

Anne, travailler à tes côtés fut un réel plaisir. Ton exubérance, ton énergie et ta passion pour la recherche ont été pour moi une source d'inspiration et de motivation. Merci d'avoir cru en moi et de m'avoir laissé une certaine liberté scientifique qui m'a permis de voler de mes propres ailes et de m'épanouir en tant que jeune chercheuse.

Giulio, où Monsieur, comme je vous ai toujours appelé, en plus de vous avoir comme promoteur de thèse, j'ai également eu la grande chance d'avoir bénéficié de votre encadrement lors de mon mémoire de fin d'études de pharmacie. Je vous remercie de m'avoir guidée ces six dernières années, que cela soit d'un point vu scientifique ou professionnel. Merci pour votre ferveur, disponibilité, humour et gentillesse.

J'aimerais également remercier les membres de mon jury d'accompagnement, les professeurs **Van Bambeke, Van Pesch** et **Saulnier**. Grâce à votre expertise, conseils et suggestions j'ai pu améliorer mon travail de recherches tout le long de ces années de thèse.

Je tiens également à remercier les Professeurs **Sarmento** et **Baron** d'avoir accepté de faire partie de mon jury de défense de thèse mais également pour la belle discussion scientifique que nous avions eue.

Outre d'avoir eu la chance d'être guidée par un panel d'experts dans leur domaine, j'ai aussi eu l'incroyable chance d'être membre non pas d'un mais deux laboratoires de recherches d'exception : **ADDB et BPBL.** Mon aventure de thèse n'aurait pas été la même sans les membres qui les composent.

C'est pour cela que je tiens à remercier mes très chers collègues d'ADDB : Mes premiers remerciements vont à mes coéquipières de la team Anne : **Viridiane, Ariane, Marie et Floriane.** Merci pour les rires, les bons moments mais également pour votre fiabilité. J'ai été ravie de partager le même espace de recherche que vous.

Outre la team Anne, je tiens chaleureusement à remercier mes collègues de bureau, **Alessio, Mingchao, Elia, Xiao et Mathilde**. Merci pour les belles discussions scientifiques et tous les bons moments passés ensemble. Cela sera dur de retrouver des voisins de bureau aussi stellaires que vous. Je n'oublie pas non plus les anciens qui m'ont guidée dans mes premiers pas de chercheurs.

De ce fait, je tiens aussi à remercier **Nikos et Thibaut**, alias Tic et Tac pour leur nombreux conseils.

J'aimerais aussi également exprimer ma gratitude envers **Bernard, Kevin et Murielle** sans qui ce laboratoire ne pourrait pas fonctionner.

La suite de ces remerciements seront dédiés à mes confrères du BPBL. Mes premiers remerciements vont au Professeur **Mireille Al Houayek.** Pendant ces années de thèse, tu as été d'un soutien indéfectible que cela soit sur le plan professionnel ou personnel. Merci pour tes encouragements, tes conseils et de m'avoir écoutée maintes et maintes fois. Mes deuxièmes remerciements vont au pôle analyse du BPBL composé de **Martin, Adrien et Romano.** Merci pour votre bonne humeur et surtout pour votre humour et taquineries qui ont toujours égayé mes passages au laboratoire. Merci aux collègues du pôle pharmaco : **Owein, Pauline et Hafsa**. Owein, merci pour tous les conseils scientifiques que tu as pu me prodiguer, Pauline merci pour tous tes petits encouragement et Hafsa pour ton sourire.

Enfin durant cette thèse j'ai eu la chance de me lier d'amitié avec d'autre membres de notre institut de recherches, notamment les membres du CMFA : **Marine, Chiara, Arina, Léopold, Romain et Alice.** Merci pour votre amitié, les soirées jeux de sociétés, vos encouragements et les quelques collaborations scientifiques que nous avions pu avoir.

La suite de mes remerciements est dédiée à ma famille et à mes amis sans qui cette thèse n'aurait pas été possible. **Clémence, Louise**, **Mary, Pauline, Laura et Azurre** merci d'avoir été toujours là pour moi que ça soit dans les bons ou mauvais moments. Votre amitié est une source de lumière dans ma vie. Je tiens également à remercier mes amis à l'international, **Yasmine, Caroline et Buthayna**, qui m'ont toujours encouragée malgré la distance.

Last but not least, je remercie du fond du cœur **mes parents** d'avoir été là pour moi, de m'avoir encouragée, aimée et choyée depuis la nuit des temps. Je n'aurais rien pu accomplir sans vous et votre soutien intarissable. Je tiens aussi à remercier mon **oncle Omar**, pour ses nombreux appels et messages bienveillants. Enfin celle que j'aimerais remercier plus que tout, c'est ma très chère tante, **Tati Noufissa**. Merci d'avoir toujours cru en moi et de m'avoir aimée comme ta propre fille. J'espère que tu es fière de moi aujourd'hui.

FOREWORD

Multiple sclerosis (MS) is a neuro-degenerative disease known for being the most common cause of non-traumatic neurological disabilities in young adults. These disabilities, among other symptoms, are caused by a pathological auto-immune response towards the myelin sheath in the central nervous system (CNS). As a result, the myelin sheath is severally damaged, and demyelination of axons occurs. Although myelin regeneration is enabled after demyelination, the efficacy of the process is progressively impaired throughout the disease. Oligodendrocyte progenitor cells (OPC) differentiation into myelinating oligodendrocytes is the heart of the myelin regeneration process, named remyelination. Nowadays, 85% of MS patients have a phase of relapse with neurological symptoms and a remission phase when those symptoms disappear. Even if these patients are stabilized under immunomodulatory therapies, the relapsing-remitting MS (RRMS) ultimately switches to the progressive form secondary progressive MS (SPMS) with a deterioration of the patient's condition over the years. It is thus crucial to develop medications that stimulate remyelination to slow down disease progression in addition to the disease-modifying treatments currently prescribed to MS patients.

Over sixteen compounds are currently in clinical trials as remyelinating therapies. Four of these compounds have been terminated after the second phase because they failed to show a significant efficiency. These compounds have previously been studied in preclinical animal models *in vivo* and *in vitro,* and in both cases, they stimulated OPC differentiation into oligodendrocytes. The question that arises from this observation is: **Why do the preclinical models results not mirror the results collected from clinical trials?**

Several hypotheses can answer this question. However, we will focus on one of them in our work: What if the issue was an inefficient biodistribution to OPC?

Lipid nanomedicines have been recently revealed to the public attention since they have been used in the composition of mRNA vaccines against the SARS-CoV2 virus. Lipid nanocarriers enabled the delivery of the mRNA inside cells by protecting them from degradation.

Hence, an exciting possibility for remyelinating therapies is implementing a similar technology to protect compounds from degradation. In the past, nanocarriers'surface have been tuned to target specific cells to maximize drug delivery. In the same scope, developing a nanocarrier that can target OPC to maximize active molecule's concentration in OPC could be a promising strategy to favor remyelination. Additionally, lipidic nanocarriers are designed to enhance lipophilic molecule solubility. Hence, they can open the door to the clinical use of lipophilic compounds that have been overlooked because of low solubility in physiological solutions. In the light of the above, **our**

work aims to use lipid nanocapsules (LNC), a lipid nanocarrier, to develop an OPC-targeted nanocarrier. This type of formulation can be loaded with potential lipophilic drug candidates and putatively enhance the therapeutic effect of the drug of interest.

The blood-brain barrier (BBB) is a formidable obstacle to drug delivery in the CNS. However, intranasal delivery has the advantage of bypassing the BBB and with this kind of administration, drugs can penetrate the CNS via the olfactory bulb. For this matter, our work will also explore the intranasal delivery of drug-loaded LNC on remyelination

This thesis manuscript will be divided into four chapters:

- **Chapter 1: Introduction.**

This chapter lays the foundation for the following chapters. We discuss concepts regarding MS physiopathology, from its inflammatory hallmarks to the role of OPC in remyelination and the available current treatments. Secondly, it will introduce lipid nanocarriers and how they can be engineered to be used in MS therapies.

- **Chapter 2: Impact of anti-PDGFRα antibody surface functionalization on LNC uptake by oligodendrocyte progenitor cells.**

This chapter reports the results we obtained regarding the development and characterization of an OPC-targeted LNC. LNC surface has been tailored with an antibody against the platelet-derived growth factor receptor α (PDGFRα), a receptor mostly expressed at the surface of OPC. We used several techniques to graft this antibody at LNC surface and assessed the uptake of this targeted formulation by primary OPC *in vitro*.

- **Chapter 3: Impact of Retinoic acid and Calcitriol loaded LNC on remyelination after intranasal delivery on a cuprizone model.**

This chapter contains our results regarding the development and characterization of retinoic acid-loaded LNC and calcitriol-loaded LNC. It also demonstrates the impact of these formulations on the differentiation of CG4-cells (an OPC cell line) and their impact on the secretion of pro-inflammatory cytokines by BV-2 cells, a microglial cell line. Finally, the formulations were administered intranasally to C57/BL6 mice to evaluate whether they could enhance myelin repair in a cuprizone model.

- **Chapter 4: Discussion and conclusion.**

This chapter highlights the results of our research and discuss their meaning and relevance, in the light of what has been reported in the literature. This chapter also explores the future perspectives that can stem from our work.

Ab	anti-Platelet-Derived Growth Factor Receptor alpha antibody
ARR	annualized relapse rate
BBB	Blood-Brain-Barrier
Cal	Calcitriol
CDP	confirmed disability progression
CIS	Clinically Isolated Syndrome
CNS	Central Nervous System
CSF	CerebroSpinal Fluid
CPPs	Cell-Penetrating Peptides
DiD	DiIC18(5) solid (1,1'-Dioctadecyl-3,3,3',3'-Tetramethylindodicarbocyanine, 4-Chlorobenzenesulfonate Salt)
DMT	Disease modifying treatment
EAE	Experimental Autoimmune Encephalomyelitis
EDSS	Extended Disability Status Score
EMA	European Medicines Agency
FA	Fatty acids
FDA	Food and Drug Administration
FGF	Fibroblast Growth Factor
GM-CSF	granulocyte-macrophage colony-stimulating factor
ICAM-1	Inter Cellular Adhesion Molecule
IGF-1	Insulin Growth factor-1
IgG	Immunoglobulin G
IFN	Interferon
IL	Interleukin
LNC	Lipid NanoCapsules
LNC-Ab	Lipid NanoCapsules with grafted Ab
MBP	Myelin Basic Protein
MOG	Myelin Oligodendrocyte Glycoprotein
MRI	Magnetic Resonance Imagery
MS	Multiple Sclerosis
NLC	Nanostructured Lipid Carriers
OPC	Oligodendrocytes Progenitor Cells
PDI	Polydispersity Index
PDGFA	Platelet-Derived Growth Factor A
PDGFRα	Platelet-Derived Growth Factor Receptor alpha
PIT	Phase Inversion Temperature

PPMS	Primary Progressive Multiple Sclerosis
RA	Retinoic Acid
RNS	Reactive Nitrogen Species
ROS	Reactive Oxygen Species
RRMS	Relapasing-Remetting Multiple Sclerosis
RXR	Retinoid X Receptor
SLN	Solid Lipid Nanoparticles
SOX	SRY-Box Transcription Factor
SPMS	Secondary Progressive Multiple Sclerosis
TCF	Transcription Factor
Th	T helper-cells
TNFα	Tumor necrosis factor alpha
Treg	Regulatory T-cells
VCAM	Vascular Cell Adhesion Molecule

TABLE OF CONTENTS

CHAPTER I	INTRODUCTION	1
CHAPTER II	IMPACT OF ANTI-PDGFRα ANTIBODY SURFACE FUNCTIONALIZATION ON LNC UPTAKE BY OLIGODENDROCYTE PROGENITOR CELLS	69
CHAPTER III	IMPACT OF RETINOIC ACID AND CALCITRIOL LOADED LNC ON REMYELINATION AFTER INTRANASAL DELIVERY IN A CUPRIZONE MODEL	97
CHAPTER IV	DISCUSSION AND CONCLUSION	123

CHAPTER I

INTRODUCTION

TABLE OF CONTENTS

I. EPIDEMIOLOGY AND ETIOLOGY 5

I.1. EPIDEMIOLOGY 5

I.2. ETIOLOGY 6

II. PHYSIOPATHOLOGY OF MS 10

II.1. T-CELLS IN MS 12

II.2. CELLS IN MS 12

II.3. MICROGLIA ROLE IN MS 13

II.4. ASTROCYTE ROLE IN MS 14

II.5. REMYELINATION 16

III. MS CLINICAL SYMPTOMS AND TREATMENTS 23

III.1. DIAGNOSTIC 24

III.2. SYMPTOMS 26

III.3. POPULAR MS MODELS IN VIVO FOR DRUG DISCOVERY 27

III.4. TREATMENTS 29

III.5. PROMOTING REMYELINATION: THE FUTURE OF MS THERAPIES? 38

IV. LIPID NANOMEDICINES 44

IV.1. OVERVIEW OF LIPID NANOMEDICINES 44

IV.2. CELL TARGETED NANOMEDICINE 49

IV.3. LIPID NANOMEDICINE ENDOCYTOSIS BY CELLS 59

IV.4. INTRANASAL DELIVERY OF NANOMEDICINE: A PRIVILEGED ROUTE FOR CNS DELIVERY? 64

V. AIM OF THE THESIS 66

I. EPIDEMIOLOGY AND ETIOLOGY

I.1. EPIDEMIOLOGY

Multiple sclerosis (MS) is a neuro-inflammatory demyelinating disease that impacts 2.8 million people worldwide with a prevalence of 35.9 per 100,000 people [1]. Although it is not deadly, MS significantly decreases patients' quality of life as it causes a series of invalidating symptoms and decreases the average lifespan of 6 to 8 years [2]. Until this day, the etiology of the disease is unknown, but the scientific community agrees that it is multifactorial.

The average age of onset is around 32 years old (but pediatric and geriatric cases are also possible), and women are twice more likely to be affected than men for unclear reasons [1]. In addition to gender and age, geographical localization also influences MS prevalence (Fig.1) [1]. Epidemiological data gathered through the years have consistently shown that countries populated with Caucasian individuals have the highest number of MS patients (e.g., North America, Europe, and Australia). This variability among the different localization is likely due to environmental factors and/or linked to the genetic heritage of the local population [1]. Indeed, some habits linked to western lifestyle such as smoking, and obesity are well-recognized risk factors for MS.

These disparities in MS prevalence may also be linked to the country's economic context. Wealthy western countries generally have an efficient healthcare system that can guarantee easy access to healthcare centers, whereas in developing countries, it is not always the case. This aspect can delay MS diagnosis in patients with limited acces to heathcare facilities and could also explain the disparity observed between western and southern countries [3] .

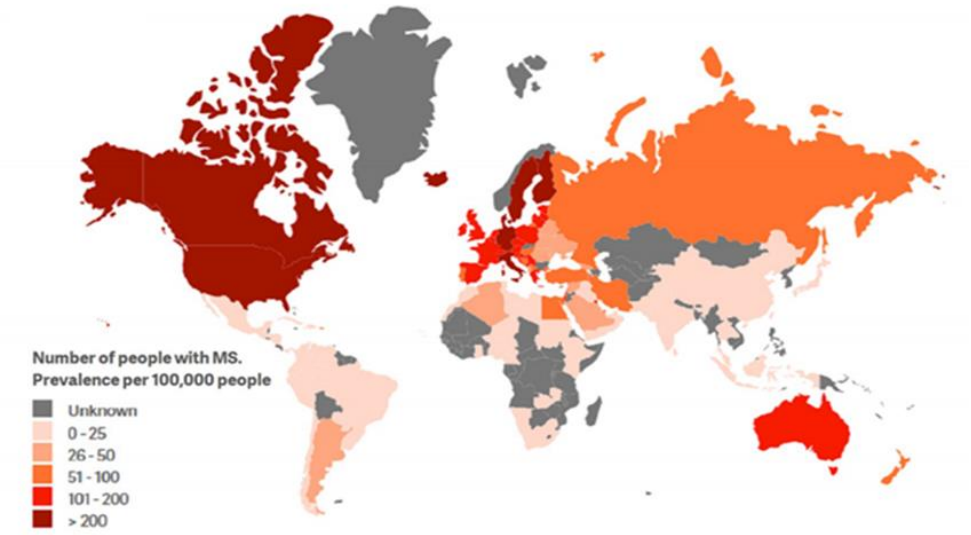

Figure 1. Prevalence of MS worldwide in 2019.[1]

I.2. ETIOLOGY

As mentioned, MS etiology is still unclear, but its onset is associated with several environmental, lifestyle, and genetic factors that we will briefly describe below (Fig.2).

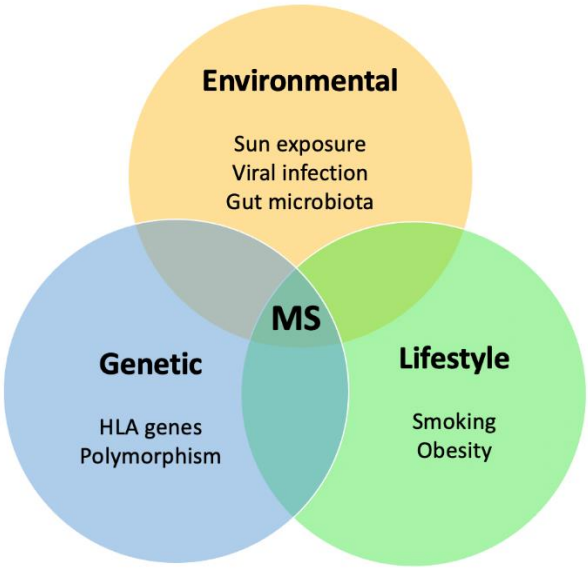

Figure 2. Etiology of MS: An illness with multiple risk factors

I.2.1. Environmental and lifestyle factors

The higher prevalence of MS in countries localized in higher latitudes highlighted the correlation between vitamin D deficiency and MS. Ultraviolet B exposition and intensity are lower in these areas, impacting 7-dehydrocholesterol conversion into vitamin D into the skin [4]. For instance, hypovitaminosis D in early pregnancy revealed a 2-fold increase in the risk of developing MS for the offspring compared with women with normal vitamin D levels [5]. Vitamin D is crucial for phospho-calcium homeostasis and has immunomodulatory properties. Conversely, vitamin D deficiency can lead to an unbalance of immune responses.

Like other autoimmune diseases, lifestyle also has an important impact on MS prevalence. Obesity is one of the key lifestyle risk factors for MS. Munger et al. reported in their study that women with a body-mass index (BMI) > to 30 kg/m^2 at age 18 had a 2-fold increased risk of developing MS compared to those with a lower BMI (18-25 kg/m^2)[6]. Other studies have confirmed these observations, but the mechanisms linking obesity to MS are still unclear. Guillemot-Legris et al.'s [7] review highlighted the relationship between obesity, constant inflammatory state, and BBB permeabilization (with occludin and claudin-5 disruption, two proteins essential in forming the

BBB tight junctions) [7]. Diet-induced obesity leads to immune cells activation and inflammatory response in many organs. Fatty acids (FA), that are increased in diet-induced obesity can activate the innate immune system through Toll-like receptors (TLRs) and activate transcription factors nuclear factor ϰB (the NF-ϰB pathway) that are known for upregulating the expression of proinflammatory mediators such as cytokines (i.e., interleukin (IL)-1β, IL-6). As a result, obesity correlated with a high number of circulating endotoxins such as lipopolysaccharide (LPS) and inflammatory mediators and the activation of immune cells in tissues such as the liver (e.g., Kupffer cells). In addition, diet-induced obesity partially translates into high adipokine rates in their blood, associated with autoimmune diseases such as MS [8].

As obesity, a western diet with a high intake of FA and sugar leads to gut microbiota dysbiosis, another factor that has been correlated to MS [9]. Although it seems unclear whether this dysbiosis is a consequence of MS or is a risk factor, several studies reported dysregulation of the gut microbiota of MS patients compared to healthy individuals. This difference is even greater when patients have an active MS with strong neurological symptoms during the relapsing phase. MS and gut dysbiosis are both tightly linked to neuroinflammation since the former is responsible for intestinal barrier inflammation and a "leaky gut" that permits translation of endotoxins, such as LPS, and gut bacteria in the secondary lymph nodes. Owing to this migration, the level of circulating immune cells increases and alters the blood-brain-barrier BBB, allowing the entrance of pro-inflammatory cues to penetrate the CNS inducing a neuroinflammatory spike [9].

Smoking is one of the other well-established lifestyle risk factors associated with MS, as several studies pinpoint a correlation between the two [10]. Pittas et al. showed that smokers have a higher relapse rate in a population of relapsing-remitting MS patients than nonsmokers [11]. Healy et al.'s cross-sectional study reported that smokers had a more rapid evolution from RRMS (relapsing-remitting MS) to secondary MS [12]. Smoking impacts the immune system as obesity and vitamin D [10]. It has been well established that tobacco smoke contains many irritating substances that generate oxygen species (ROS) that lead to lung inflammation. Inflamed lungs form a niche of activated macrophages and T-cells that produce pro-inflammatory cytokines. Some scientists reasoned that by molecular mimicry and epitope changing, myelin-reactive immune cells could arise from these cascades [13]. They can then get into the CNS through a leaky BBB (i.e. a BBB impaired by cigarette smoke) and have neurotoxic effects [14, 15]. However, it is interesting to note that smoking impact is dose- and duration-dependent [13].

Viral infections, especially the Epstein-bar virus (EBV), have been suggested as another risk factor for developing MS. EBV is a virus from the herpes virus family that affects 95 % of the world's adult population.

It often relies on dormant immune cells, and when activated, it can onset mononucleosis. In a cohort study including 1047 patients, only 3.3 % of MS patients were EBV negative compared to 6% in a healthy control population [16]. In line with the previous study, Bjornevik et al. calculated the risk of developing MS after EBV infection in a cohort of more than 10 million people [17]. They found that the risk of MS increased 32-fold after infection after EBV infection but did not increase after infection with other viruses, including the cytomegalovirus, another common virus in the world's adult population [17]. Therefore, the authors suggested that EBV might be the leading cause of MS. Although several studies underlined the link between EBV and MS, it is not easy to decipher if EBV is one of the primary causes behind MS since it is ubiquitous in the adult population.

Several theories suggest how EBV plays a role in MS etiology, and the most popular is based on the molecular mimicry theory. The molecular mimicry theory relies on autoimmune activation in the periphery by EBV antigens due to their resemblance to myelin antigens. Another hypothesis involves the expression of αB-crystallin in lymphoid cells via EBV infection of peripheral B cells triggering an immune response towards αB-crystallin, expressed in oligodendrocytes [18].

EBV transformation of B cells into pathogenic plasmablasts is another hypothesis that could explain EBV's role in MS [19]. After EBV infection, B-cells may express proteins specific to EBV, such as latent membrane protein 2A (LMP2A). LMP2A can then mimic B cell receptor signaling and trigger B-cells/T-cells signaling that may lead to a putative auto-immune response that could be one of the factors that triggers MS [19].

In addition to its putative role in MS onset, EBV may also contribute to aberrant activation of $CD8^+$ T-cells and trafficking of CNS-reactive immune cells, resulting in disease relapses.

I.2.2. Genetic factors

MS is not a hereditary disease; therefore, even people with no MS family history can be affected. Nevertheless, studies found that 15%–20% of MS patients had a family member with MS and had a 30-fold higher chance of developing MS than the general population (4% for siblings, 2% for parents, 2% for children vs. 0.1%–0.3% for the general population) [20]. These data indicate that genetic parameters can be considered as risk factors and lead scientists to perform genome-wide association studies (GWAS) to uncover the genes that could be linked to MS. Thanks to those studies, around 200 genes were associated with an increased risk of developing MS. Most of them are related to human leucocyte antigens (HLA). Type I HLA encodes for proteins involved in presenting antigens to T-cells. Among the genes associated with MS, the HLA DRB1*1501 haplotype is the most frequent one [18]. Homozygote individuals for this allele have an odds ratio

of 6 of developing MS [21]. This mutation may allow an optimal presentation of CNS myelin auto-antigen, thus increasing the probability of MS onset [22]. GWAS also showed that single-nucleotide polymorphisms (SNPs) in several genes, non-HLA related (LRP2 gene associated in axone guidance and MBP gene), could be linked to MS. Most of them are near the *loci* of genes related to the adaptative or innate immune system. Nonetheless, the association degree is weaker than for the HLA-dependent gene [22].

Overall, all these risk factors have one common point: they all have the potential to trigger inflammation, which is the main component in MS physiopathology. Although none can directly provoke the disease, they can undoubtedly be considered risk factors.

II. PHYSIOPATHOLOGY OF MS

MS is a demyelinating disease where a cascade of neuroinflammatory events leads to the death of oligodendrocytes and the destruction of the myelin sheath (demyelination). The myelin sheath in the CNS has two significant roles. Firstly, it is responsible for the swift conduction of actions potential throughout the axon via a process of saltatory conduction (50–100 times faster than unmyelinated axons) [23]. Myelin enables saltatory conduction through regular intervals of myelin interruption named nodes of Ranvier where there is a cluster of voltage-gated sodium channels. These channels open when depolarization occurs, allowing extracellular sodium to enter the axon. This influx of sodium induces a depolarization of the adjacent node and initiates the propagation of an action potential to the next node. The cycle then continues through the axon [24]. Secondly, myelin also plays a part in the metabolic support of axons. Monocarboxylate transporters on oligodendrocytes allow lactate transmission to the axons. They provide the substrate for ATP production in the axons via the citric acid cycle [25]. Hence, the destruction of the myelin sheath creates a massive delay in neuronal information transmission and leaves the axon without trophic support that ultimately triggers neurodegeneration.

For a long-time, MS has been considered an autoimmune disease, but all the criteria to be qualified as such are not fully met. By definition, an autoimmune illness implies that all patients produce IgG (immunoglobulins) or IgM antibodies against the same autoantigen. In MS, auto-IgG are present in the patients' cerebrospinal fluid, but these antibodies are directed against various antigens such as myelin oligodendrocyte glycoprotein (MOG), myelin basic protein (MBP), and alpha-crystallins. For this reason, MS is considered more as an immune-mediated disease [26]. The neuroinflammatory context led by the immune system aberrant activity towards the myelin sheath in MS is the principal cause of demyelination. Nonetheless, how the CNS becomes the stage of inflammation in MS is still an open question. Two main theories are considered:

The first claims that the inflammation originates in the CNS. For instance, in 2004, Barnett and Prineas suggested that oligodendrocytes apoptosis is the root source of demyelination, followed by neuroinflammation due to microglia and macrophages activations [27]. They reasoned that oligodendrocyte apoptosis might be caused by a viral infection or an undetermined neurodegenerative process that begins in the CNS. Infiltration of peripheral immune cells still occurs, but in this scenario, it is considered more as a consequence of CNS inflammation than its cause. The second, and the most popular theory, is based on an auto-antigen presentation to B-cells and T-cells outside the CNS ("outside-in") (Fig.3). This theory implies that following a viral

infection, most likely EBV, APC presents an antigen sharing structural components with myelin at their surface (Fig.3.1). This leads to B-cell and T-cell activation against myelin by molecular-mimicry followed by an inflammatory response and recruitment of other immune cells.

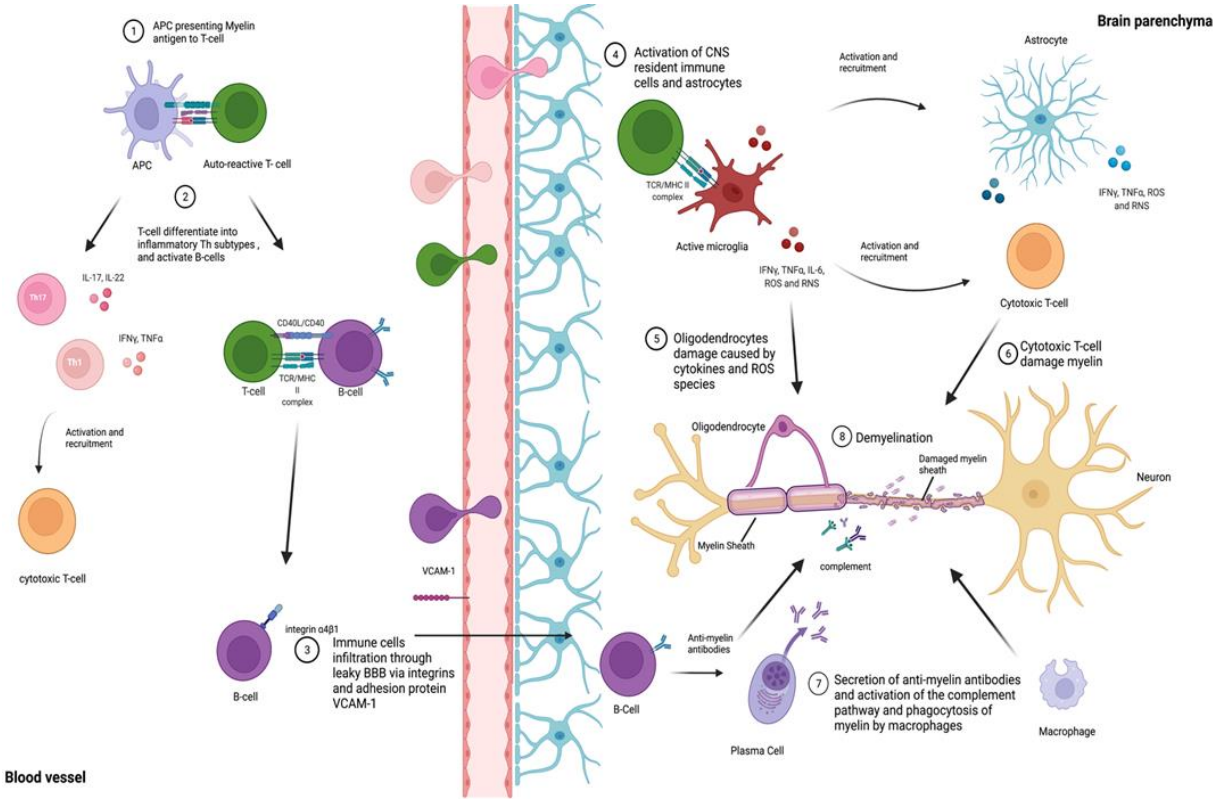

Figure 3. Overview of the neuroinflammatory cascade leading to demyelination according to the "outside-in" theory.

In the "outside-in theory," APC present myelin antigen to auto-reactive T-cells in the periphery, thus triggering their activation and differentiation into Th17 and Th1-cells. Th-cells secrete pro-inflammatory cytokines that onset the recruitment of other immune cells such as cytotoxic T-cell ($CD8^+$) and B-cells. Auto-reactive T-cells ($CD4^+$) can also act as APC and activate B-cells and $CD8^+$ T-cells toward myelin. This activation leads to the up-regulation of integrin expression at the surface of the immune cells that can cross the BBB via cell adhesion proteins (i.e., VCAM-1). Once in the CNS, T-cells and B-cells interact with microglia and astrocytes, which onset and perpetuate neuroinflammation by secreting pro-inflammatory cytokines. On the one hand, these cytokines can trigger oligodendrocyte apoptosis, and on the other hand, they contribute to the recruitment of immune cells that contribute to oligodendrocyte death (i.e., cytotoxic T-cells). In parallel, auto-reactive B-cells differentiate into plasmocytes that produce anti-myelin antibodies. Via the complement pathways, antibodies contribute to oligodendrocytes' death. The cascade of these events fatally leads to demyelination.

APC = antigen-presenting cells, IL = interleukin, IFN = interferon, ROS = reactive oxygen species, RNS= reactive nitrogen species,Th cells = T helper-cells; TNFα = tumor necrosis factor alpha, IFN γ = interferon γ

Usually, regulatory T-cells destroy self-activated T-Cells in the thymus, but due to central tolerance failure, they are released into the bloodstream [28]. Thus, $CD4^+$ T-cells and $CD8^+$ T-cells are activated by APC, and $CD4^+$ T-cells differentiate into their T helper (Th1 and Th17) (Fig.3.2) phenotypes. Along with activated B-cells and monocytes, they infiltrate the CNS by passing through a leaky BBB (Fig.3.3).

The BBB is dysfunctional at the early phase of the illness, resulting in the local recruitment of pathogenic T and B-cells. Pro-inflammatory cytokine secretion and expression of integrins and chemokines receptors by infiltrating lymphocytes have been identified as causes of BBB disruption [29]. Th17 lymphocytes, for instance, can efficiently disrupt tight junctions at the BBB via granzyme B and foster the recruitment of other $CD4^+$ cells from the systemic circulation into the CNS. Regardless of the hypothesis, the same course of events occurs immune cell recruitment, microglia activation, astrocyte activation, and demyelination.

In its complexity, the inflammatory response involved in MS is mediated by different immune cells that work together to initiate and maintain the inflammatory response observed in the disease. In the following paragraphs, the role of these different cells in the inflammatory response and demyelination will be briefly depicted.

II.1. T-CELLS IN MS

T-cells are a key player in MS. They can bind to a myelin epitope, activate macrophages that harm the myelin sheath through phagocytosis, and contribute to the outburst of pro-inflammatory cytotoxic mediators [22]. $CD8^+$ T-cells, more numerous than $CD4^+$ T-cells in lesions, are a cytotoxic subset directly contributing to oligodendrocytes and neuronal death through granzymes and perforin release [29]. Moreover, under inflammatory conditions, CNS resident cells can express class 1 major histocompatibility complex (MHC) molecules and present peptides derived from endogenous antigens (self or viral antigens), becoming potential targets for $CD8^+$ T-cells and thus contributing to tissue damage. Associated with the inflammatory outburst, an imbalance of pro-inflammatory and anti-inflammatory $CD4^+$ lymphocytes subtypes settle. Indeed, the upregulation of Th17 and Th1, with secretion of tumor necrosis factor α (TNF), Interferon γ (IFN γ), and IL-17 and downregulation of regulatory T-cells (Treg) and Th2 (with the secretion of IL-4 and IL-10) [21] enable macrophage and monocyte recruitment but also local T-cell, B-cell activation, and differentiation.

II.2. B-CELLS IN MS

B-cells have multiple roles in MS physiopathology. Firstly, they can differentiate into plasma cells and secrete antibodies directed against myelin-like antigens that contribute to oligodendrocytes' death. Anti-Myelin-like antibodies can induce demyelination through different mechanisms: (1) antibody-dependent cell-mediated cytotoxicity, (2) release of inflammatory mediators via stimulation of Fc receptors on natural killer cells or macrophages, and (3) opsonization of myelin, or complement activation (Fig.3.7) [30]. The presence of IgG in the cerebrospinal fluid (CSF) is

one of the hallmarks of MS. Nonetheless, only 60% of MS patients have antibodies directed against myelin. Although there is a considerable diversity of antigens among these antibodies, anti-MOG and anti-MBP antibodies are the most frequent and have been associated with highly active MS lesions. Of note, these antibodies are not specific to MS and can be detected in other diseases (i.e, anti-MOG in MOG antibody disease) [31]. Besides anti-myelin antibodies, antibodies against other types of CNS autoantigens can be found in the CSF of MS patients. For example, Svristava et al. identified antibodies against potassium channel KIR4.1, expressed at the surface of astrocytes and oligodendrocytes [32].

Secondly, B-cells play a role as APC [33] and secrete pro-inflammatory cytokines [34]. B-cell isolated from MS patients have shown a dysregulation of their cytokine profile. Indeed, compared to healthy patients, their B-cells secrete pro-inflammatory cytokines such as lymphotoxin-α, IL-6, and granulocyte-macrophage colony-stimulating factor (GM-CSF) that are toxic components towards oligodendrocytes and induce their death [34]. In addition to these functions, evidence has shown that B-cells may also have a role in T-cell recruitment. Although the precise mechanisms of interaction between those two cell types still need thorough investigation, patients treated with the anti-CD20 rixitumab (a B-cell targeted therapy) had a lower number of B-cells and a lower number of CD4+ and CD8+ T cells, and a decreased concentration of IFNγ and IL-17 in the systemic circulation [35]. These data highlight B-cell key role in the recruitment and/or the activation of T-cells by cytokine secretion or via their role as APC [35].

II.3. MICROGLIA ROLE IN MS

Microglia are considered as resident macrophages in the CNS and patrol the environment looking for signs of infection and injury. They represent 12% of the total CNS cells in rodents and 16% in humans [36]. During embryogenesis, they are responsible for neural precursor migration and synaptic pruning and they support myelination through the secretion of growth factors [35]. For a long time, the scientific community considered that microglia cells had two main phenotypes: the pro-inflammatory M1 phenotype associated with secretion of cytokines such as IL-1β and TNF-α and the anti-inflammatory M2 phenotype associated with anti-inflammatory cytokines such as IL-10, Insulin growth factor (IGF-1). It was also admitted that they could switch from one phenotype to another in response to their environment, but the latest evidence invalidated this dichotomy [37]. Llyod et al. suggested that a microglial cell does not switch from one phenotype to another but rather that pro-inflammatory microglia had to undergo necroptosis for pro-regenerative microglia to rise [38]. In addition, more than two subtypes of microglia can be found depending on the brain area, state of health, disease, or age [35, 39]. For example, $CD11c^+$ is one of the

microglia subtypes localized in the corpus callosum and is involved in the remyelination process in MS [40]. In a physiological context, microglia are in their "resting state" (Tmem119+, P2RY12+), but an activated microglia population (p22phox$^+$, iNOS$^+$, CD86$^+$and Trem2$^+$) arises in the context of CNS injury or in MS [39]. Microglia are involved in different ways in MS physiopathology. They contribute to neuroinflammation and can be found in active RRMS lesions alongside monocytes autoreactive B and T-cells infiltrates. In later phases of the disease, they have also been detected at the rim of the lesions, alongside macrophages, where they release inflammatory cytokines and reactive oxygen species (ROS) that lead to the apoptosis of mature oligodendrocytes (Fig.3.5). Microglia can also indirectly contribute to neuroinflammation by acting as APC for T-cells through the expression of class I and II MHC and cytotoxic T-lymphocyte-associated antigen 4 (CTLA4). This interaction induces T-cell proliferation, differentiation, and pro-inflammatory cytokine secretion [41]. Although numerous pieces of evidence pinpoint microglia participation in demyelination, counterintuitively, it also participates in remyelination [42]. Among the numerous microglial phenotypes, the pro-regenerative/anti-inflammatory phenotype (Arginase-1$^+$, IGF-1$^+$) is involved in myelin debris clearance, a mandatory process for remyelination [39, 43] but also stimulates OPC differentiation, partly via the secretion of the growth factor such as Activin-A [42].

II.4. ASTROCYTE ROLE IN MS

Astrocytes are the most abundant glial cells in the CNS. Similar to microglia, they can have different phenotypes. The first significant heterogeneity resides in their morphology and their localization. White matter astrocytes are called fibrous astrocytes, while grey matter astrocytes are called protoplasmic [44]. White matter astrocytes have small cell bodies and elongated morphology. Protoplasmic astrocytes have several primary processes and a higher degree of branching than fibrous astrocytes. Astrocytes have several crucial functions. They contribute to synapse formation and pruning, regulate extracellular concentrations of ions and neurotransmitters, synthesize metabolic substrates for neurons (i.e., glycogen and lipoproteins)[44]. They also participate in the BBB formation and integrity. In addition to their trophic support to neurons, they also contribute to the neuroinflammatory process and immune response. Depending on their surroundings, astrocytes can also bear a pro-inflammatory and anti-inflammatory subtype [45].

In the scope of MS, astrocytes intervene at multiple levels by playing a role in inflammation and subsequently in demyelination. Firstly they mediate innate immunity and express pattern recognition receptors (PRRs) that bind to diverse pathogen-associated molecular patterns (PAMPs) [44]. Astrocytes' tight link with the BBB basal lamina allows them to regulate the barrier permeability to facilitate the migration of peripheral immune cells by (1) the expression of adhesion

molecules such as intercellular adhesion molecule-1 (ICAM-1) and vascular cell adhesion molecule-1 (VCAM), (2) the secretion of pro-inflammatory cytokines such as TNFα, IL-6, et IL-1ß that impact the tight junctions of the BBB endothelial cells [44].

Furthermore, the secretion of chemokines such as MCP-1 and IL-8 by astrocytes allows the attraction of peripheral immune cells and resident cells. They also express MHC I and II at their surface, contributing to T-cell and B-cell activation. Regarding demyelination, astrocytes contribute to oligodendrocyte/myelin toxicity by producing ROS and nitrogen reactive species (RNS) [45]. Furthermore, astrocytes play a crucial role in regulating the extracellular concentration of glutamate, an excitatory neurotransmitter with multiple physiological functions. However, in the context of inflammation and damage, glutamate concentration increases to a level that becomes toxic to surrounding cells, mostly neurons and oligodendrocytes (a phenomenon called excitotoxicity). In MS, astrocytes fail to regulate this glutamate outburst because of decreased glutamate uptake [44]. Due to rising glutamate levels, AMPA/kainate glutamate receptors are activated in oligodendrocytes and axons, triggering calcium influx in the cytoplasm due to rising glutamate levels. Following this calcium outburst, calcium-dependent enzymes associated with neurodegeneration and cell death are activated and cause membrane breakdown and cytoskeleton alteration [45]. Finally, astrocytes impair efficient remyelination by being a significant "glial scar" component. These "scars" are localized in the demyelinating area of the brain and are mainly composed of proliferating astrocytes, oligodendrocyte progenitor cells (OPC) (with impaired differentiation), and finally, fibromeningeal cells [46].

The purpose of these scars is to prevent damage and injury from spreading to the nearby healthy tissues.

Nevertheless, the formation of scars inhibits remyelination and axonal regeneration via the secretion of different factors by astrocytes such as fibroblast growth factor-2 (FGF) and Ephrins (EPH). The first promotes OPC proliferation and survival but impedes differentiation hence remyelination [44]. The latter is secreted around MS lesion by astrocytes, creating a basal lamina around damaged areas contributing to scar formation. Moreover, EPH induces collapse of the axonal growth via activation of axon-bound EPH tyrosine-receptor kinase.

Overall, all immune cells mentioned above contribute to triggering and perpetuating neuroinflammation, leading to demyelination. Unmyelinated axons suffer from mitochondrial toxicity enabled by ROS and RNS species via mitochondrial DNA mutation with time and chronic inflammation. With mitochondrial deficiency, the amount of available ATP decreases, which impairs the function of the Na+/K+ ATPase pump, limiting Na^+ extrusion. The high

concentration of cytoplasm causes the $Na^+/Ca2^+$ exchanger (NCX) to operate in a reverse mode, importing $Ca2^+$ and triggering harming secondary cascades and axonal injury. Calcium aberrant influx into the axon in the context of impaired ionic homeostasis, partly due to glutamate outburst, triggers NO synthase (NOS) activation, proteases, and proteolytic enzymes that lead to axonal degeneration [28].

II.5. REMYELINATION

Following demyelination, an endogenous process called remyelination is set to regenerate the damaged myelin sheath [25]. Experimental data obtained in rodent MS models have shown that remyelination is enabled by new oligodendrocytes that stem from oligodendrocyte progenitor cells (OPC) [47]. OPC represents around 6% of the CNS total cell number and are localized at several CNS regions, where their primary role is to replenish the mature oligodendrocyte cell pool. OPC are multipotent and self-renewing cells [25]. They can differentiate into oligodendrocytes, astrocytes, and in some pathological conditions (i.e., MS or spinal cord injury) into Schwan cells (usually considered exclusive to the peripheral nervous system). In this regard, OPC fit the definition of a CNS stem cell. While the signaling pathways involved in remyelination are still under investigation, there is no doubt that OPC have a starring role in the process.

Nevertheless, other glial cells such as astrocytes, microglia, and macrophages also have a capital role in remyelination by either cleaning myelin debris, for the latter, or secreting promyelinating factors [42]. The process of remyelination can be broken down into three different phases: (1) OPC activation, (2) Proliferation and migration, and (3) Differentiation and remyelination and illustrated and summarized in Figure 4.

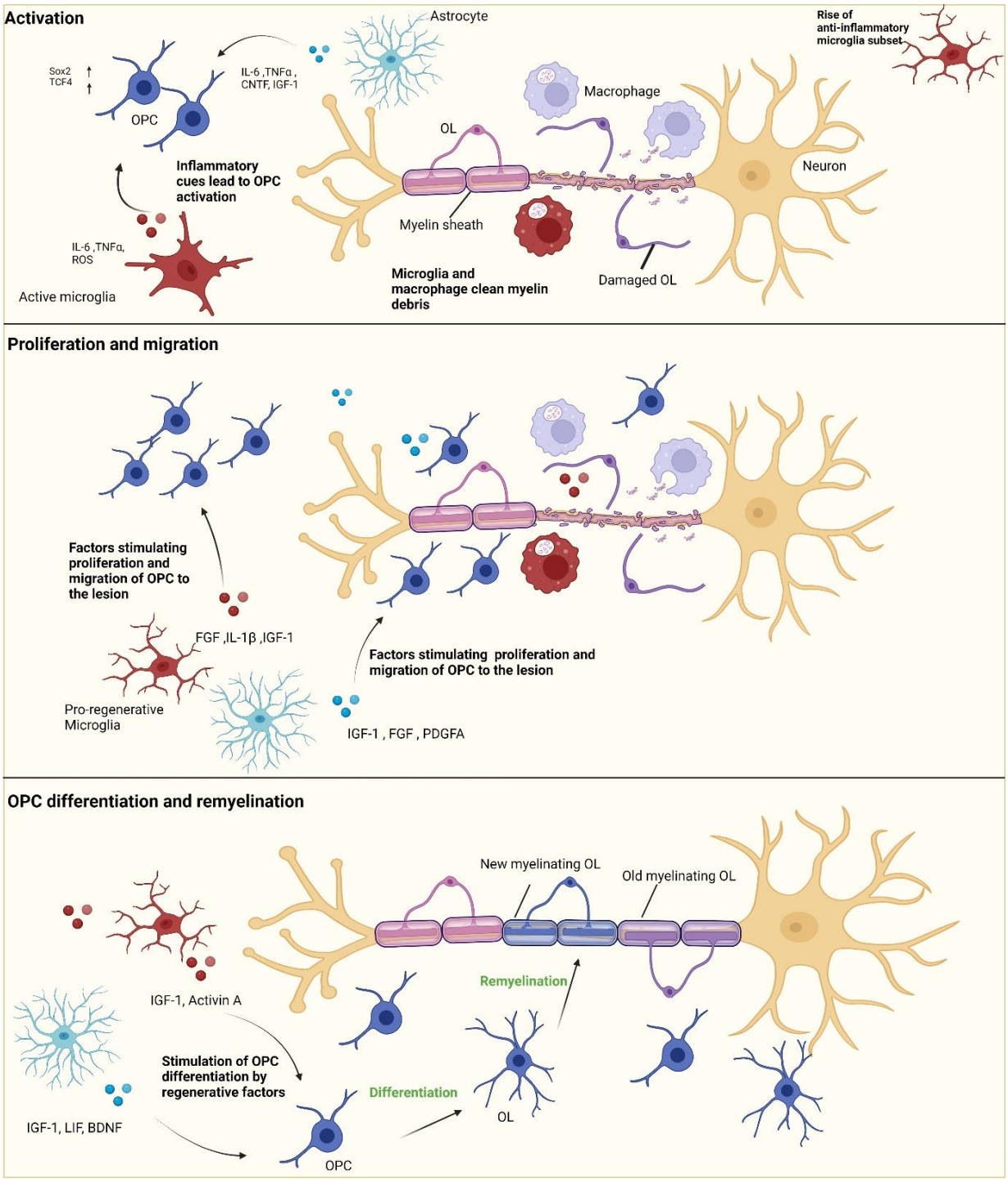

Figure 4. Overview of the three stages of remyelination.

(1) Activation: Following demyelination, OPC are activated by inflammatory signals enabling the upregulation of genes involved in proliferation and differentiation. **(2)** Proliferation and Migration: Pro-regenerative microglia and astrocytes at the lesion's periphery secrete chemoattractants and other factors that promote OPC migration towards the demyelinated axons and their proliferation. **(3)** Differentiation and remyelination: Finally, under the stimulation, several factors such as activin A and IGF-1, OPC differentiate into new myelinating oligodendrocytes. Upon demyelination, although some old oligodendrocytes can survive and reform a new myelin sheath. IGF-1 =Insulin Growth factor, LIF =Leukemia inhibitory factor factor, BDNF = Brain-derived neurotrophic factor, FGF= fibroblast growth factor, PDGFA = Platelet-derived growth factor A, IL = Interleukin, TNF = tumour necrosis factor,OL= oligodendrocyte.

II.5.1. OPC activation

After demyelination, microglia and astrocytes start secreting a myriad of pro-inflammatory cytokines that activate astrocytes and later launch the signal for OPC proliferation and differentiation via the secretion of factors such as IGF-1 and ciliary neurotrophic factor (CNTF) [48]. During this phase, the transcriptome of OPC switches, enabling their "regeneration mode" and up-regulating transcription factors such as SRY-Box Transcription Factor-2 (SOX2) and transcription factor-4 (TCF4). Microglia and macrophages are critical in clearing up myelin debris detrimental to remyelination (Fig.4) [42]. Microglia activation for myelin debris clearance is through the CX3C chemokine receptor-1, present at the surface of pro-inflammatory microglia.

II.5.2. Proliferation and migration

Following their activation, OPC begin to migrate towards the damaged region then start proliferating. In parallel, near the lesions, cells of the innate immune system and astrocytes start secreting pro-regenerative cytokines. Astrocytes and microglia secrete chemoattractants such as the semaphorin 3F protein (Fig.4) [49] or proliferation factors such as FGF and PDGFA to ensure proper remyelination by attracting OPC to the lesions and stimulating their multiplication. Pro-regenerative microglia have also been described to secrete activin A, IGF-1, and IL-1ß [42]. As reviewed by Lubetztki et al. [23], remyelination efficiency is dependent on several parameters, and a sufficient number of OPC at the lesion site is a vital prerequisite. Unfortunately, the latter can be quite variable depending on the demyelinated lesion as, in some cases, the lesion can be devoid of cells of the oligodendroglial lineage or contain OPC that cannot differentiate. Therefore, the extent of remyelination can differ from one lesion to another [23].

II.5.3. Differentiation and remyelination

To differentiate into oligodendrocytes, OPC require the up-regulation of a new set of genes that are repressed while they are in proliferation mode [50]. Therefore, OPC must exit the cell cycle of division and proliferation for differentiation to occur. This shift is favored by regenerative factors such as IGF-1, activin A or BDNF secreted by astrocytes and microglia(Fig.4) [51]. Several proteins and transcription factors are involved in this transition, like the MYC proto-oncogene protein and the transcription factor E2F1 [25, 52]. The kinetic transition between the multiple differentiation stage and the myelin sheath formation is crucial for proper remyelination (Fig.5).

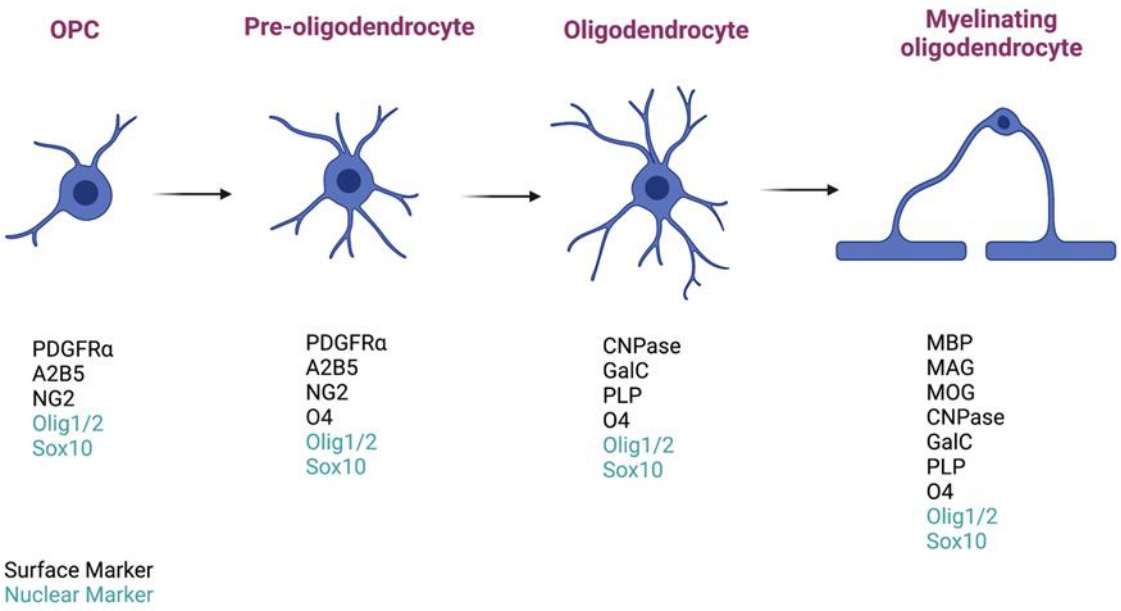

Figure 5. The different stages of OPC differentiation into myelinating oligodendrocytes. These stages are identified by their different morphology and expression of different markers (some nuclear some at the surface) CNPase, = 2',3'-cyclic nucleotide 3'-phosphodiesterase; GalC = galactocerebroside C, MAG =myelin associated glycoprotein , MBP =myelin basic protein , MOG, myelin oligodendrocyte glycoprotein , PLP= proteolipid protein.

The differentiation of OPC into myelinating oligodendrocytes is a multistep process where cells change their phenotype and morphology under the stimulation of growth factors, cytokines, and neurotransmitters. The process can be summarized by four main stages/phenotypes: OPC, pre-oligodendrocytes, oligodendrocytes, and myelinating oligodendrocytes (Fig.5). Each of these stages is defined by several markers that allow their identification [53]. OPC are bipolar cells that express the PDGFRα at their surface (receptor for PDGFA, the most potent OPC growth factor) and other surface proteins like A2B5 and NG2. At the pre-oligodendrocytes stage, these markers remain but the cell morphology is more complex with the appearance of filamentous myelin outgrowths, and a new surface protein, O4, is produced. Between the switch from pre-oligodendrocytes to oligodendrocytes PDGFRα, A2B5 and NG2 are not expressed anymore [53]. Oligodendrocytes have more developed arborization than their predecessors and are characterized by the expression of news markers like 2', 3'-cyclic-nucleotide 3'-phosphodiesterase (CNPase), a myelin-associated enzyme early myelin components such as galactocerebroside (GalC) and the transmembrane protein proteolipid protein (PLP). At the final differentiation stage, oligodendrocytes cytoplasm extend to wrap around the axon. Myelinating oligodendrocytes express a plethora of surface proteins such as MBP, myelin-associated glycoprotein (MAG) and MOG [53]. In postnatal murine-derived oligodendrocytes, MBP and MAG emerge between day 5 and 7, whereas MOG appears one to two days later [53].

The three transcription factors Olig1, Olig2, and SOX10, are present throughout the whole oligodendroglial lineage [54]. Their expression has been described to be a critical element in the promotion of OPC differentiation.

Any disturbance of the process results in a failure of remyelination. Even if remyelination is efficient, the newly formed myelin sheath is thinner than its predecessor.

During developmental myelination, the thickness of the myelin sheath is proportional to the thickness of the axon, but in remyelination, this correlation is lost for unclear reasons. This change is more apparent for larger axons, where the newly formed sheath is thinner than the original one. However, for thinner fiber, like in the corpus callosum, the thickness of the myelin the newly formed myelin mostly remains to the original one [55].

In the latest decade, there has been a real effort to uncover the mechanisms behind remyelination and, notably, the role of the myriad of secreted factors during remyelination. Furthermore, it was also critical to determine what aspect of remyelination was more likely to fail in MS patients. Along this line, Woodruff, and colleagues [56] demonstrated, using a transgenic mice model overexpressing PDGFA, that OPC proliferation permitted their migration at the lesion site but did not manage to improve remyelination compared to wild-type mice. Their results suggested that OPC differentiation seems to be the limiting step for efficient remyelination [56]. Therefore, unraveling the pathways that inhibit or promote OPC differentiation seemed crucial to find effective drug targets to improve OPC differentiation [23]. Many inhibitory pathways (Fig.6) [23] have been discovered, such as the Notch Pathway or the Wnt pathway, but so far, only Lingo-1 and the muscarinic receptor signaling have been a source of interest to researchers since antagonistic antibodies for the former and molecules for the latter have been taken to clinical trials (see below). Among the pathways that favor differentiation, we can cite the activation of the retinoid X receptor (RXR), thyroid hormone, and vitamin D that mediate their effect via heterodimerization of the RXR.

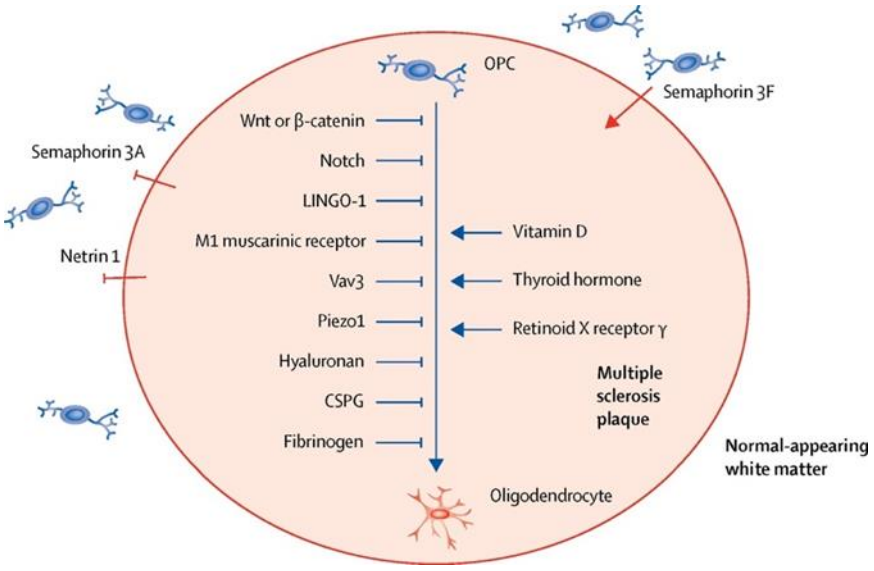

Figure 6. Pathways involved in OPC differentiation [23].

At the left of the central blue arrow are listed some of the proteins that inhibit OPC differentiation. The elements that promote OPC differentiation are listed at the right of this same arrow. Semaphorin 3A and Netrin I hinder OPC recruitment at the lesion, whereas Semaphorin 3F favors their recruitment.

CSPG=chondroitin sulfate proteoglycan. Vav3=rho GTPase-regulating guanine nucleotide exchange factor.

Nonetheless, recent findings by Yeung et al. call into question most of the discoveries made in animal models regarding how important OPC differentiation is for myelin sheath regeneration and the role of damaged oligodendrocytes in the process of regeneration [57]. They used C^{14} datation in shadow plaques (i.e. partially remyelinated lesions) to show that the newly remyelinated lesions were mainly composed of older oligodendrocytes and not recent ones. Furthermore, another study found reduced amounts of mRNA correlated with OPC (SOX6 and PDGFRA mRNA) in shadow plaques of post-mortem brains from MS patients compared to healthy subjects [58]. In addition, they also discovered that different subsets of mature oligodendrocytes existed and that they differ between areas of normal-appearing white matter in MS patients and healthy individuals (some subtypes were depleted in MS patients). In the last two years, discoveries made on animal models (zebrafish and rodents) strengthened the idea of oligodendrocytes participating in remyelination [59]. For example, Bacmeister et al. used a cuprizone model and followed damaged oligodendrocytes in mice [60]. They observed that these oligodendrocytes could reform the myelin sheath but are less involved in the process than new oligodendrocytes stemming from OPC differentiation [59, 60]. In line with these observations, Duncan et al. found that in the demyelinated spinal cord of cats, mature oligodendrocyte cell bodies were seen to extend their processes to mature myelin sheaths and thinly remyelinated axons. They also observed by electron microscopy the same phenomenon in rhesus macaques in the spinal cord [61].

Taken together, these observations suggest that old oligodendrocytes, in addition to OPC, also contribute to remyelination in humans and rodents (Fig.7). Thus, the long-time postulate placing only OPC differentiation in the center of remyelination is obsolete, leading to the conclusion that oligodendrocytes can also be the target of new medicines that can potentially restore their ability to generate myelination. We highlighted how essential myelin is for axon protection and the high velocity of action potentials conduction. Therefore with remyelination, all myelin functions are recovered and thus axonal degeneration. Hence, remyelinating molecules can be the rise a new class of therapeutic agents that could be prescribed alongside the existing immunomodulatory treatments discussed in the following paragraphs.

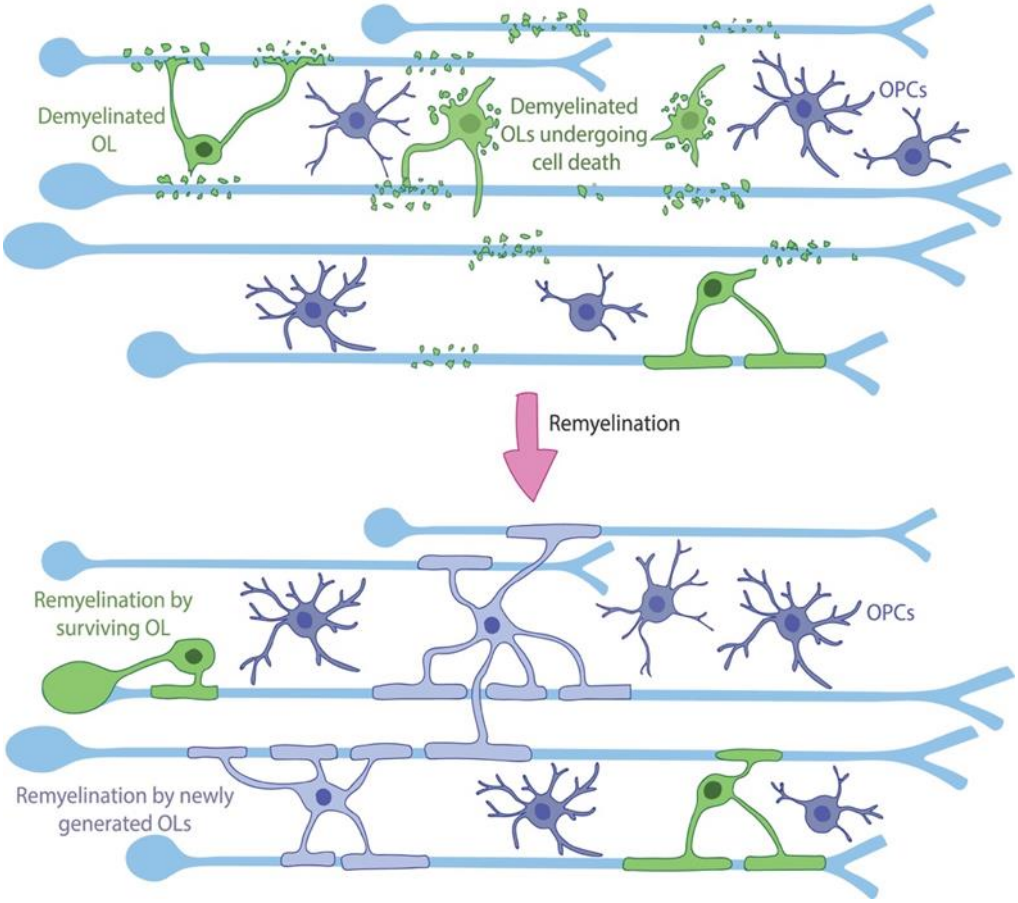

Figure 7. Remyelination by oligodendrocytes and OPC [59].
After demyelination, some oligodendrocytes survive, losing some or all of their myelin sheaths whereas others die, leading to OPC activation. During remyelination, OPC can generate new myelinating oligodendrocytes and the surviving oligodendrocytes can contribute to remyelination, but to a limited extent. OL = Oligodendrocytes

III. MS CLINICAL SYMPTOMS AND TREATMENTS

Demyelination and neuroinflammation are the root cause of the various symptoms observed in MS.

As its variable clinical symptoms, the disease can have several clinical courses that depend on its "form." MS patients are usually classified in one of the three main forms of MS (Fig.8).

- The relapsing-remitting form affects 85% of the patient.
- The primary progressive form (PPMS) affects less than 10% of the patients.
- The secondary progressive (SPMS) form that is considered the long-term evolution of the RRMS developed by the majority of a patient within 15-20 years after RRMS manifestation: 10% after 10-years, 50% after 20-years, and 93% after 30-years of disease onset [62]. In the younger population (disease onset at 14 years old), this conversion from RRMS to SPMS is slower than in adults. The switch occurs more rapidly for an elderly population (disease onset over 55 years old).

In RRMS, patients experience acute inflammatory episodes and symptoms followed by months or years of remission, whereas in the progressive form, there is a continuous degradation of the patients' neurological function (Fig.8) [63] [64].

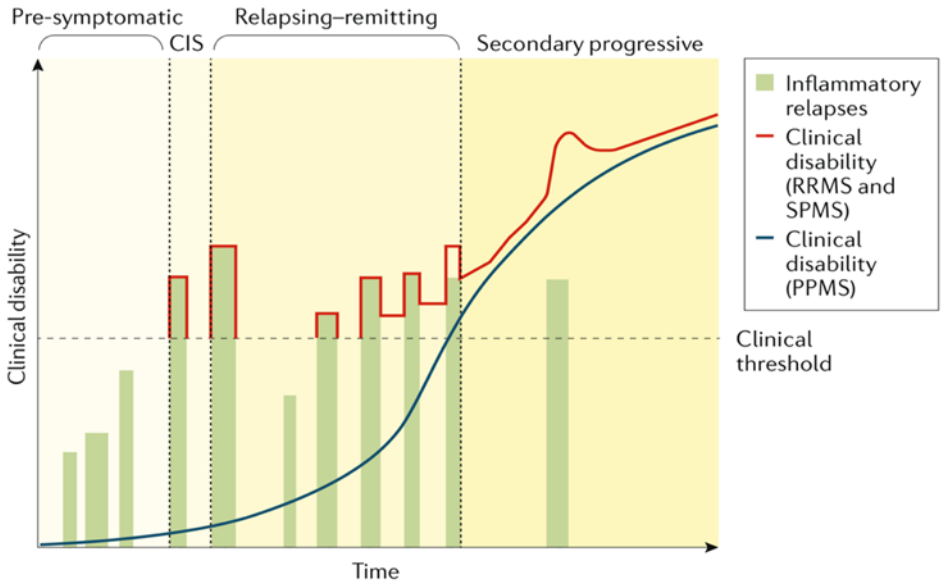

Figure 8. Clinical course of MS [64].

MS diagnosis is always preceded by a clinically isolated syndrome (CIS) phase where patients experience their first neurological attack. These symptoms can only be a one-time event and don't necessarily evolve into MS. Depending on the type of MS, clinical disability progresses differently throughout time. However, all MS patients can suffer from chronic symptoms such as fatigue, cognitive difficulties or residual deficits from previous relapses

III.1. DIAGNOSTIC

MS first manifestations are generally isolated neurological deficits that can differ from one patient to another due to the localization of the demyelinated lesions in the CNS. One of the most common initial symptoms in MS are vision problems due to optical neuritis. Symptoms can be temporary loss of vision, blurry vision, or eye pain that gets worst with movement. These symptoms occur 90% of the time in one eye and rarely in both eyes. Inflammation in the spinal cord (myelitis) is the second common symptom that declares disease onset. It translates in muscle weakness, reduced limb sensation and bowel and bladder dysfunction. This acute inflammation can resolve or develop into spasticity. The Lhermitte sign, which consists of an electrical shock-like sensation going down the spine or limbs induced by neck movements or urinary urgency, is also a diagnostic indication of MS. Other symptoms such as vertigo, caused by cerebral lesions, or uncoordinated voluntary movements of the limbs, cognitive disorders, and mood swings can also be MS symptoms [65]. It is difficult to establish at the beginning of the onset whether the patient has MS. A first clinical episode is called a clinically isolated syndrome (CIS), and it may take weeks or months for another relapse to occur. With a large and complex clinical picture, the McDonald criteria (Table 1) have been established to help physicians diagnose MS with sufficient sensitivity and specificity [66]. These criteria are based on clinical symptoms, magnetic resonance imaging (MRI), and laboratory findings (oligo bands that show IgG presence in the CSF). Demyelinating lesions in MRI can be observed in T-2 weighted and T-1 weighted images where they appear as hyperintense and hypointense, respectively [66]. In summary, the disease's dissemination in time and space must be demonstrated and other causes excluded to confirm a diagnosis of MS.

Table 1. The 2017 McDonald Criteria for diagnosis of MS in patients with an attack at onset [66]. Dissemination in time: the appearance of the new lesion over time; Dissemination in space: the appearance of a lesion in another location in the brain

	Number of lesions with objective clinical evidence	**Additional data needed for a diagnosis of multiple sclerosis**
≥2 clinical attacks	≥2	None
≥2 clinical attacks	1 (as well as clear-cut historical evidence of a previous attack involving a lesion in a distinct anatomical location)	None
≥2 clinical attacks	1	Dissemination in space demonstrated by an additional clinical attack implicating a different CNS site or by MRI
1 clinical attack	≥2	Dissemination in time demonstrated by an additional clinical attack or by MRI OR demonstration of CSF-specific oligoclonal bands
1 clinical attack	1	Dissemination in space demonstrated by an additional clinical attack implicating a different CNS site or by MRI **AND** Dissemination in time demonstrated by an additional clinical attack or by MRI OR demonstration of CSF-specific oligoclonal bands

For example, having a CIS such as optic neuritis does not necessarily mean that the syndrome is related to MS. Even if CIS are related to demyelination, they can be a one-time syndrome that can swiftly disappear. Nonetheless, individuals having CIS have a higher chance of developing MS. The probability is lower if patients' have no brain lesions visible with MRI at the time of the CIS (10-year risk of 20% chance of meeting the McDonald criteria for MS) but if the same attack is observed with evidence of brain lesion, the risk increases (10- year risk of 90% of meeting the McDonald criteria)[65]

III.2. SYMPTOMS

MS symptoms can be very different from one person to another. The physician can grade the degree of disability with the extended disability status scale (EDSS). The EDSS scale ranges from 0 to 10, with a higher scoring representing a higher disability. For example, a scoring from 1 to 5.5 refers to people with MS who can walk without any aid. The highest score of 10 corresponds to the patient's death because of MS. The nature of the symptoms mainly depends on the demyelination lesion localization, but overall, they have a significant impact on patients' lives. In 2018, Barin et al. reported the frequency of symptoms in patients with RRMS (611 participants and PMS 244) [67]. Interestingly the three most frequent symptoms were different from one subtype to another. For RRMS, it was paresthesia (77.1%), fatigue (74.1%), and weakness (54.8%), whereas PMS patients had gait problems (90.6%), balance problems (84.0%), and fatigue (83.2%). In the elderly population, in addition to the symptoms cited above, cognitive impairment is widespread. Roth et al., compared cognitive performance of elderly individuals (60-80 years old) with MS and those with amnestic mild cognitive impairment healthy (unaffected by MS)[68]. Their data suggest that MS patients affected individuals exhibited worse performance on measures of processing speed (speed with which information can be perceived, understood, and responded to). Either way, MS patients display a large panel of symptoms with different frequencies (Fig. 9) [67].

The study by Barin et al. also reports the measurement of the participants' health-related quality of life (HRQoL) [67]. The HRQoL was assessed using the EQ-5D-5L self-assessment questionnaire that considers patients' 5-component scale, including mobility, self-care, usual activities, pain/discomfort, and anxiety/depression [67]. The study showed that for RRMS patients, gait and balance problems and fatigue are the symptoms that most affected their quality of life, whereas, for PPMS, it was spasticity (abnormal muscle tightness that creates a resistance to movement) and paralysis.

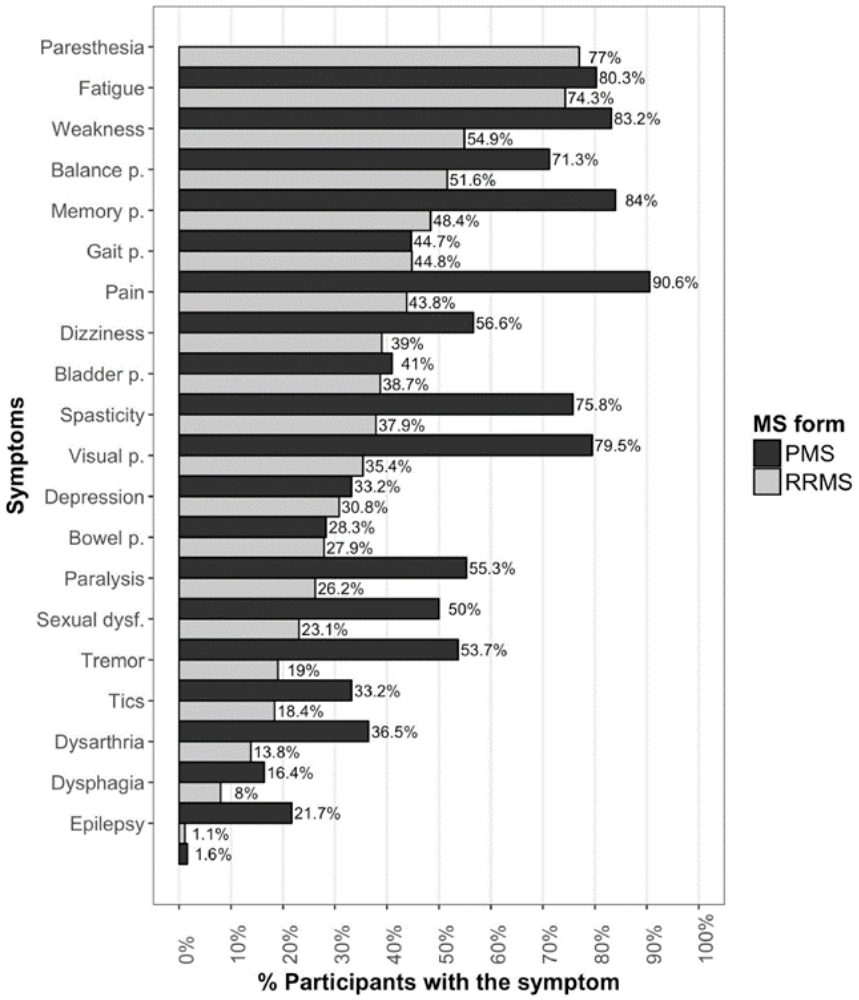

Figure 9. Frequency of reported symptoms in participants with RRMS and PMS [67]. RRMS = relapsing-remitting MS, PMS = progressive MS, dysf. = dysfunction, *p.* = problems

III.3. POPULAR MS MODELS *IN VIVO* FOR DRUG DISCOVERY

Efficient preclinical models are essential for drug discovery. Like other diseases, animal models have been developed for MS. While a single model does not capture the complexity of MS, they are valuable tools to test new therapies and decipher disease machinery. Several models permitted establishing the efficacy of the molecules that clinicians have nowadays at their disposal to tackle MS. In this paragraph, we will briefly introduce 3 of the most popular models and discuss their limit and the scope of their use.

Experimental allergic encephalomyelitis (EAE): EAE is one of the most popular animal models to study MS, whether for understanding its complex immunopathology or testing new drugs. EAE has been induced in rats, mice, guinea pigs and monkeys, nonetheless, C57BL/6 mice are the most used [69]. Most MS treatments discussed in the upcoming paragraph were tested in the EAE model in preclinical studies. This model is particularly interesting since it shares many

common characteristics with MS such as inflammation, demyelination, axonal loss, and gliosis [69]. The induction of such inflammation results in MS-like symptoms in mice that are graded with a "clinical" score (as an example : 0, no disease; 1.0, limp tail; 2.0, weakness in hind legs; 3.0, ataxia; 4.0, paralysis of both hind legs; 5.0, hind and foreleg paralysis; 6.0, moribund/dead).

EAE is based on encephalomyelitis induction by immunizing the animal with proteins or peptides from the myelin (generally a fragment of a myelin-related protein such as MOG or PLP). For instance, to stimulate the immune system activation towards the antigen in C57BL/6, a standard protocol is to use a peptide from the myelin oligodendrocyte glycoprotein (MOG35–55) emulsified into complete Freund's adjuvant [69]. Depending on the sex of the animal, the inflammatory response may differ in regard of some aspects. Although female and male mice have a similar clinical score 20 days post-immunization, female mice had more spinal cord infiltrating cells and demyelination than males [70]. Even if EAE has been used to study the impact on remyelination of a given compound, it may not be the most suitable model to do so. Considering the strong neuroinflammation induced in this model, it is challenging to decipher whether the myelin sheath regeneration is induced via the modulation of inflammation or by the induction of OPC differentiation and proliferation [69].

Cuprizone: This murine model is based on chemical-induced demyelination. Cuprizone is a copper-chelator that is specifically toxic towards oligodendrocytes. Oligodendrocytes fail to maintain their very high metabolic activity due to copper deficiency, leading to their apoptosis and thus demyelination [69]. It is typically mixed with chow ingested by rats or mice. Although several grey and white matter regions are affected, demyelination is quite significant in the corpus callosum. Actually, this region is the most studied one due to its high myelin content [71]. Even if the demyelination observed in the cuprizone model is not inflammation-mediated, inflammatory markers are increased in the CNS. Indeed, innate immune cells are activated as a reaction to oligodendrocytes 'apoptosis with prominent gliosis due to microglial accumulation and astrogliosis. Of note, microglia infiltration in the later stage of demyelination appears to clear myelin debris and secreting factors, such as FGF, essential for OPC proliferation [72]. This model is particularly interesting to study remyelination as it can inform the kinetic process. Usually, after 5-6 weeks of 0,2% cuprizone chow ingestion in mice, the corpus callosum has attained a significant loss of myelin (less than 25% of the myelinated area) [71]. Upon removal of cuprizone from the diet, remyelination starts and is completed after 6-8 weeks. Therefore, using this model makes it easier to appreciate the effect of a given molecule on the speed of remyelination.

Lysolecithin (LPC): The use of LPC, a phospholipase A activator, is another type of chemical demyelination [73]. Contrary to the two previous models, LPC is used to induce a local

demyelination plaque by administering a 1% solution using stereotactical injection methods. In the literature, the most common site of injection are the corpus callosum and the spinal cord [73]. As the cuprizone model, demyelination is quickly followed by remyelination. OPC start repopulating the lesion around 5 days after LPC injection and remyelination is complete between 14 to 28 days post lesions. The speed and degree of remyelination depend on the animal's age but are also site-dependent [69]. Like the cuprizone model, LPC models are used to study the mechanistic of remyelination or to appreciate the impact of a molecule on remyelination.

Although these animal models permitted to uncover several physiopathological elements linked to MS and test the efficiency of all approved MS drugs we want to highlight that these models have their limitations. Indeed, animal models of MS feature demyelinating lesions that can be induced via multiple mechanisms, but these plaques' characteristics do not reflect all the complexity and subtypes of human MS lesions [74]. To address some of these limitations, new humanized chimeric animal models have been developed. They are based on the transplantation of human oligodendrocytes from a healthy human donor in immune-deficient mice or pups that allow xenograft. With this kind of model, the biology behind the myelination process can be studied with a higher correlation with human biology. To study the physiology behind remyelination or evaluate the impact of a given compound, cells can also be grafted after demyelination [75].

III.4. TREATMENTS

To this date, MS is an incurable disease. However, the treatments available help limit the disease's progression and positively impact patients' lives (Fig.10) [76]. Treatments can be divided into (i) clinically isolated syndrome treatments, (ii) disease-modifying treatments, and (iii) symptomatic treatments that manage patients' symptoms. Since MS is an immune system-related disease, all treatments are either immunomodulatory or immunosuppressive. Below the main treatment options available will be listed, and their main mechanisms of action will be briefly described.

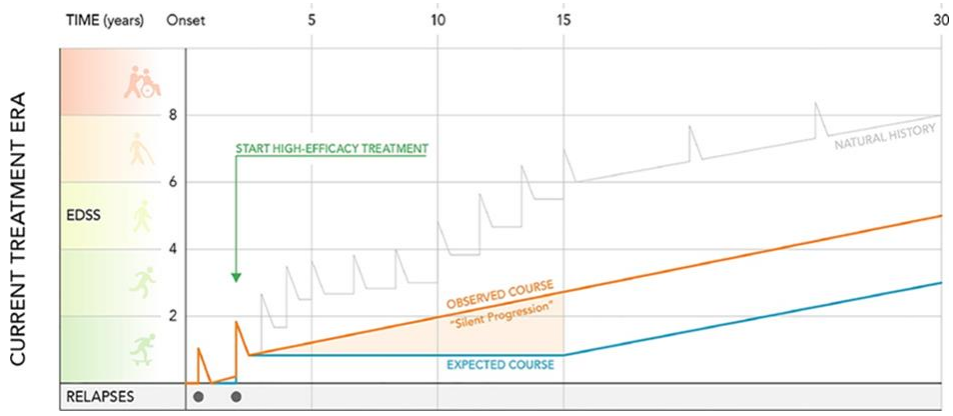

Figure 10. Progression of EDSS in MS during the years after disease onset [76]. The figure shows the progression of MS with the current treatment. With the use of nowadays therapies, attacks fairly decreased in most patients. However, even during relapses, there is still an evident disease activity that the authors termed "silent progression."

The CIS patients present one or several symptoms of neurological deterioration with or without MRI lesions that lasts more than 24h, without any sign of fever or infection, and that resolves by itself. With this kind of neurological manifestation, patients are highly likely to develop MS. While most neurologists use high doses of intravenous (IV) corticosteroids (3–5 days course) to accelerate relapse recovery, the aftermath management can differ from one physician/hospital to another. Indeed, to delay the manifestation of other neurological attacks, patients do not receive any treatment in some cases. However, in some practices, patients can receive as a first intention treatment IFN-β or glatiramer acetate [65].

Disease-modifying treatments (DMT):

In MS, a DMT is an immunomodulatory drug that acts on the dysregulated immune system. The primary purpose of these treatments is to prevent relapses, limit CNS inflammation, and reduce the development of new lesions. However, they generally do not significantly improve preexisting MS symptoms. Nowadays, there are 10 type of DMT for RRMS and one, Ocrelizumab, approved for PPMS. IFN-β and Glatiramer acetate are part of these 10 types of therapies approved for RRMS. We listed them as first-line and second-line treatments.

First-line treatments

IFN-β: IFN-β is the first drug authorized by the Food and drug administration (FDA) (1993) and the European medicine agency (EMA) (1995) for MS [77]. There are different types of IFN-β on the market (IFN-β-1a, β-1b or PEGylated IFN-β). IFN-β-1a is produced in chinese hamster ovary

cell line and its amino acid sequence is identical to the native IFN-β. On the other hand, IFN-β-1b is produced in Escherichia coli, has a subtle different amino acid sequence from the natural IFN-β [77]. These differences result in lower efficiency thus leading to the administration of higher doses. Those preparations are self-injected by the patient either by intramuscular (IM) or by subcutaneous (SC) administration. IFN-β activates IFNAR1/2 inducing the phosphorylation of signal transducers and activators of transcription such as (STAT)1-STAT2 factors. It induces a shift from a Th1 to a Th2 response associated with the secretion of anti-inflammatory cytokines such as IL-10. In addition, this activation of IFNAR decreases MHC II and thus inhibits the presentation of auto-antigen and T-cell activation. IFN-β also diminishes immune cell trafficking across the BBB by decreasing the expression of adhesion molecules very late antigen-4 (VLA-4) and cleavage of endothelial vascular cell adhesion protein (VCAM) [77].

Glatiramer acetate is a polypeptide of 4 amino acids (l-alanine, l-lysine, l-glutamic acid, and l-tyrosine) SC self-administrated. This peptide is supposed to mimic myelin auto-antigen and thus serve as a decoy for the immune system [66]. However, the exact mechanism of action of this drug is still unknown. The suggested mechanism of action is that glatiramer acetate decreases myelin auto-reactive T cells by biding to MHC II of APC cells, thus limiting the presentation of myelin-like antigen. It favors the differentiation of activated T-cells into a Th2 and T-reg phenotype that secretes anti-inflammatory factors [78].

Dimethyl fumarate: Dimethyl fumarate is also a small molecule taken per os indicated for the treatment of RRMS and is the most prescribed oral drug for RRMS in the US [74]. The mechanism of action of dimethyl fumarate is still unclear, but it is known to activate the nuclear transcription factor erythroid-derived 2 (Nrf2). Nrf2 is a ubiquitarian redox sensor that regulates oxidative stress. The Nrf2 pathway is activated by dimethyl fumarate via cysteine residues of the Keap1 protein, Nrf2 inhibitor, resulting in its dissociation from Nrf2 [74]. Upon dissociation from Keap1, Nrf2 migrates to the nucleus and increases the transcription of anti-oxidative genes (i.e., genes coding for oxydo-reductase enzymes)[74]. Since ROS production is a hallmark of demyelination and axonal degeneration, dimethyl fumarate anti-oxidant action result in a neuroprotective effect. Moreover, it also has an anti-inflammatory effect mediated by the inhibition of the NF-Kβ pathway that decreases anti-inflammatory cytokine secretion and lymphocyte activation and production [74].

Teriflunomide: Teriflunomide is an oral drug indicated for RRMS and is the active metabolite of leflunomide prescribed for rheumatoid arthritis. It limits the de novo synthesis of pyrimidines by inhibiting a mitochondrial enzyme named dihydro-orotate dehydrogenase [75]. In all cells, pyrimidines are essential for DNA, membrane phospholipids, and glycoproteins synthesis. Nevertheless, proliferating T-cells and B-cells are mainly dependent on this pathway. Therefore,

by depleting the pyrimidine pool in these cells, teriflunomide acts as an immunosuppressive molecule by decreasing circulating T-cells and B-cells [75].

Second-line treatments

Fingolimod and Siponimod: Fingolimod was the first oral therapy released, in 2010, for RRMS. After phosphorylation it acts on the sphingosine-phosphate receptors (S1PR1, S1PR3 and S1PR5) that are crucial for lymphocyte migration from the lymphoid organs to the bloodstream [73]. Phosphorylated fingolimod binds to its receptor and sequestrates the auto-reactive lymphocytes in the lymph nodes, limiting their accumulation into inflamed CNS lesions. Its main effect is primarily on T- and B -cells, but a few studies demonstrated that fingolimod can also act on gliosis and OPC differentiation in vitro [73]. In clinical trials, fingolimod the number of CD4+ cells and CD8+ cells [73]. Siponimod, like fingolimod, is administered per os and acts on sphingosine phosphate receptors; however it appears to be more specific. Indeed, it modulates the S1PR1 and S1PR5 receptors [72]. This confers to siponimod a better safety profile. Indeed, fingolimod, likely due to its binding to S1PR3, caused atrioventricular nodal block (a heart arrhythmia) and macular edema in some patients. Siponimod also blocks lymphocyte migration from lymph nodes resulting in a decrease of circulating auto-reactive lymphocytes [74]. Siponimod is indicated for relapsing or active secondary progressive MS.

Ocrelizumab: Ocrelizumab is a humanized monoclonal antibody approved for RRMS and PPMS. Like all monoclonal antibodies, is administrated intravenously It is the first drug approved for PPMS and also the first drug focusing on B-cell targeting [33]. Ocrelizumab blocks the CD20 glycoprotein present in most B-cell lineage, except for stem cells and antibody-secreting plasma cells. Therefore, it manages to deplete the circulating mature and immature B-cells by inducing antibody and complement-dependent cytotoxicity. Ocrelizumab efficacy in PPMS underlined how B-cells have an essential role in MS physiopathology, that is not limited to antibody secretion by plasma cells [33]. These findings also led to questions about the different physiopathology between the progressive form of MS and the RR form [79].

Natalizumab: This monoclonal antibody is an anti-α4-integrin receptor. The α4-integrin is present at the surface of lymphocytes, monocytes, and eosinophils. It interacts with a vascular VCAM-1 that is overexpressed on endothelial BBB cells in the context of inflammation. VCAM-1 and α4-integrin association is essential for lymphocytes to cross the BBB. Moreover, it has been reported that VCAM-1 and α4-integrin interaction also triggers activation of lymphocytes proliferation, and secretion of local cytokines that recruit more immune cells and further promote adhesion and

transmigration of these cells into inflamed tissues. Hence by blocking lymphocytes migration, lower immune cell infiltration in lesions and decreased neuroinflammation were reported [80]. Natalizumab is a high efficiency medication. Its downside however is that it has been linked with John Cunningham virus (JC virus) activation. The JC virus is ubiquitous in the population, generally benign for immunocompetent individuals but can be responsible for progressive multifocal leukoencephalopathy in immunosuppressed individuals. During phase 3 clinical trial, natalizumab triggered the activation of the previously dormant virus, inducing progressive multifocal leukoencephalopathy. For this reason, patients that are prescribed natalizumab are tested for this virus.

Alemtuzumab: Alemtuzumab is a recombinant humanized monoclonal antibody directed against CD52. CD52 is localized at T-cell, B-cell, and NK cell surfaces. Alemtuzumab binding to CD52 causes antibody-dependent cellular cytotoxicity and complement-dependent cytotoxicity [81]. Therefore, it activates pro-apoptotic pathways that lead to the depletion of T-and B-cells in the blood and lesions (according to the observation made in the EAE model) [81]. After treatment, a new population of T-cells and B-cells arises. A clinical study evaluated the new population of T-cells in patients after treatment. It showed that regulatory T-cells repopulated much faster and were more present in the Th2 phenotype, thus promoting the secretion of anti-inflammatory cytokines. Th1 and Th17 were slower to repopulate (3months vs. 12 months) and were present to a lesser extent in patients [81].

Cladribine: Cladribine is a small molecule analog of deoxyadenosine [70]. It is usually prescribed for highly active MS in case of other treatment failure and for active SPMS. Cladribine is a prodrug that needs to be phosphorylated to its active triphosphate form by intracellular deoxycytidine kinase. The deoxycytidine kinase is highly expressed in lymphocytes, favoring the selectivity of the drugs for these cells. Being a deoxyadenosine analog, it intercalates in the DNA and induces a strand breakage, resulting in cell death by apoptosis or autophagy [70]. Among the lymphocytes, B cells (CD19+) were depleted to a greater extent than T cells (CD3+, CD4+ or CD8+) and natural killer cells. In addition to lymphocytes depletion, this drug also impacted serum levels of ICAM-1 and E-selectin, two adhesion molecules that play a role in the entry of inflammatory cells into the brain of MS patients) [71].

Mitoxantrone: This molecule is an established cytotoxic antineoplastic molecule administrated intravenously and already used as treatment against several cancers (e.g., breast cancer and advanced prostate cancer, lymphoma, and leukemia) [75]. Mitoxantrone is a topoisomerase-2 inhibitor, an enzyme having a pivotal role in DNA replication. Consequently, mitoxantrone promotes DNA breakage and deterioration, resulting in cell death. In addition to being a cytotoxic

agent, this molecule has immunosuppressive properties via depletion of T-cell, B-cell, macrophages, and APC [75].

The choice of DMT by the physicians is mainly based on the efficacy/safety profile of the medicine, the patients' medical history, and the disease activity. There are different algorithms of treatment that physicians can follow to initiate treatment. For a while, IFNβ−1a and glatiramer acetate were considered first-line treatments due to their safety profile and their ability to be self-administrated [76]. Further, the traditional approach uses drugs of moderate effectiveness and then switches to an efficient compound when the illness activity increases. Nonetheless, nowadays, the paradigm has changed. Studies suggest that early use of high efficacy therapy such as ocrelizumab improves long-term outcomes. The following table summarizes DMTs' characteristics in their place in MS management (Table 2) [76].

Table 2. Overview of DMTs' characteristics approved for Multiple Sclerosis (adapted from Hauser et Al.)[76]ARR, annualized relapse rate; CDP, confirmed disability progression.

Drug	Mechanism of action	Indication	Route of and frequency of administration	Efficacy data	Common adverse events
Highly effective					
Ocrelizumab	Anti-CD20 mAb	RMS and PPMS (1st line)	IV infusion, every 6 months	RMS: Relative reduction in ARR compared with IFN-β- a:47% PPMS: Relative reduction in 12-week CDP compared with placebo: 24%	RMS: Infusion-related reaction, upper respiratory tract infection, headache, and urinary tract infection PPMS: Infusion-related reaction, upper respiratory tract infection, and oral herpes infection
Natalizumab	α4β1 integrin inhibitor	RRMS (2nd line)	IV infusion, every 4 to 6 weeks	Relative reduction in ARR compared with placebo: 68% Relative reduction in sustained disease progression compared with placebo: 42%	Fatigue and allergic reaction, JC virus activation Progressive multifocal leukoencephalopathy (PML)
Alemtuzumab	Anti-CD52 mAb	RMS (1st line)	IV infusion, once daily. During 5 days (year 1) and 3 days (year 2)	Relative reduction in ARR compared with placebo: 49–69%	Headache, rash, nausea opportunistic infections brain hemorrhage secondary autoimmunity, and fever

Mitoxantrone	DNA intercalator	RMS, SPMS (2nd or 3rd line)	IV infusion, every month or 3 months	Relative reduction in relapses compared with placebo: 61%	Dose-related cardiomyopathy, promyelocytic leukemia
Moderately effective					
Fingolimod	Sphingosine- 1- phosphate inhibitor	RMS (2nd line)	Oral, once daily	Relative reduction in ARR compared with placebo: 48–60%	Bradycardia, atrioventricular conduction block, macular edema, elevated liver-enzyme levels, mild hypertension,shingles, Herpes infections and PML
Siponimod	Sphingosine 1- phosphate receptor modulator	CIS, RMS, active SPMS (1st Line)	Oral, once daily	Relative reduction in 12-week CDP compared with placebo: 21%	Headache, nasopharyngitis, urinary tract infection
Dimethyl fumarate	Activation of the Nrf2 pathway	RMS (1st line)	Oral, twice daily	Relative reduction in ARR compared with placebo: 48–53%	Flushing, diarrhea, nausea, upper abdominal pain, decreased lymphocyte counts, and elevated liver aminotransferase

Cladribine	Not fully known	RMS (2nd or 3rd line)	Oral, 4–5 days over 2-week treatment courses	Relative reduction in ARR compared with placebo: 55–58%	Headache, lymphocytopenia, nasopharyngitis, upper respiratory tract infection, nausea, Shingles, cutaneous rash, hepatic cytolysis.
Modestly effective					
Teriflunomide	Dihydroorotate dehydrogenase inhibitor	RMS (1st line)	Oral, once daily	Relative reduction in ARR compared with placebo: 32–36%	Nasopharyngitis, headache, diarrhea, and alanine aminotransferase increase
Glatiramer Acetate	Not fully known	RMS (1st line)	SC injection, once daily or 3 times weekly	Relative reduction in ARR compared with placebo: 29%	Injection-site reactions
IFN-β	Not fully known	CIS and RMS (1st line)	SC injection, every 2 weeks	Relative reduction in ARR compared with placebo: 39%	Injection-site erythema, influenza-like illness, pyrexia, headache, hepatic cytolysis and lymphopenia

III.5. PROMOTING REMYELINATION: THE FUTURE OF MS THERAPIES?

As explained in section 1.2.5, myelin regeneration is crucial to restore saltatory conduction, metabolic support to axons, and preventing neurodegeneration. Thus, promoting remyelination in MS patients seems to be the next logical step to slow the evolution of the disease. Several animal models have shown that remyelination limits the development of disabilities. Extensive research on the process of remyelination led to the discovery of several signaling pathways in OPC or outside OPC (Fig.6). Here, we will review some of the significant compounds that showed promising preclinical results on animal models and completed their phase 2 clinical trial.

Opicinumab: Opicinumab is an antibody that targets LINGO-1, a protein expressed on OPC surface that is upregulated during MS. LINGO-1 downregulates OPC differentiation and myelination by activating ras homolog gene family member A (RhoA) and inhibiting protein kinase B signaling pathways [82]. Opicinumab promoted remyelination in animal models such as EAE [83, 84] and the cuprizone model [85]. Therefore, it was taken through clinical trials and reached phase 2 (RENEW study) [86]. The RENEW study was a double-blind, placebo-controlled trial in patients with the first episode of acute optic neuritis. Clinicians used a primary outcome the measure of the recovery in Visual evoked potential (VEP) latency after an episode of optic neuritis. VEP is used to evaluate the visual conduction pathways through the optic nerves and brain. In healthy patients, the VEP latency is about 100 ms, but when the optic nerve is damaged, as in optical neuritis, this latency is longer.

Regarding the secondary outcome, the thickness of the retinal nerve fiber layer (an optical coherence tomography parameter) was considered in the affected versus the unaffected eye. For both primary and secondary outcomes, no changes were observed between the treatment and placebo groups [86]. However, after a per-protocol analysis that implied the removal of the patients that did complete the study in the opicinumab-treated patient group, a significant improvement was seen over the placebo group [86]. With these results, a change of protocol was explored. In the SYNERGY study (NCT01864148), opacinumab was used in a dose-ranging study on RRMS and SPMS in association with IFN-β with different primary outcomes: ambulation (25-foot walk), cognition, and EDSS [87]. Although some functional improvements were observed for 10 and 30 mg/kg doses, none of the primary outcomes were met [87]. Thus, Biogen decided to discontinue opicinumab development.

Clemastine: Clemastine is a first-generation anti-histamine approved by the FDA for allergic rhinitis via its antagonism for the H1 receptor that also have an affinity for muscarinic receptor [88]. Its interest in MS was put forth in 2014 by Mei et al., who screened a micropillar array system

for high-throughput screening for possible therapeutics MS [89]. Their system used 96 well plates with micropillar to evaluate OPC capability to differentiate into myelinating oligodendrocytes that can wrap their membrane around the microarray, forming concentric myelin rings. They screened 1000 bioactive molecules, and upon automated detection and quantification of MBP immunofluorescent signal, they found that anti-muscarinic compounds could stimulate OPC differentiation, among which clemastine. Following positive preclinical results on the EAE model, the ReBUILD study (NCT02040298) was used to evaluate clemastine efficiency vs. placebo in RRMS patients and chronic demyelinating optic neuropathy [90]. The first group of patients was given clemastine for 60 days (10 mg), then a placebo for 90 days, and the second group the contrary. Results showed a significant decrease in the VEP latency. With those encouraging results, other trials are investigating the effect of clemastine at different doses, 12 mg/day for one week then 8 mg for 3 months (ReCOVER trial NCT02521311) and in a cohort with progressive MS (ReBUILD) [91]. In terms of safety profile, clemastine did not induce any life-threatening conditions, but patients under treatment experienced a high fatigue in the ReBUILD trial [90]. Although the results were promising, having an actual clinical trial that showed the efficacy over a placebo would be more relevant to proving clemastine efficacy on VEP latency reduction in individuals with a diagnosed MS and not only optical neuritis. In addition to clemastine, benztropine, another FDA-approved antagonist of the M1 muscarinic receptor, has shown promising results in EAE by stimulating remyelination and decreasing EAE score and favored remyelination in the cuprizone model [92]. However, for now, this molecule was not taken to a clinical trial for MS or optic neuritis. Nevertheless, these findings are interesting because they open the paths for discovering or designing new M1 antagonists' molecules that can be efficient to favor remyelination.

BEXAROTENE AND RXR AGONISTS: The retinoid X receptors family (RXR) are nuclear receptors that can either act as a homodimer (RXR/RXR association) or can bind to other receptors, for instance, retinoic acid receptors (RARs), thyroid hormone receptors, vitamin D receptors (VDRs), peroxisome proliferator activator receptors (PPARs) and liver X receptors (LXRs) as a heterodimer. These complexes bind to retinoic acid response elements (RAREs) and modulate the expression of genes involved in cell proliferation and differentiation [92]. The RXR complex then migrates to the nuclei and acts as a transcription factor. Several studies in animals showed that RXR agonists could promote remyelination. Huang et al. showed that in an LPC model, during remyelination, there was a rise of the RXR gene expression pathway [93]**.** A more thorough investigation showed that the expression of the RXR-03B3 receptor was up-regulated in cells of the oligodendroglial lineage. In addition, 9-cis-retinoic acid, an RXR and RAR agonist, induced

OPC differentiation *in vivo* [94]. Carradori et al. demonstrated that all-trans retinoic acid, a RAR agonist that leads to RAR heterodimerization with RXR, also promoted remyelination in an LPC-induced lesion in rats [95]. To investigate the RXR agonist effect on human remyelination [96], bexarotene, an FDA-approved molecule to treat skin lymphoma, was selected for a randomized, double-blind, placebo-controlled phase 2 clinical trial: the CCMR One study (registered in the ISRCTN Registry under 14265371) [97]. They used as a primary endpoint the change in mean lesional magnetization transfer ratio (MTR) between month 0 and month 6 for several lesions per patient. Lesional MTR is a parameter obtained via MRI that allows myelin integrity quantification that decreases in the demyelinated lesion. Unfortunately, in the CCMR One study, there was no statistically significant change in the mean MTR between the bexarotene and the placebo groups of all lesions combined. Surprisingly, when lesions were subdivided by location, bexarotene significantly impacted the cortical grey matter, deep grey matter, and brainstem lesions. Moreover, in per-protocol studies, bexarotene reduced VP latency compared to placebo in individuals that had have been previously affected by optical neuritis.

Nonetheless, the authors did not recommend using bexarotene as an MS treatment since its number of adverse effects was too high, in addition to the poor efficacy of treatment. Central hypothyroidism and hypertriglyceridemia were the main adverse effect observed. These events are the consequences of an off-target RXR agonist action. Hypothyroidism resulted from bexarotene binding to RXR present in thyrotrope cells in the pituitary gland, inducing TSHß gene expression and leading to a fall of TSH secretion and, consequently, T3 and T4 serum levels [98]. As for hypertriglyceridemia, bexarotene can bind to RXR that forms a heterodimer with LXRs, mainly expressed in the liver, thus inducing very-low-density lipoproteins (VLDL) production and up-regulated factors, angiopoietin-like protein three and apoCIII, that inhibits triglyceride hydrolysis [99].

As a rexinoid, calcitriol's (Cal) effect on remyelination is mediated by RXR. Cal binds to VDR, forming a heterodimer complex that up-regulates a series of genes involved in remyelination [100]. Cal and vitamin D have been investigated for a long time in the context of MS. Several preclinical studies depicted exciting data on the effect of high doses of vitamin D on remyelination in *ex vivo* brain slices [100] and *in vivo,* such as the cuprizone model [101] and LPC induced lesions model [101]. Furthermore, Cal has immunomodulatory properties on anti-inflammatory T-reg cells and decreases the difference of Th1 and Th17 cells in EAE models [102].

Nevertheless, despite these very encouraging results, most of the placebo-controlled clinical trials involving Cal or vitamin D intake kept on failing to achieve immunomodulation in MS and

remyelination [102]. These failures can be explained by a too low dose or a too-short treatment duration. Hence, several studies investigated different dose regimens, larger study groups, and longer treatment duration in the last years. In the Soilu-Hanninen et al. placebo-control study performed on RRMS patients [103], vitamin D3 was given to RRMS patients with an IFN-β1b. In one year, the patients under vitamin D supplementation showed fewer T2/T1 lesions and reduced disability accumulation than the placebo group [103]. However, no difference was observed between the two groups regarding the relapse rate. Camus et al. study also observed similar findings in a placebo-controlled two-year study with 100,000 IU vitamin D supplement per week [104]. Overall, to draw further conclusions on Vitamin D supplementation in MS management, additional studies need to be performed at different time/dose regimens. Nowadays, there are still some clinical trials that are ongoing to assess Vitamin D impact on MS patients

Although no therapy targeting remyelination reached the market, several clinical trials are ongoing as summarized in Table 3 [105].

Table 3. Ongoing clinical trial for remyelination therapies (adapted from Cunniffe et al.) [105].

Drug	Type of study	Primary outcome	Status/result
Liothyronine (MST3K, **NCT02760056**)	A phase I, randomised, double-blind, placebo-controlled, dose-finding trial of liothyronine sodium (L-T3) given for 1 week to people with any type of MS	Maximum tolerated dose of L-T3 as measured by hyperthyroid symptom scale	Completed. Results awaited
CNM-Au8 Nanocrystalline gold (**NCT03536559**)	A phase II, randomised, double-blind, placebo-controlled, parallel group study in 150 people with MS and evidence of chronic optic neuropathy	Multifocal visual evoked potential latency at 24 weeks	Recruiting
Domperidone (**NCT02493049**)	A phase II randomised, open-label, single-blind study of domperidone 10 mg three times daily in people with RRMS and new Gd-enhancing lesions	Texture analysis and MTR in enhancing lesions over 32 weeks	Ongoing
rHIgM22 (**NCT02398461**)	A phase I randomised, double-blind, placebo-controlled study of rHIgM22 compared to placebo in 27 people with RRMS following a relapse	Safety and tolerability end points	Completed.Results awaited

There is a list of reasons that could explain why these trials were not successful: (1) low bioavailability due to drug degradation, (2) failure to cross the BBB, (3) inadequate route of administration, and (4) debilitating adverse events. These criteria are obstacles to an optimal pharmacological effect of a drug, partially explaining why no putative pro-remyelinating molecules met their primary outcome in their respective clinical trials. Hence, having an optimal biodistribution of these drugs into the CNS and, more specifically, to OPC could tremendously increase treatments efficacy. Therefore, there is a need to develop strategies to 1) protect these molecules against degradation, 2) increase their transport across the BBB to improve their delivery in the CNS, 3) improve their solubility, 4) deliver them precisely to OPC and limit off-target effect. These hurdles may be overcome by using advanced drug delivery techniques such as drug-loaded nanoparticles.

IV. LIPID NANOMEDICINES

The COVID-19 pandemic is the perfect example of how nanomedicines can be used to develop efficient vaccines. The mRNA spike protein of the SARS-CoV2 virus has been encapsulated in lipid-based nanoparticles to prevent degradation of the vaccine mRNA. Therefore, these nanoparticles facilitated an optimal delivery to the cells to express the spike protein that encounters T-Cell that triggers the start of the humoral immune response, protecting the individual against future exposure to the SARS-CoV2 virus. As these lipid-based nanoparticles have been efficient in playing their part in the Pfizer© and Moderna© vaccines, we believe nanoparticles can be a safe choice to deliver a pro-remyelinating lipophilic drug specifically to OPC. Further, functionalizing their surface to make them specific to OPC and avoid adverse side-effects, as the hypothyroidism observed with bexarotene, can be an innovative approach. In the second part of this thesis introduction, we will focus on lipid nanomedicines, specifically Lipid nanocapsules (LNC), and how they can be of use for remyelinating treatments in MS.

IV.1. OVERVIEW OF LIPID NANOMEDICINES

(adapted from the review of surface modification of lipid-based nanoparticle, under revision for ACS Nano)

Among the vast array of nanomedicines, lipid-based nanoparticles are some of the most popular. For instance, liposomes were used to formulate Doxil®, the first FDA-approved product based on nanomedicine, to improve the safety profile of doxorubicin. Lipid nanoparticles present several advantages that make them attractive when nanocarriers are needed. Lipid nanoparticles are biodegradable and biocompatible and present low immunogenicity. Their lipid components allow efficient lipophilic drugs encapsulation, which is critical as the proportion of new lipophilic drugs increases. These nanoparticles' size and surface properties can be easily tuned using lipids with different physicochemical characteristics, such as their molecular weight, charge, and lipophilicity.

Over the last several decades, the array of lipid-based nanoparticles has rapidly expanded. In this section, the main types of lipid nanoparticles will be briefly introduced, i.e., nanoemulsions (NE), liposomes, solid lipid nanoparticles (SLN), nanostructured lipid carriers (NLC) [106-109], lipid nanocapsules (LNC), and lipid–polymer hybrid nanoparticles (hybrids) (Fig.11). NEs are colloidal dispersions prepared by combining water, oils, and surfactants, with the most important NEs being self-nanoemulsifying drug delivery systems (SNEDDS) for oral drug delivery [110]. Liposomes are composed of a phospholipid bilayer that surrounds an aqueous core, thereby being suitable for

encapsulating lipophilic, hydrophilic, and amphiphilic cargoes [111]. SLN and NLC can be classified as solid core nanoparticles. They both have a strong protective effect on the incorporated therapeutics[107, 112]. LNC present a lipoprotein-like structure organized with an internal liquid or semiliquid oily core and an external PEGylated rigid membrane [113]. Hybrids are more novel core-shell lipid-based nanostructures that combine a polymeric core encapsulating a payload and a phospholipid shell (e.g., a lipid-polyethylene glycol (PEG) layer). Hybrids can display the merits of both systems (liposomes and polymeric nanoparticles) [114-119]. The detailed preparation techniques, physicochemical properties, and pharmacological applications of these lipid nanoparticles have been reviewed elsewhere [116, 120, 121].

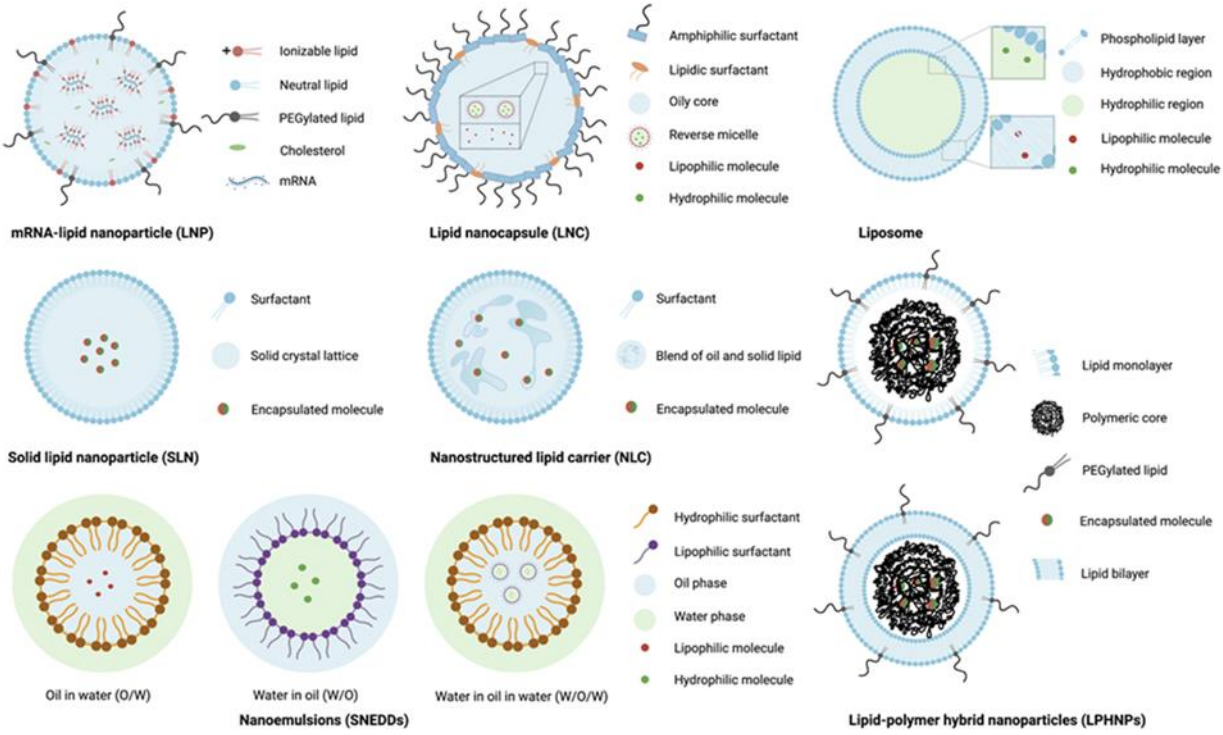

Figure 11. Structures of different types of lipid-based nanoparticles

Focus on LNC

Among lipid nanoparticles, LNC are particularly interesting since they are described as a hybrid between polymeric nanocapsules and liposomes because of their oily core surrounded by a rigid membrane [122]. LNC can have a tunable size below 100 nm, which will allow them to pass epithelium fenestration [113]. LNC has an oily core composed of Labrafac® WL 1349, a triglycerides liquid mixture, a shell composed of an amphiphilic surfactant (Kolliphor HS®15; a PEG mixture of PEG 660 and PEG 660 hydroxy stearate) and of a lipid surfactant, named Lipid® S100 (a mixture of phosphatidylcholine from soybean). Our laboratory uses this composition to

formulate LNC, but the protocol can vary and include other triglycerides (as Captex® 8000) or lipid surfactants. LNC is an ideal nanocarrier to deliver lipophilic drugs that are insoluble in physiological solutions. Encapsulating these molecules in LNC increases their solubility since, after encapsulation, the LNC formulation is miscible in a saline-based solution (0,9% NaCl) and can be administrated intravenously. Moreover, LNC can protect the drug from enzymatic degradation; in line with this characteristic, hydrophilic compounds can also be encapsulated in LNC via an inverse micelles protocol [123]. In these scenarios, LNC are more used for drug protection instead of their "anti-degradation" properties since they can prevent drug enzymatic degradation (i.e cytochrome metabolization). Their PEGylated capsule can shield them from enzymatic degradation and opsonization by the immune cell system, increasing their half-life. LNC are polyvalent nanocarriers. As their surface can be functionalized with peptides or antibodies to enhance cell internalization they can be of use to target specific cells [124], but they can also serve as carriers for several types of bioactive molecules (i.e., cytotoxic, nucleic acids) or theragnostic agents (e.i fluorescent dyes and radioactive molecules) [113].

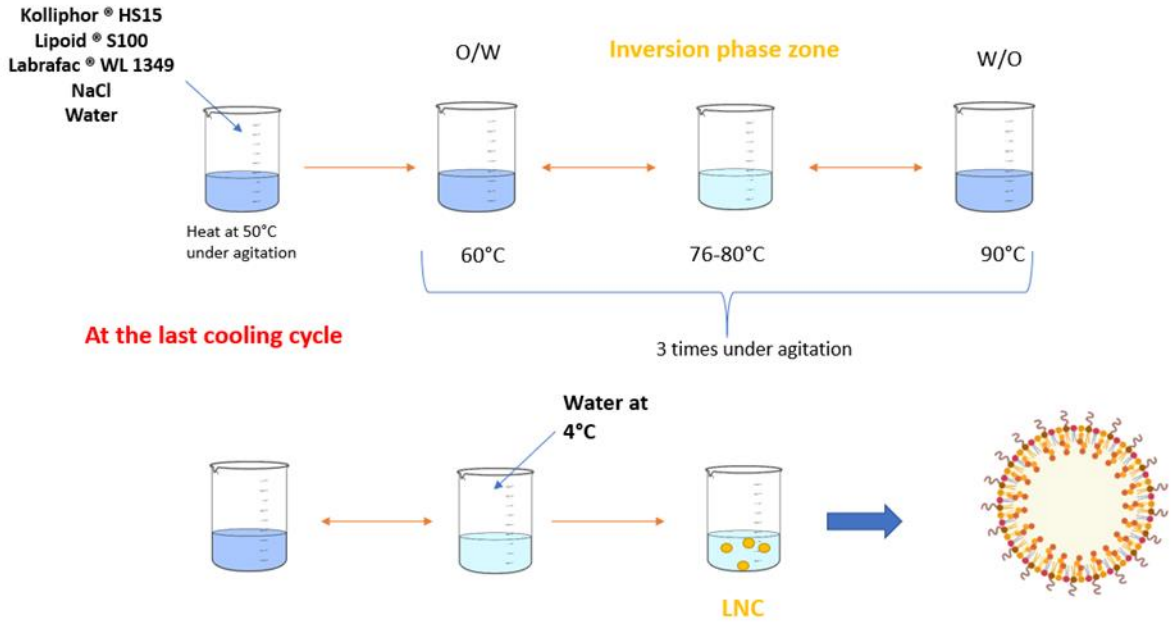

Figure 12. LNC production based on the phase inversion method.

Briefly, 0.846 g of Solutol HS15, 0.075 g of Lipoïd®, 0.089 g of NaCl, 1.028 g of Labrafac® and 2.962 ml of water were mixed under magnetic stirring for 5 min at 50 °C. Next, three temperature cycles of heating/cooling were done between 60 °C and 90 °C, also under magnetic stirring. During the cooling of the last cycle, at the PIT , 12.5 ml of cold water (4°C) were added, under high-speed stirring.The resulting LNC are filtered with 0.2 µm filter and stored at 4°C.

One of LNC's most significant advantages is its solvent-free production process. Briefly, Labrafac, Kolliphor HS 15®, Lipoid®, NaCl, and Milli-Q water are mixed at 50°C allowing all these

components to mix. Next, three temperature cycles are made under stirring, going from 60 to 90 °C. During these cycles, there is a change in Kolliphor HS®15 solubility, impacting the emulsion type. At high temperatures (>80°C), it is lipophilic (dehydration of the polyoxyethylene chains), forming a water in oil (W/O) emulsion, while at low temperatures (<60°C), it is hydrophilic forming an oil in water (O/W) emulsion (Fig.12)

At the phase inversion temperature (PIT) that occurs around 77 C°, there is a balance between the W/O and the O/W emulsion that can be visually recognized by its transparency [125]. At this precise moment, cold Milli-Q water is added to the formulation, allowing a fast cooling that breaks the microemulsion system present at the PIT and forms stable nanocapsules [113] (Fig.12).

To encapsulate lipophilic molecules inside LNC, two strategies can be used: 1) the bioactive compound can be directly solubilized in Labrafac at the beginning of the process or 2) the bioactive compound is solubilized in an organic solvent (such as ethanol in a very high concentration) and then added at the last cooling cycle under stirring just before the PIT. LNC preparation can be easily scaled up for industrial production. In 2013, a pilot study to scale-up LNC and Ibuprofen loaded-LNC was conducted at Angers University. The test was successful, and LNC stability and Ibuprofen encapsulation efficiency were assessed. LNC size, zeta potential, and polydispersity index (PDI) did not significantly vary in 12 months with the scale-up process, and ibuprofen encapsulation efficiency was superior to > 97%, which is similar to the lab process.

Nowadays, two types of lipid nanocarriers are approved by the FDA and the EMA: liposomes and lipid-based nanoparticles (LNP) [126]. The former was introduced in the 90s, with Doxyl®, a doxorubicin loaded-liposome formulation, and the latter in 2018, with Onpattro®, a siRNA loaded in LNP for the treatment of polyneuropathy in patients with hereditary transthyretin-mediated amyloidosis. LNC has some advantages summarized in Table 4 [118] compared to these lipid formulations.

Table 4. Advantage and drawbacks of LNC and FDA-approved lipid-based nanomedicines (adapted from Thi et al.) [126].

Name	Composition	Size	Advantages	Drawbacks
Liposome	Phospholipid, cholesterol, essential oils	10-1000 nm	- -Drug protection - -Controlled release, - -Encapsulation of lipophilic and hydrophilic therapeutic agents - -High bioavailability, and biodistribution	- -Not crossing the stratum corneum barrier - -Rigid structure - -Moderate encapsulation of lipophilic drugs - -Process of fabrication involves organic solvent
LNP	Solid and liquid lipids (fats and oils), surfactants	50–1000 nm	- -Biocompatible and biodegradable ingredients - -High cell uptake - -Good protection of drugs - -Long shelf life - Ease of drug entrapment	- Optimization required of the ratio of solid/liquid lipids
LNC	Solid and liquid lipids (lecithins and tryglicerides), surfactants	20-100 nm[113]	- -Same as Liposomes + higher enhancement of the solubility of hydrophobic therapeutic agents - -Solvent free process[113]	- Multi-step Process [113]

Another attractive feature of LNC is the possibility of modifying their surface with targeting moieties to achieve selective, cell-specific targeting. The goal behind cell-targeting is to maximize the distribution of the bioactive compounds but in the desired cell to 1) maximize the therapeutic effect and 2) limit the off-target effect on other cell types and organs, which can result in adverse effects. In other words, these strategies aim for a better efficacy and safety profile of nanomedicines. In the next paragraph, we will discuss the targeting strategies and the different technics that have been used in the literature to tailor lipid nanocarriers.

IV.2. CELL TARGETED NANOMEDICINE

Targeted nanomedicine has been the "magic bullet" dream of nanoscale drug delivery systems [127, 128] to recognize actively, bind to, and be taken up by the targeted cell population. Specific cell targeting is achieved by linking a ligand to the surface of a nanoparticle. This ligand molecule should recognize another molecule, such as a receptor, present in the targeted cells in a selective or specific manner.

IV.2.1. Ligands

The choice of the ligand is crucial. Antibodies are obvious ligands, as their function is to target a specific antigen. Alternatives include antibody fragments, nanobodies, other types of proteins, peptides, aptamers, oligonucleotides, and small molecules such as folic acid or carbohydrates [129, 130]. Each ligand has its pros and cons (Table 5), and a particular ligand should be selected according to the targeted cell type, the lipid nanoparticle and the range of molecules available.

In addition to antibodies, smaller fragments, peptides and aptamers have been developed to replace full-size antibodies. Peptides can recognize specific receptors such as integrins with the arginine-glycine-aspartate (RGD) peptide or improve cell penetration when positively charged (cell-penetrating peptides). Aptamers are short single-stranded nucleic acid sequences with more affinity and selectivity for their designed antigen than antibodies that are heat-stable and nonimmunogenic. The main polymeric ligand is HA, which targets the CD44 receptor that is overexpressed in many cancer cells, such as ovary cells [131]. Finally, small molecules include sugars, such as mannose against dendritic cells or folate used for cancer targeting.

Table 5. Lipid nanoparticle targeting ligands (a non-exhaustive list).

Ligand (example)	Size	Advantages	Disadvantages
Proteins			
Antibody (Trastuzumab, Rituximab)	150 kDa	Available for a large range of antigens, selectivity improvement by protein evolution[132], good specificity	Large, unstable, immunogenic, need of proper orientation
Fab [133]	50 kDa	Vs. antibodies, smaller, more stable, less immunogenic, same targeting capacity	
scFv[134]	25 kDa		
Nanobody[135]	12-15 kDa		
Affitin/affibody[136]	<10 kDa		
Transferrin	80 kDa	-	
Peptides[130]			
RGD[137]	350 Da	Vs proteins, smaller, more stable, modulable immunogenicity, easier production	Limited colloidal stability
CPP (R6H4[138]	1.5 kDa		
TAT[139])	1.6 kDa		
Aptamers [130]			
AS1411[140], Transferrin receptor targeting	10 kDa	Very high affinity and specificity heat-stable, non-immunogenic, nucleic acid chemistry	Faster biodegradability
Polymers			
HA[141]	5-1500 kDa	Adjustable size and density	Limited targets
Small molecules[130, 142]			
Mannose	180 Da	Vs macromolecules, more stable	Low choice, limited targets
Folate	441 Da		

CPP: Cell-penetrating peptide; Fab: Fragment antigen-binding; HA: Hyaluronic acid; scFv: Single-chain variable fragment

IV.2.2. Grafting of ligands onto lipid nanoparticles

Grafting of ligands onto lipid nanoparticles must 1) maintain the integrity and functionality of the ligand as well as of the nanoparticle; 2) expose the ligand at the surface of the particle; 3) stabilize the ligand in the blood and biological medium, and 4) preserve the affinity of the ligand for its target. Ideally, the grafting technique should present the following characteristics: i) stereospecificity to control the localization of the conjugation on the ligand and to ensure that the ligand is oriented outwards; ii) simplicity and reproducibility; iii) easy scale-up and characterization, and iv) a high yield to limit costs [133]. The methods used to graft targeting ligands onto liposomes have been previously reviewed [143].

IV.2.3. Noncovalent grafting

Lipid nanoparticles do not usually present reactive groups on their surface and do not tolerate organic solvents after being formulated. Moreover, chemical reactions add some complexity and the risk of destabilization of the nanoparticles. Therefore, noncovalent techniques have been developed to decorate lipid nanoparticles with targeting ligands (Fig.13).

A common form of noncovalent grafting is the integration of a lipid anchor into the lipid nanoparticle during formulation. This lipid anchor is often previously coupled with a polymer, such as PEG as a spacer, with a terminal reactive group to react with the ligand [144]. Such lipid anchors include i) phospholipids, with the most popular being 1,2-distearoyl-sn-glycero-3-phosphatidylethanolamine (DSPE)[145, 146]; ii) cholesterol [144, 146]; or iii) a single fatty chain, such as stearate [145, 147, 148].

Alternatively, lipid anchors can be post-inserted once nanoparticles have been formed. Post-insertion into lipid nanoparticles is time-, temperature-, and lipid concentration-dependent[149, 150]. However, this method is widely used because the insertion is stable and easy to perform. Conditions can be optimized by adjusting the temperature and the ligand/lipid ratio [151]. Post-insertion has been mainly used for liposomes[145, 152, 153], but it has also been adapted with success to phospholipid nanomicelles [154], lipid-coated polystyrene nanoparticles [109], LNC [155], and exosomes using sonication to increase the efficacy of the post-insertion [156]

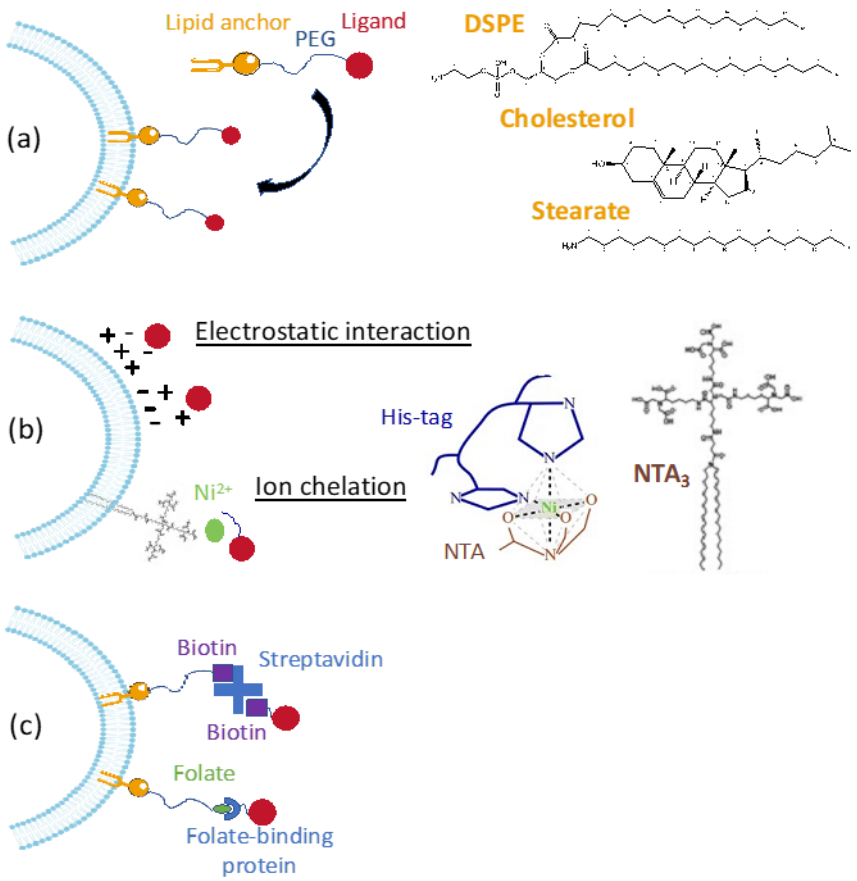

Figure 13. Noncovalent grafting techniques
(a) Lipid anchor inserted in the membrane during formulation or by post-insertion and examples of lipid anchors. (b) Ionic interaction by electrostatic or NTA-Nickel-His-Tag chelation. (c) Biological interaction by streptavidin-biotin or folate-folate binding protein.

Ionic interactions have been used to adsorb targeting ligands on the surface of lipid nanoparticles (i.e., electrostatic adsorption and chelation). Ionic interactions are quite weak, and biological media can induce their dissociation or ion exchange [157]. Therefore, multiple ionic interactions are needed. The objective is to pair up a charged nanoparticle with an oppositely charged ligand. This is the simplest method when feasible, as it does not need a chemical reaction. By default, lipid nanoparticles tend to have a slightly higher negative surface charge [138, 158]. Therefore, it is possible to adsorb a positively charged ligand, such as a cell-penetrating peptide, to the surface of a lipid nanoparticle. Another strategy is to add a cationic lipid surfactant to the formulation to produce positively charged nanosystems that can then interact with a negatively charged ligand [159, 160]. As a drawback, cationic nanoparticles can be toxic and are quickly cleared from the blood [138, 161]. Therefore, ideally, the nanoparticle surface charge should be neutralized by the adsorption of the negative ligand before IV administration. Ionic interactions can also be used for chelating strategies. It is indeed possible to create a stable noncovalent binding between nitrilotriacetic acid (NTA), nickel (Ni^{2+}), and a His-tag coupled to the targeting ligand by aqueous

incubation at room temperature [162]. However, Ni-based chelation is unstable after IV administration and the associated ligand can be lost by competition with endogenous proteins, or endogenous chelators can remove the nickel [162, 163]. Ni-NTA has thus been replaced by porphyrin-phospholipid to create a metallo-porphyrin-phospholipid bilayer in the presence of $cobalt^{(II)}$ ions, resulting in more stable binding with His-tagged proteins [163], [164], and improving the final coupling yield by spatial interaction. Biological interactions can also be used for the non-covalent coupling of ligands. The advantages are that conjugation happens in physiological media with good specificity. The biological interaction with the highest affinity and most stability is between biotin and streptavidin. The last technique, which does not require a chemical reaction, is gene engineering. Indeed, exosomes can be produced via previous transfection of the exosome-producing cells with a vector associating lamp2b, an exosomal membrane protein, with the desired targeting peptide [165, 166]. The produced exosomes then have a targeting ligand at their surface without the need for further modifications.

IV.2.4. Covalent grafting

Noncovalent grafting offers several advantages for the targeting of lipid nanoparticles, but the links it creates can be less stable and versatile than covalent coupling [129, 144]. A covalent link is the result of a reaction between the ligand and a head reactive group at the end of a PEGylated lipid [129]. To be compatible with fragile ligands, the reaction should be in an aqueous solvent and free from side-product formation, such as ligand-ligand or particle-particle association. Meeting these criteria significantly reduces the number of chemical reactions that can be used. We consider here the direct covalent coupling between a preformed lipid particle and the targeting ligand, but the same reactions can be used to link the ligand with a lipid polymer before formulation or post-insertion [129] (Fig.14).

Amide bond coupling between an amine and a carboxylic group is one of the most popular techniques to form a covalent link between a ligand and a lipid nanoparticle [167]. It is used for nanoparticles showing either carboxylate or amine moieties. *para*-Nitrophenylcarbonyl (pNP) can also be added to the formulation to react with primary amines in an aqueous buffer between pH 8 and 9.5. This reaction does not need any adjuvant molecule or special conditions, except a pH change [168]. Forming a thioether bond has also been used to attach a targeting ligand. Usually, a linker bearing a maleimide group reacts specifically with thiols in the pH range of 6.5-7.5 by a Michael addition reaction [167]. The ligand must contain a thiol group via a cysteine or by thiolation using e.g. Traut's reagent (2-iminothiolane). This reagent is a cyclic imidothioester that can react

with primary amines at pH 7-10 in a ring-opening reaction to exhibit a free sulfhydryl group [133]. *N*-Succinimidyl 3-(2-pyridyldithio)propionate (SPDP) can also be used to add a thiol group.

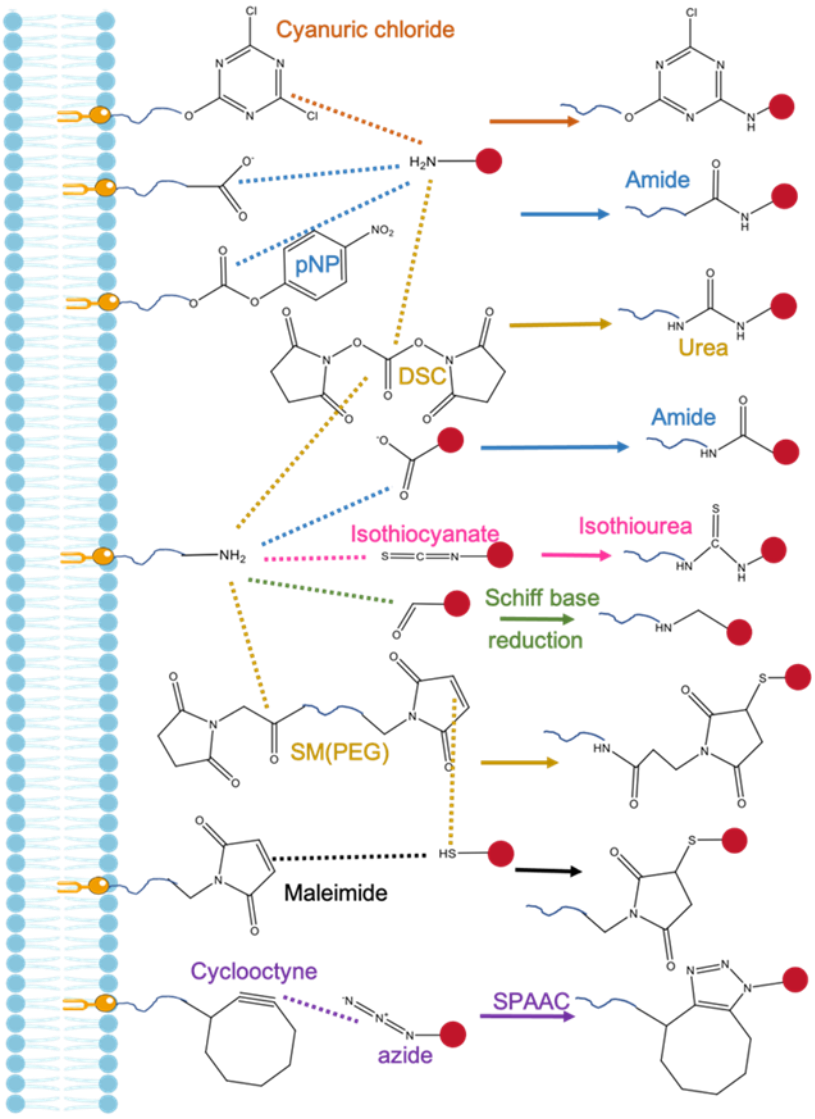

Figure 14. Covalent grafting techniques.

pNP: para-nitrophenyl; DSC: N,N'-Disuccinimidyl Carbonate; SM(PEG): succinimidyl-[(N-maleimidopropionamido)-tetracosaethyleneglycol] ester; SPAAC: copper-free strain-promoted cycloalkyne−azide cycloaddition

The *N*-succinimidyl portion reacts with amine groups, whereas the pyridyldithiopropionate moiety can be reduced to a thiol by tris(2-carboxyethyl) phosphine hydrochloride (TCEP) or dithiothreitol (DTT). Once the ligand has reacted with the maleimide moiety, it is advised to inactivate he remaining maleimide by adding cysteine [169]. Another strategy is to use a cross-linking agent that will successfully bind to lipid nanoparticles and ligands thanks to two adapted reactive groups. The cross-linking agent can be homobifunctional or heterobifunctional. The latter option has the

advantage of preventing homologous ligations between two lipid nanoparticles or ligands. A wide variety of commercial cross-linking agents is available [133]. Two other bonds can also be created by reacting with an amine group on the lipid nanoparticle surface. The formation of a labile Schiff base with an aldehyde group can be further reduced to produce a stable secondary amine bond [170], while reaction with an isothiocyanate produces an isothiourea bond [171]. Stable triazole bonding is obtained by click chemistry with copper-free strain-promoted cycloalkyne−azide cycloaddition (SPAAC) based on the Cu(I)-catalyzed Huisgen 1,3-dipolar cycloaddition of azides to terminal alkynes. In aqueous medium, this reaction is orthogonal against other biological functional groups and proceeds in good yield. Finally, cyanuric chloride is a reagent with three aromatic chlorides that can react by nucleophilic substitution at basic pH. Each substitution requires specific temperature and time conditions, allowing selectivity. No derivatization is necessary, and unmodified proteins will be coupled by nucleophilic amino acids [133]. Other techniques, such as disulfide bond or hydrazone bond formation, have been used in the past. Disulfide bonds are unstable in reducing and acidic environments [172], and hydrazone is also sensitive to hydrolysis. Active ligand targeting is not the only way to achieve cell targeting. For instance, a lipid nanoparticle's main constituents can help selectively deliver its cargo to a targeted population. As an example, cholesterol-based NLC show selectivity towards overexpressing low-density lipoprotein (LDL) receptor cells, such as some tumor cells [173]. In this case, cholesterol is not exposed at the surface but constitutes 60% of the NLC excipients. The same LDL receptor was recently used in a study where squalene-based nanoparticles were designed to interact with lipoproteins and be carried towards tumors by LDL [174]. Therefore, there is a place for innovative strategies for tissue and cell targeting.

Lipid-based nanoparticle surface decoration has not only been used for cell-targeting, but it has also been investigated for crossing biological barriers such as the BBB. Crossing this barrier to get the bioactive molecule to the CNS is one of the biggest challenges encountered by MS therapies delivery and all other CNS diseases.

The BBB is an anatomical barrier that protects the CNS composed of endothelial cells, tight junctions, pericytes, astrocytes, and neurons (Fig.15) [175]. Therapeutic compounds commonly administered intravenously or orally need to pass through the BBB to reach the CNS and generally display very low availability [122]. Nanomedicines can improve drug availability, but even then, their crossing of the BBB is not very efficient. This is the reason why nanoparticle surface modification strategies have been proposed. The two major surface modifications that have been applied to lipid nanoparticles are based on either cationic polymer adsorption or grafting of a ligand that will interact with a receptor-based on the endothelium to highjack receptor-mediated

endocytosis. For the latter, transferrin, lactoferrin, insulin and low-density lipoprotein receptors (LDLRs) have mainly been targeted [176]. One of the most popular strategies targets the transferrin receptor (TrF), highly expressed on BBB endothelial cells [124], or the LDLR. LDLs enter the CNS by binding to this receptor, followed by transcytosis [177]. Examples of nanoparticle surface modification aiming for TrF or LDLR are collected in Table 4. A less usual strategy was proposed by Hui et al. They used borneol, a bicyclic monoterpene extracted from *Dryobalanops aromatica,* at the surface of SLNs to open the BBB tight junctions [175].

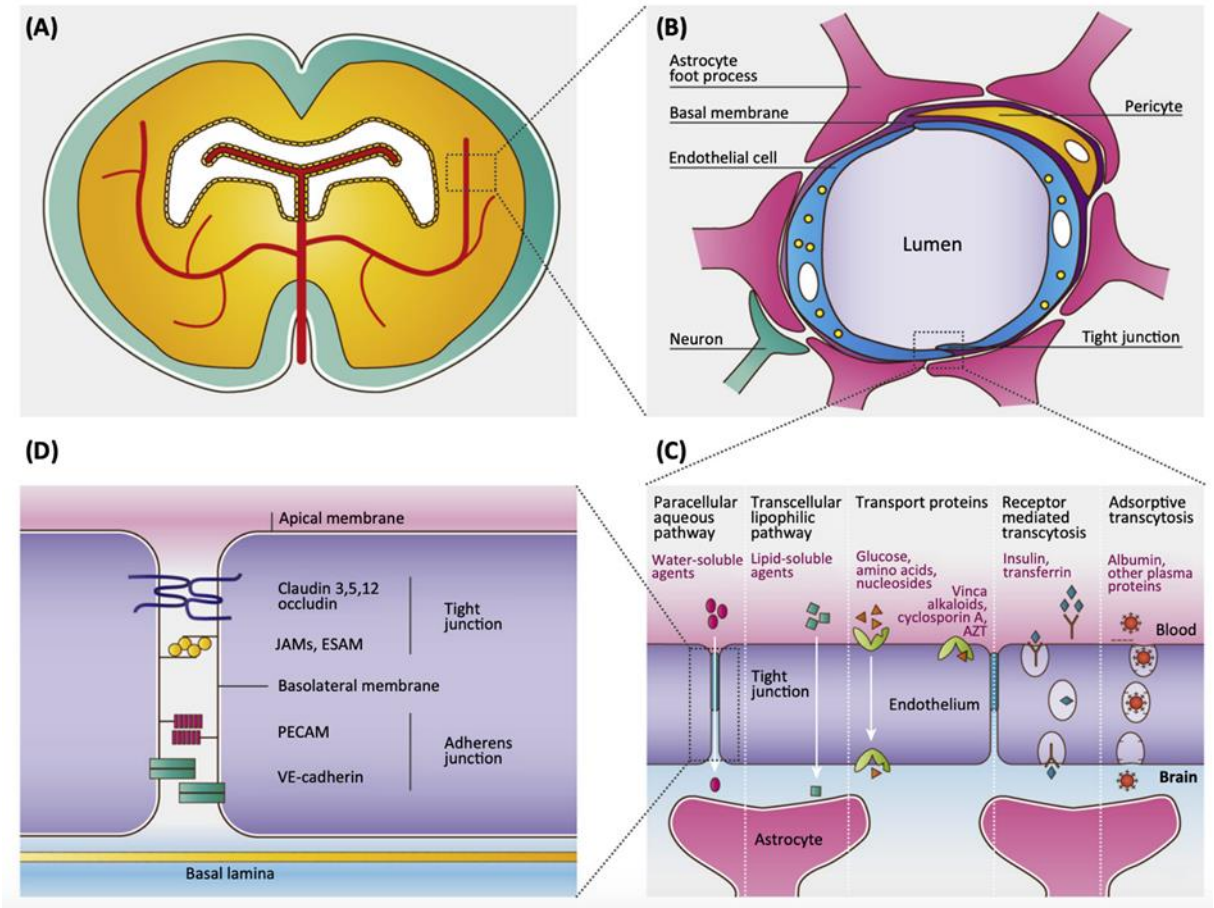

Figure 15. A schematic representation of the blood–brain barrier and pathways across this barrier [178]

(A) Brain barriers. The brain has several barriers, including (1) the BBB, (2) the outer blood–cerebrospinal fluid (CSF)–brain barrier, and (3) the blood–CSF barrier. (B) BBB structure. The BBB is formed by endothelial cells that are in close association with astrocyte end feet and pericytes (C) Routes for molecular trafficking across the BBB are shown. Hydrophilic compounds can only pass through tight junctions of the BBB, which ultimately limits their penetration in the brain. Large molecules, such as insulin and transferrin, require receptors, whereas small molecules require carrier-mediated transport to move across the barrier. On the other hand , small lipophilic molecules can pass the BBB via passive diffusion. (D) Tight junctions. Tight junctions are typically located on the apical region of endothelial cells. The tight junctions form complex networks that result in multiple barriers that restrict the penetration of polar drugs into the brain. AZT= azidothymidine

As specific targeting moieties used to decorate lipid nanocarrier's surface often target receptors, these nanocarriers are often related to receptor-mediated endocytosis mechanisms. As example, transferrin functionalized nanoparticles are known to be internalized via clathrin-mediated endocytosis. Clathrin-mediated endocytosis is one of the many internalization routes that functionalized nanomedicine can take. In the following paragraph, we will discuss nanoparticles uptake by cells and why it is primordial to understand the endocytosis process used by nanocarriers.

Table 4. Examples of lipid nanoparticle surface modifications for BBB targeting.

Nanocarrier	Surface modification	Grafting technique	Modification outcome	References
Target Transferrin receptor				
cationic solid lipid nanoparticles	OX26	Thiol-maleimide reaction	Enhancement of the PK profile of Baicalin in the cerebrospinal fluid	[179]
LNCs	OX26	Thiol-Maleimide	In vitro: LNC-OX26 interacted with cells expressing TrF	[124]
Liposome	Transferrin receptor DNA aptamere	Thiol –maleimide reaction	Better accumulation of DAL-TRAM in the brain parenchyma than non-coated liposome.	[180]
			reduce cocaine-induced hyperlocomotion better than the non-coated liposome *in vivo*	
Liposome	RI7217	Thiol-Maleimide or Avidin-biotin	enhancement on permeability value on BBB in vitro model hour after hour. No control (	[181]
			hCMEC/D3 cell monolayers).	
			Confocal microscopy. after 2h incubation	
SLNs	OX26	Thiol-Maleimide	Permeability enhanced in vitro (ECs) derived from hematopoietic stem cells	[182]
Tight junction opening				
SLNs	Borneol	Amide reaction	-enhancement on permeability value on BBB in vitro model	[175]
		with succinic anhydride as the linker.	-enhancement of the HBMEC cell uptake.	
			-higher and faster accumulation in the brain.	
Target LDLR				
SLNs	Apolipoprotein E	Avidin-biotin	enhancement on permeability value on BBB in vitro model (	[183]
			hCMEC/D3 cell monolayers)	
Combination strategy				
Liposome	ApoE, anti-TfR and TREG	Thiol-Maleimide	In vivo: multi-functionalized liposome has a higher penetration in the brain compared to the dua labeled ApoE and anti-TrF liposome	[184]

IV.3. LIPID NANOMEDICINE ENDOCYTOSIS BY CELLS

One can think that the higher the accumulation of a drug-loaded nanoparticle in the cell, the higher the biological effect, but things are not that simple. In Malfanti et al.'s study, folated polyplexes nanoparticles had lower cell uptake by the breast cancer cell line MDA-MB-231 than their unfolated counterparts [185]. However, when the biological effect of these siRNA-loaded polyplexes was assessed, the unfolated formulation was more efficient in silencing the genes of interest. After investigation, they found that the folated polyplexes escaped lysosomes fusion hence degradation, and were internalized via caveolin pathway, explaining their efficacy. Hence, a better knowledge of the fate of nanoparticles at a subcellular level is crucial to achieve efficient drug biodistribution. Furthermore, it is essential to understand how they are internalized by the cells of interest to predict their subcellular fate. Indeed this will allow adapting the surface modification strategy based on the endocytosis mechanism.

Depending on the localization (i.e., cytoplasmic, nuclear, mitochondrial) of the target of the drug that has to be delivered, some endocytosis pathways are more beneficial than others. There are five main endocytosis pathways: (1) phagocytosis, (2) macropinocytosis, (3) clathrin-dependent endocytosis (4) caveolin-dependent endocytosis (5) clathrin- and caveolin-independent endocytosis (Fig.16) [186]. Each of these endocytosis pathways is linked to a distinct intracellular trafficking mechanism. Nanoparticles endocytosis by cells remains quite complex to solve since it depends on several factors such as the size, shape, surface charge, and composition of the nanoparticles. In addition to these criteria, nanoparticles endocytosis is also cell-dependent.

IV.3.1. Endocytosis pathway

Phagocytosis

Phagocytosis mainly involves pathogen and cell debris or non-endogenous material clearance by immune cells triggered by cell surface receptors such as Fc receptors or complement receptors. Nanoparticle clearance is mainly mediated by opsonization and adsorption. After internalization, nanoparticles are found in phagosomes that later fuse with lysosomes, giving birth to a new structure: the phagolysosomes [186]. The content of phagolysosomes is then enzymatically digested; thus, the nanoparticle should avoid this internalization route. Adding PEG chains at the surface of nanoparticles is one of the most common strategies to limit nanoparticle opsonization. However, the disadvantage of this strategy is that with repeated administration PEG immunogenicity may increase, leading to the production of anti-PEG antibodies directed towards these nanoparticles leading to loss of therapeutic efficacy [187].

Macropinocytosis

Macropinocytosis is also a non-specific endocytosis pathway that primarily relies on the uptake of extracellular fluids and solutes but includes other elements such as nanoparticles [188]. After signaling, the cell membrane extends itself through an action-stabilized mechanism to engulf fluids or other elements (for this matter, nanoparticle). Following internalization, nanoparticles are in a large vesicle called macropinosomes (up to 1,5 μm) that can also fuse with the lysosomes [186]. The advantage of macropinosomes is that they are leaky; therefore, nanoparticles could more easily escape them and be released in the cytoplasm.

Clathrin-dependent endocytosis

Clathrin-mediated endocytosis is a receptor-mediated endocytosis pathway often involved in surface-modified nanoparticle internalization. It is activated when ligands bind to their cell membrane receptors. For example, transferrin receptors and low-density lipoprotein receptors are involved in clathrin-dependent endocytosis [186]. Upon binding of the ligand, a clathrin-coated pit is formed. This step induces plasma membrane bending and invagination followed by scission of the upper part of the invagination to form an intracellular vesicle. Clathrin proteins unbound themselves from the vesicle that will fuse with an endosome. Later, this endosome will mature to a late endosome and either fuse with a lysosome for degradation or be recycled to the surface (mechanism involved in cell membrane receptors recycling) [186].

Caveolin-dependent endocytosis

Caveolin-mediated endocytosis is another receptor-mediated type of endocytosis. The process is more or less similar to the clathrin-dependent pathway, except that the pits are coated with caveolin proteins. The vesicle formed afterward is called caveosome [186]. This kind of vesicle is typically trafficked through the cytoplasm to the Golgi apparatus or the endoplasmic reticulum. Hence comparatively to the clathrin-dependent endocytosis, transportation via caveosome seems to avoid degradation or exocytosis, making the caveolin endocytosis pathway particularly interesting if the drug of interest needs to be delivered to the cytoplasm or organelles. Of note, caveosomes can also merge with lysosomes and can be degraded. As reviewed by Donahue et al., nanoparticle surface modification with folic acid, albumin, and cholesterol seems to favor this kind of endocytosis [186]. Moreover, it seems that this type of endocytosis in epithelial cells results in transcellular transportation of caveola, making this type of endocytosis also interesting for crossing barriers. Hence, surface modification to favor caveolin-dependent endocytosis seems to be a promising strategy to deliver drug-loaded nanoparticles.

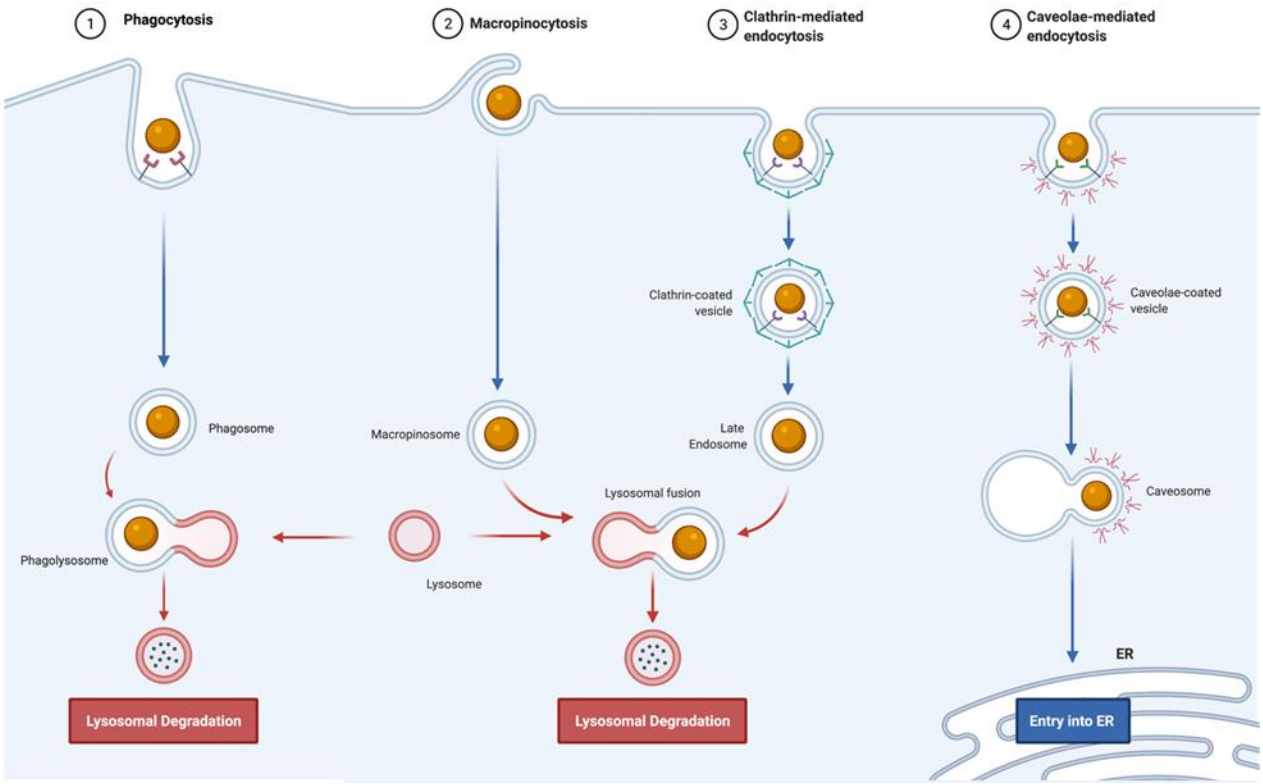

Figure. 16 Endocytosis pathways potentially used by nanoparticles to penetrate cells.
ER=Endoplasmic reticulum

Clathrin- and caveolin-independent endocytosis

Unspecific endocytosis pathways do not involve receptor/ligand interaction and are clathrin- and caveolin-independent routes. This unspecific endocytosis mechanism often involves lipid raft-mediated endocytosis, rich cholesterol, and sphingolipid domain that can invaginate into the cell. This mechanism is undertaken by some nanoparticles, viruses, or toxins but is mainly involved in interleukins internalization by immune cells. Lipid composition of the cell membrane can critically impact nanoparticle internalization, as demonstrated by Carradori et al. [189]. NFL (NFL-TBS.40–63 peptide) functionalized LNC (NFL-LNC) have a higher penetration rate in subventricular zone-neural stem cells (SVZ-NSC), however almost none in central canal-NSC stem cells (CC-NSC). They showed that depending on the localization of these stem cells (brain vs. spinal cord), the proportion of the different types of lipids were different. Cholesterol in SVZ-NSC membranes was 2-fold higher than in CC-NSC membranes and proportions ceramides and sphingomyelins were also higher in SVZ-NSC than in CC-NSC membranes. Since lipid rafts are enriched in sphingolipids, such as sphingomyelins and cholesterol, the authors hypothesized that SVZ-NSC have more lipid rafts involved in NFL-LNC endocytosis [189].

As reviewed, nanoparticles can undertake different endocytosis pathways to deliver their cargo. The endocytosis of nanoparticles can be impacted by different parameters, such as their size or surface charge. Hence, this knowledge can help researchers engineer efficient nanomedicines to escape intracellular degradation. These parameters will be discussed in the following section:

IV.3.2. Size and Shape

Generally speaking, large particles, superior to 500 nm, are uptaken either by phagocytosis and/or micropinocytosis [188]. Smaller molecules are uptaken by clathrin or caveolin endocytosis. Particles around 60 nm are uptaken by the former, and larger particles around 120 nm -250 nm by the latter [188]. In any case, it is complicated to set up a strict correlation between nanoparticles size and subsequent endocytosis pathway for two main reasons: the first is that endocytosis mechanisms are rarely exclusive, and most of the time, several pathways are involved. Secondly, the process is cell-dependent. For example, Albanese et al. report that in Hela and A549 cells, monodispersed gold nanoparticles with a size of 30 nm were better uptaken than 170 nm gold nanoparticle aggregates. However, the polydisperse particles were more internalized in MDA-MB-435 cells (a human melanoma cell-line) than the monodisperse nanoparticles when using another cell line.

Aside from the size, the other morphological element that influences particle uptake is shape. For instance, Xie et al. [190] synthesized different shapes of gold nanoparticles (stars, rods, and triangle) and assessed their uptake by macrophages. All nanoparticles were internalized by clathrin-mediated uptake. Rods were also internalized via caveolae/lipid raft-mediated endocytosis and triangles via additional actin and dynamin-dependent pathways (possibly phagocytosis and/or macropinocytosis) [190].

IV.3.3. Surface Charge

Based on Coulomb's law, positively charged nanoparticles penetrate the negatively charged cell membrane more easily than their neutral and anionic counterparts [188, 191, 192]. Nevertheless, a positively charged surface is not a prerequisite for cell internalization, and negatively charged nanoparticles can also successfully penetrate the cells [193, 194]. To appreciate the charge at the surface of a nanoparticle, the zeta (ζ) potential is measured by scientists as a routine characterization. When a nanoparticle has a net surface charge, ions of opposite charge of the buffer they are dispersed in, clusters around the nanoparticle (Stern layer) (Fig.17). A second diffuse outer layer is composed of loosely associated ions. The zeta potential is a measure of the difference in potential between the fluid in which a particle is dispersed (slipping plane) and the

layer of fluid containing the oppositely charged ions that is associated with the nanoparticle surface [195].

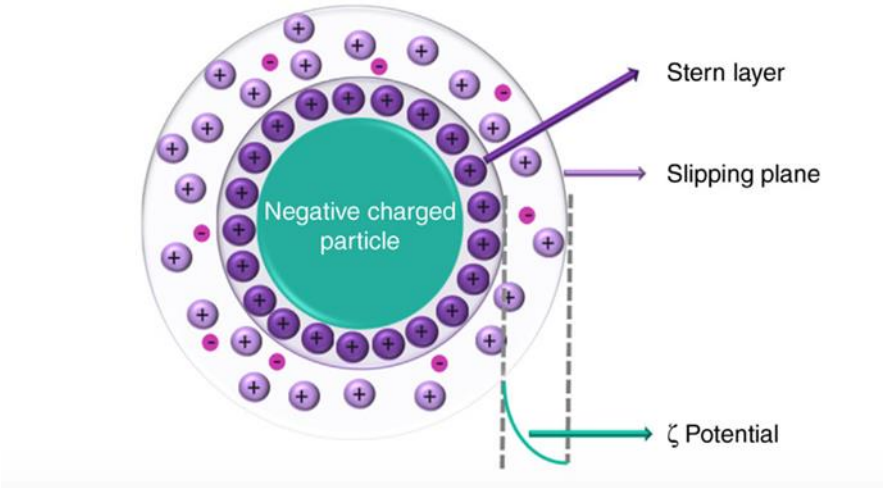

Figure 17. Zeta potential at the surface of nanoparticles

The magnitude of the zeta potential provides information about particle stability. The higher the magnitude of the zeta potential, the higher is the electrostatic repulsion between particles. These repulsions forces limit the flocculation of particles and thus increase the stability of a colloidal solution [195]. Zeta potential is a buffer-dependent parameter and is often measured in water or saline but does not represent surface charge in biological fluids such as blood. Hence in water and serum, for instance, it can be quite different. Furthermore, nanoparticles are generally surrounded by a corona of negatively charged serum proteins in biological fluids.

IV.3.4. Surface modification

The presence of ligands on nanoparticles' surface can impact their uptake by the cells, as these ligands often bind to cell membrane receptors. The binding often triggers receptor-mediated endocytosis via clathrin or caveolin-dependent internalization. For instance, epidermal growth factor functionalized gold nanoparticles are uptaken through clathrin-mediated endocytosis [188]. To increase their stability or increase their half-time, nanoparticles can also be decorated with citrate to give the particle a repulsive negative charge to avoid flocculation or with PEG to escape phagocytosis by immune cells. A surface modification with one or the other molecule leads to a different endocytosis route. Gold nanoparticles coated with citrate were taken up by macropinocytosis as well as clathrin- and caveolae-mediated endocytosis, whereas when this same nanoparticle was functionalized with PEG, they were internalized via clathrin- and caveolae-mediated endocytosis only [188].

Besides peptides, antibodies are also used to functionalize nanoparticles' surfaces. Due to their high affinity towards their antigen, they can be a suitable choice to achieve cell-targeting. Many studies showed that an antibody's grafting impacted the nanoparticle's internalization inside the cell of interest. For instance, grafting of cetuximab, an antibody directed against the epidermal growth factor receptor (EGFR) at the surface of PLGA nanoparticles, enhanced their association in PANC-1 cells and BxPC-3, two cancer cell-line, expressing EGFR [196].

Although antibody bestow high specificity, their Fc region can mediate cell uptake via Fc receptor highly expression immune cells. This can ultimately favor their elimination by the immune system (antibody-dependent cellular cytotoxicity and phagocytosis). Hence, an alternative is to use antibody fragment as mentioned in section 2.2.2. These fragments are devoid of the Fc region and are only composed of the Fv region. In Lee et al.'s study, cytotoxic T-cell targeting was achieved by grafting fragments of an anti-CD8a antibody on PLGA nanoparticles' surface [197].

IV.4. INTRANASAL DELIVERY OF NANOMEDICINE: A PRIVILEGED ROUTE FOR CNS DELIVERY?

(adapted from the "Extracellular vesicles for the treatment of central nervous system diseases" published in Advanced drug delivery review)

There are many hurdles limiting drug delivery to the brain. Indeed, following systemic administration, therapeutic agents may be metabolized or taken up by other tissues thus reducing the amount of drug delivered to the CNS [198]. Furthermore, the CNS is protected by the BBB, which regulates molecular transport and cellular trafficking between the blood and the brain. It consists of endothelial cells, which are linked by tight junctions, pericytes, which have the ability to control the diameter of the vessels, a basement membrane, which provides an additional barrier and finally astrocytes, which provide a link between neurons and vessels. The BBB plays a major role in the protection of the neural tissue from pathogens and toxins. However, certain molecules need to cross the BBB, essentially for CNS homeostasis, for which specific modes of transport exist across the BBB. Transporters such as GLUT1 (glucose), CAT-1 (cationic amino-acids) and LAT-1 (neutral amino-acids) are enriched on the surface of CNS endothelial cells. Passive diffusion through the BBB is possible for molecules presenting a high lipid solubility, a molecular weight < 400 Da and less than 8 hydrogen bonds. These stringent conditions limit the number and type of drug molecules that can reach the CNS parenchyma. Moreover, efflux transporters (e.i. P-glycoprotein) are also expressed by CNS endothelial cells. They limit toxin, but also therapeutic drug, entry into the CNS. All in all, the BBB excludes more than 98% of small molecule drugs and almost 100% of large molecule therapeutics from the brain [199]. The intranasal administration is

a particularly interesting non-invasive approach as it provides direct access to the brain [198]. Several reviews underline the growing interest of the nose-to-brain transport for treating CNS diseases. Indeed, the intranasal administration route offers several advantages, including a non-invasive entry to the brain, a rapid onset of action with reduced systemic side effects and an ease of administration with a potential for self-medication. Moreover, the intranasal drug delivery route is of particular interest in chronic situations when multiple dosing regiments are required. Although the exact mechanisms of the nose-to-brain drug delivery are not fully understood, several evidence suggest four main pathways. In brief, after instillation, the drug can be directly transported to the brain via the trigeminal nerve, present in both the olfactory and respiratory regions of the nasal cavity, or the olfactory nerve, considered to be the most direct pathway in humans [198, 200] (Fig.18). In both cases, the drug is either transported alongside the nerves via bulk flow processes and/or reaches the brain by transneuronal retrograde transport. The drug can also be transported through or along the supporting cells of the olfactory epithelium. Since the respiratory region of the cavity is well vascularized, a fraction of the administered drug can also enter the systemic circulation and reach the brain depending on its ability to cross the BBB [200]. To promote deposition to the olfactory region, several devices have been developed including Vianase an electronic atomizer developed by Kurve Technology® and Opt-Powder by Optinose®, a bi-directionnal delivery device [201].However, the nasal cilial clearance diminishes drug residence time in the nasal cavity and drugs administered via the nasal route can be metabolized by the nasal mucosa enzymes. To address the challenges, another strategy is to encapsulate the bioactive molecules in nanosized delivery systems to protect them and increase their bioavailability during the nose-to-brain transport.

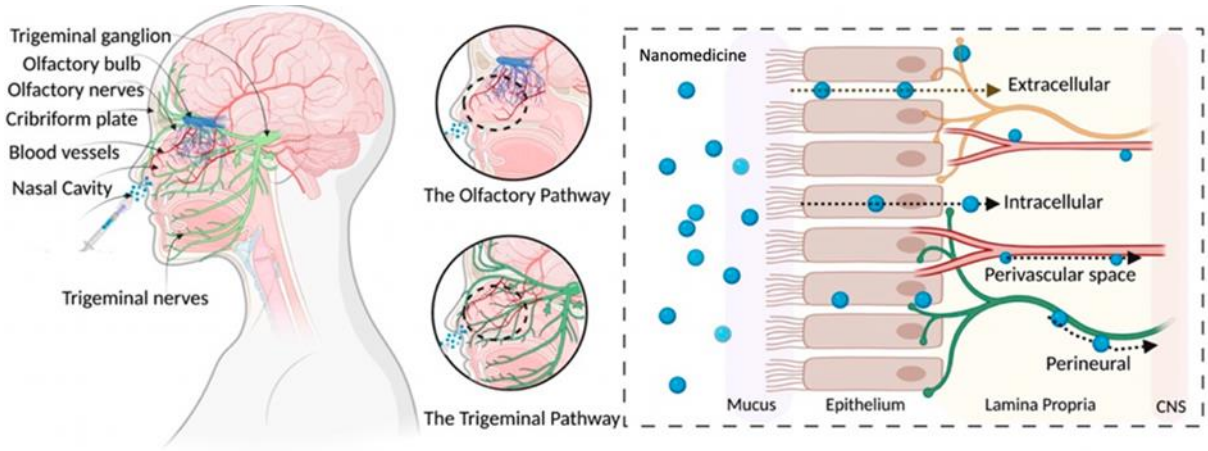

Figure 18. Intranasal administration of nanomedicine [202].
Pathways of nanomedecine distribution after intranasal administration.Compounds pass through the nasal epithelium to reach the lamina propria primarily via extracellular transport.

V. AIM OF THE THESIS

Nowadays, numerous clinical trials are ongoing to evaluate molecules that successfully promote myelin repair in animal models. Unfortunately, other molecules got to this point in the past but never made it out of phase 2 due to lack of efficacy or side effects. Some of the factorst that might cause these failures are : 1) The drugs may have a poor biodistribution, because of the BBB, in the CNS and consequently in OPC. 2) Another theory is that even if they manage to get through the BBB, the concentrations that reach OPC are not high enough to favor their differentiation effectively. 3) Lipophilic molecules offer an additional challenge as they are insoluble in physiological solutions thus cannot be administrated intravenously without a proper formulation or chemical modification (i.e prodrug). Hence, they are taken *per os* most of the time, making them subject to hepatic first-passage and diminishing their plasma concentration. **Our work will aim to improve the properties of lipophilic pro-remyelinating molecules by encapsulating them inside LNC to 1) increase their solubility and 2) address them to OPC to foster their differentiation into remyelinating oligodendrocytes (Fig.18).**

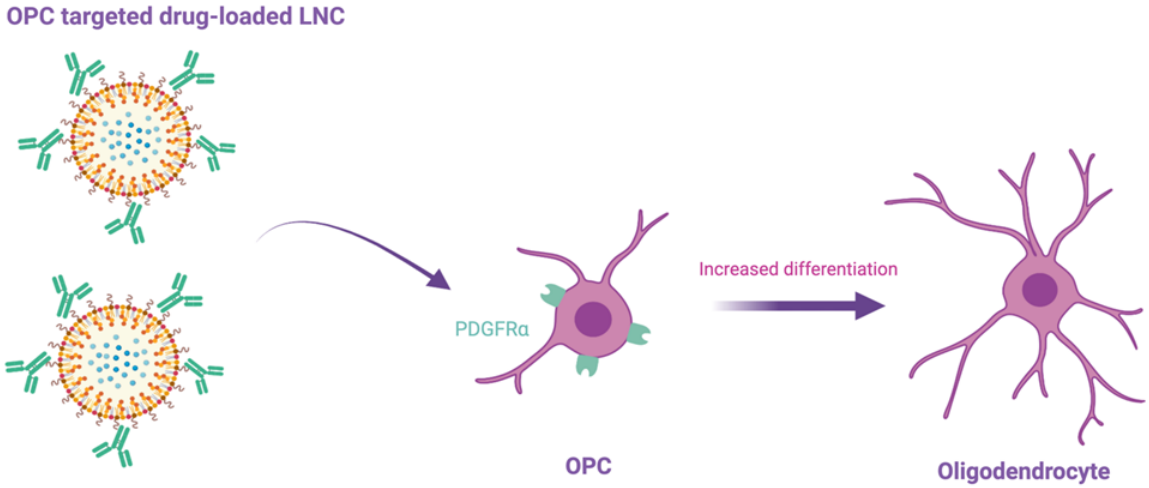

Figure 18. Aim of the thesis

The first part of the thesis focused on the development of OPC-targeted LNC. To achieve OPC targeting, we grafted an anti-PDGFRα antibodies at the surface of the LNC. This tyrosine-kinase receptor is predominantly expressed at OPC surface in the CNS in humans (and rodents) and it undergoes endocytosis upon binding with its ligand, the PDGFAA growth factor. We hypothesized that interactions of the anti-PDGFRα at the nanoparticle surface with PDGFRα at the OPC membrane will ultimately increase LNC uptake by OPC. To graft the anti-PDGFRα we explored

three different techniques. We selected the most effective formulation to evaluate the impact of the anti-PDGFRα antibody at LNC surface on their uptake on primary OPC culture (**chapter 2).**

The second part of the thesis explored the intranasal delivery of pro-remyelinating lipophilic molecules. The advantage of this administration route is its direct access to the CNS. Indeed, the nasal epithelium is the only part of the human body that connects the CNS to the outside work [199]. After administration, compounds can get to the brain either by the olfactive bulb and get to the brain by transcellular or paracellular means or pass via the trigeminal nerve by endocytosis or transcellular transport [199]. The success of the nose-to-brain administration depends on several factors: drug solubility, residence time, metabolic stability, and rate of mucociliary clearance of the nasal epithelium. Using LNC as a nanocarrier for these lipophilic compounds of interest can limit their clearance, facilitate their endocytosis, and prevent their degradation by enzymes of the nasal cavity [203]. However, more importantly, it will solubilize them and avoid the administration of a suspension with aggregates that will be an obstacle for their delivery. To evaluate whether pro-remyelinating therapies could be effective when delivered intranasally, we encapsulated in LNC two bioactive molecules lipophilic compounds showing encouraging data in animal models: *all-trans*-retinoic acid (RA) [204-206] and Cal [101, 207]. Their logP of 6.3 and 5.5 respectively make them the perfect candidates to be encapsulated in LNC to improve their nose-to-brain delivery and *in-fine* their efficacy. Therefore, we evaluated *in vitro* and *in vivo,* using a cuprizone model, the effect of RA-loaded LNC, Cal-Loaded LNC, and the combination of those two formulations to explore a possible synergistic effect between those two compounds **(chapter 3).**

CHAPTER II

IMPACT OF ANTI-PDGFRα ANTIBODY SURFACE FUNCTIONALIZATION ON LNC UPTAKE BY OLIGODENDROCYTE PROGENITOR CELLS

ADAPTED FROM :

Labrak, Y., Heurtault, B., Frisch, B., Saulnier, P., Lepeltier, E., Miron, V. E., .Muccioli, G. & Des Rieux, A. (2022). Impact of anti-PDGFRα antibody surface functionalization on LNC uptake by oligodendrocyte progenitor cells. International Journal of Pharmaceutics, 121623.

ABSTRACT

Impairment of oligodendrocyte progenitor cell (OPC) differentiation into oligodendrocytes and chronic inflammation are key determinants of poor remyelination observed in diseases such as multiple sclerosis. For many pro-myelinating molecules, the therapeutic potential is hindered by poor solubility or limited access to the targeted cells. A promising approach to improve the delivery of those molecules to OPC is to encapsulate them in functionalized Lipid Nanocapsules (LNC). We aimed to develop the first OPC-targeting LNC, by grafting an anti-PDGFRα antibody on the surface of the LNC using several strategies and evaluating the interaction with PDGFRα via ELISA. We found that only site-selective click-chemistry grafting allowed the grafting of an average of 5 antibodies per LNC. Additionnaly with this approach anti-PDGFRα/PDGFRα association was mainted after the antibody association with LN (40% of association compared to control), confirmed *in vitro* on primary rat OPC. In conclusion, we demonstrated that it was possible to produce anti-PDGFRα functionalized LNC, confirmed the antibody's ability to recognize its receptor after grafting and optimized techniques to characterize antibody functionalized LNC.

KEYWORDS

Lipid nanocapsules, Surface modification, Multiple sclerosis, Nanomedicine Remyelination

TABLE OF CONTENTS

I. INTRODUCTION 73
II. MATERIALS AND METHODS 75
II.1. MATERIALS 75
II.2. PREPARATION OF ANTI-PDGFRA LIPID NANOCAPSULES (LNC-AB) 75
II.3. CHARACTERIZATION OF LNC-AB 79
II.4. IMPACT OF THE GRAFTING ON THE INTERACTION OF ANTI-PDGFRA WITH ITS TARGET 80
II.5. OPC PRIMARY CULTURE 81
II.6. LNC CYTOTOXICITY ON OPC 81
II.7. LNC-AB ASSOCIATION WITH OPC 82
II.8. STATISTICAL ANALYSIS 82
III. RESULTS 83
III.1. CHARACTERIZATION OF LNC-AB OBTAINED WITH THE MALEIMIDE COUPLING STRATEGY 83
III.2. IMPACT OF PEG-MALEIMIDE INSERTION METHOD ON AB GRAFTING EFFICIENCY 84
III.3. IMPACT OF GRAFTING ON THE INTERACTION BETWEEN ANTI-PDGFRA AND PDGFRA 84
III.4. IMPACT OF THE CLICK CHEMISTRY METHOD ON AB ACTIVITY 85
III.5. IMPACT OF AB GRAFTING AT LNC SURFACE ON LNC INTERACTIONS WITH OPC 87
IV. DISCUSSION 91
V. CONCLUSION 94
VI. SUPPLEMENTARY DATA 95

I. INTRODUCTION

The myelin sheath, formed by oligodendrocytes in the central nervous system (CNS), is crucial in the transduction of electrical impulses along the axons and neuron metabolic support. In demyelinating diseases, such as multiple sclerosis (MS), loss of the myelin sheath causes invalidating symptoms such as cognitive dysfunction, impaired locomotor function and disorders such as optical neuritis [208]. In MS, demyelination results from a complex physiopathological process involving a targeted immune response towards the myelin sheath [47]. Until now, the trigger of this autoimmune disease is still unknown, but the onset of MS is most likely multifactorial (i.e. genetic, environmental, hypovitaminosis D, viral) [64].

Endogenous repair of myelin sheaths occurs via the recruitment and differentiation of oligodendrocyte progenitor cells (OPC) into new myelinating oligodendrocytes [47]. As a result, a new functional myelin sheath is rebuilt around axons, restoring efficient electrical impulse conduction. However, with time and MS progression, this mechanism becomes less efficient. Several mechanisms are at cause and limited OPC differentiation into myelinating oligodendrocytes is one of them [28, 47].

Most MS therapies focus on reducing peripheral inflammation and on lengthening remission time between relapses. However, no treatments stimulating remyelination are currently available [209]. To reach this goal, one strategy is to enhance remyelination by promoting OPC differentiation into mature oligodendrocytes [23]. For the last decades, researchers have been working to decipher OPC differentiation pathways to find molecules that would enhance remyelination [23]. A few drugs have been tested, in preclinical or clinical settings, in this context. For instance, retinoic acid and calcitriol have been studied *in vitro* for their differentiating potential of OPC. Bexarotene, a lipophilic retinoid X receptor gamma (RXRγ) agonist, showed some interesting results on remyelination in a recent clinical trial involving relapsing-remitting MS patients [97]. However, the trial was interrupted due to two major off-target effects, hypothyroidism and hypertriglyceridemia.

Using targeted nanomedicines is one strategy to reduce side effects. In this context, lipid nanocapsules (LNC) are gaining interest. Indeed, LNC are very efficient in solubilizing lipophilic bioactive drugs, are biocompatible, can protect their cargo from degradation and facilitate their transport across membranes [210]. Moreover, their surface can be modified to favor the interaction with a cell or tissue. For instance, LNC surface has been modified to target a specific cell type [158, 211-213], mainly by adsorption of a targeting peptide [214-216]. As platelet-derived growth factor

receptor α (PDGFRα) is specifically expressed by OPCs in the CNS [217, 218], we hypothesized that grafting an anti-PDGFRα antibody at LNC surface would favor the targeting of OPC.

Thus, here we compared three different approaches to graft an anti-PDGFRα at LNC surface (LNC-Ab). Two are based on thiol-maleimide chemistry but involved different approaches to link the maleimide at LNC surface (transacylation *vs* post-insertion) and the third one is based on copper less click-chemistry. Following an extensive characterization of the obtained LNC-Ab, we assessed their targeting ability, first using a custom-made ELISA assay and then *in vitro*, in rat OPC primary cultures.

II. MATERIALS AND METHODS

II.1. MATERIALS

Labrafac® provided by Gattefosse SA (France) and Lipoïd® S100 by Lipoid Gmbh (Germany). Kolliphor HS15®, poly-D-Lysine hydrobromide (70000–150000 Da), fluorescamine, 2-Iminothiolane•HCl and propidium iodide were purchased from Sigma (United-States). 1,2-Distearoyl-sn-glycero-3-phosphorylethanolamine-PEG $_{(2000)}$-Maleimide (DSPE-PEG-Maleimide) and NH_2-$PEG_{(5000)}$- Dibenzocyclooctyne (NH_2-PEG-DBCO) were purchased from Nanocs (United-States). NH_2-PEG $_{(5000)}$-Maleimide was purchased from Creative PEGWorks (United-States). Anti-PDGFRα was purchased from BioLegend (United-States). Anti-rat-HRP, DMEM (41966-029), HEPES, Pen/Strept, DMEM 0.05% trypsin-EDTA (1x), Presto blue Cell Viability Reagent, DiD'solid, SiteClick™ Antibody Azido Modification Kit and Alexa-488-Phalloidine were purchased from Thermo Fisher Scientific (United-States). Platelet-derived growth factor A (PDGFAA) and fibroblast growth factor 2 (FGF) were purchased from Peprotech (United Kingdom). rmPDGFRA/Fc chimera (soluble PDGFRα) has been purchased from R&Dsystems. Spectra-Por Float-a-lyzer G2 300 kDa dialysis membrane and Rotilabo®-syringe sterile 0.22 µm filters were purchased from Carl Roth GmbH (Germany).

II.2. PREPARATION OF ANTI-PDGFRA LIPID NANOCAPSULES (LNC-AB)

II.2.1. Preparation of the LNC

LNC were prepared following the protocol developed by Heurtault et al. [125]. Briefly, 0.846 g of Solutol HS15, 0.075 g of Lipoïd®, 0.089 g of NaCl, 1.028 g of Labrafac® and 2.962 ml of water were mixed under magnetic stirring for 5 min at 50 °C. Next, three temperature cycles of heating/cooling were done between 60 °C and 90 °C, also under magnetic stirring. During the cooling of the last cycle, at 77 °C, 12.5 ml of cold water (4°C) were added, under high-speed stirring. The resulting nanoparticle of 126mg/ml were filtered with a 0.2 µm filter for sterilization and stored at 4 °C until use. LNC concentration was calculated by the total weight of Kolliphor HS 15, Lipoïd® and Labrafac® divided by the final volume the LNC formulation [219].

Fluorescent LNC, obtained by loading DiD into LNC (14,7 µg/ml of DID in LNC), were used for confocal and uptake experiments [220]. DiD was added before the heating/cooling cycles.

II.2.2. Preparation of LNC-PEG-Maleimide

To graft Ab to the surface of the LNC, two approaches based on the coupling between thiol and maleimide moieties were used. The first one consisted of the transacylation of PEG chains (Kolliphor) exposed at LNC surface using NH_2-PEG-Maleimide (Approach 1), while the second one consisted of the post-insertion of DSPE-PEG-Maleimide in the PEG corona of the LNC (Approach 2) (Fig.1A). For both approaches, the thiolated antibody was covalently coupled to the PEG by reaction with the maleimide moiety.

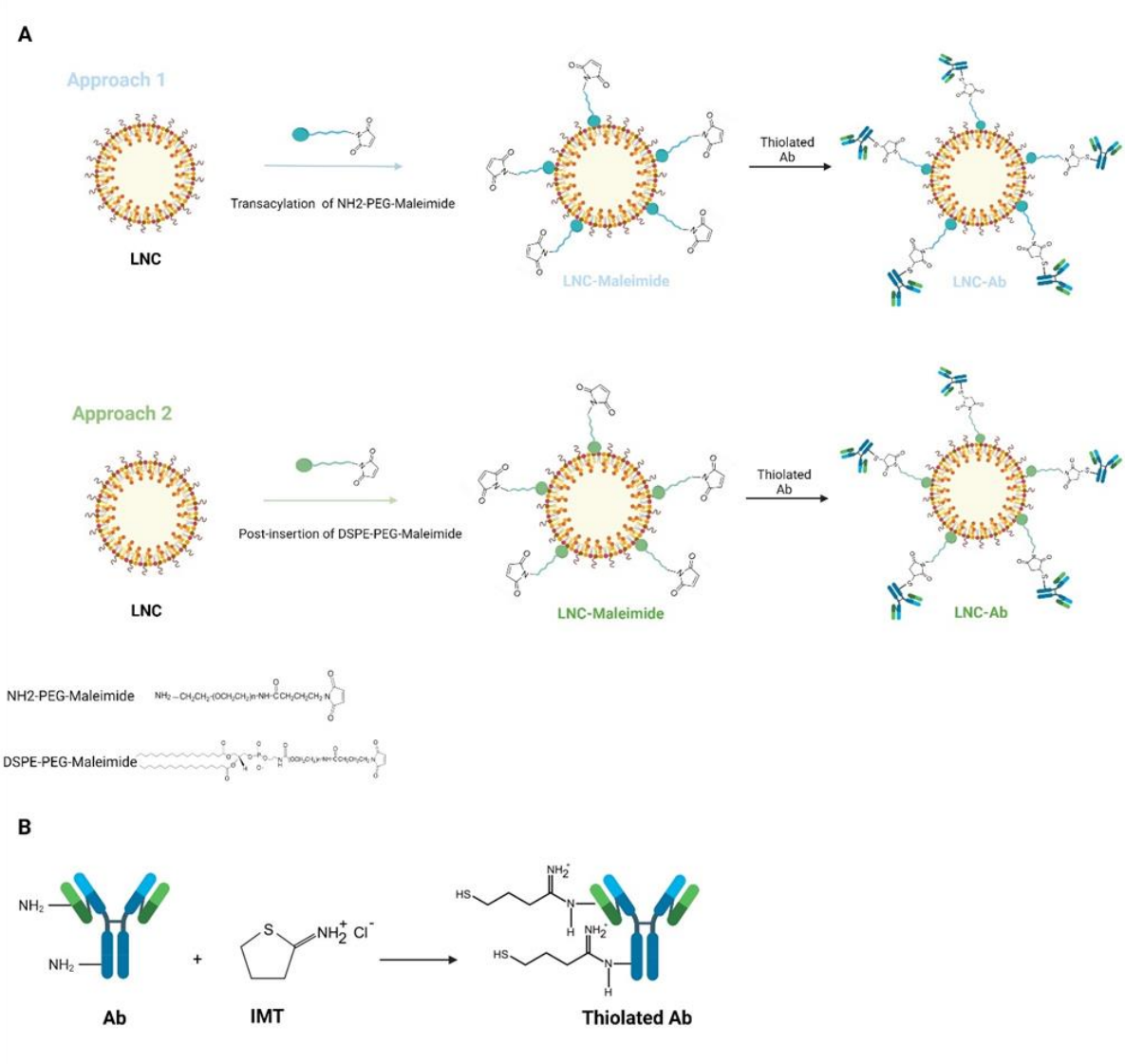

Figure 1. Preparation of LNC-PEG-Maleimide and grafting of Ab (created with Biorender.com)
(A) The PEG-Maleimide conjugate was added to the surface of the LNC using two different approaches: Approach 1 consisted of the transacylation of NH_2-PEG-Maleimide, and Approach 2 involved the post-insertion of DSPE-PEG-Maleimide. Both led to the formation of LNC-Maleimide.
(B) The Ab (anti-PDGFRα) was thiolated by using IMT (2-iminothiolane•HCl). Then, the thiolated Ab formed a thioether bond with the maleimide moiety present at LNC surface. Unattached Ab were removed by dialysis.

Transacylation of NH_2-PEG-Maleimide (Approach 1): Transcylated LNCs were made according to Messaoudi et al protocol [221]. Briefly, 5 mg of NH_2-PEG-Maleimide (1:100, molar ratio of Maleimide: Kolliphor HS®) with 2 ml of LNC and 100 µl of NaOH (10 M) were incubated under agitation for 15 minutes. Then 2 ml of glycine buffer (50 mM of glycine and 5 mM of HCl, pH= 2) were added. NH_2 reacted with the hydroxystearic acid moiety of the Kolliphor HS®, to form an amide bond linking the LNC to the NH_2-PEG-Maleimide. After NH_2-PEG-Maleimide covalent grafting at the surface of the LNC, the formulation was dialyzed for 48h (cut-off 300 kDa) against water to remove the unbound PEG-maleimide.

Post-insertion of DSPE-PEG-Maleimide (Approach 2): Post-inserted LNC were made according to Perrier et al. protocol [222]. Briefly, DSPE-PEG-Maleimide (1:100 molar Ratio of PEG-Maleimide: Kolliphor HS®) dissolved in PBS was incubated for 1 h at 60°C under agitation. Afterward, 300 µl of this solution were added to 400 µl of LNC prepared as described in section 2.2.1. The resulting mixture underwent seven cycles of 15 min incubation at 60°C under stirring followed by 15 minutes of incubation on ice.

II.2.3. Preparation of LNC-PEG-DBCO

NH_2-PEG-DBCO was covalently grafted to the surface of the LNC by transacylation as described in section 2.2.2 (Approach 3) (Fig. 2). Five mg or 10 mg of NH_2-PEG-DBCO (1:100 or 1:50 molar ratio of PEG-DBCO : Kolliphor HS®) with 2 ml of LNC and 100 µl of NaOH (10 M) were incubated under agitation for 15 minutes. Then, LNC-PEG-DBCO were separated from unreacted components as described in 2.2.2.

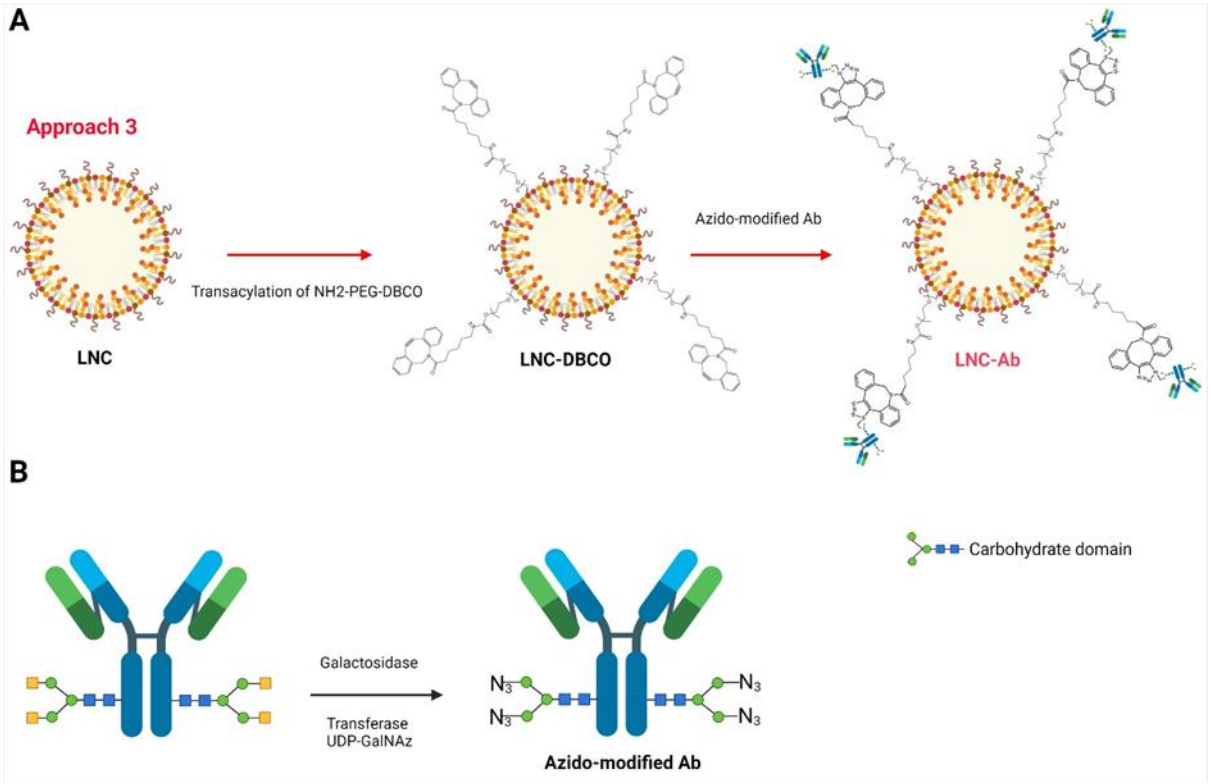

Figure 2. Preparation of LNC-PEG-DBCO and grafting of Ab (created with Biorender.com)
(A) A transacylation reaction was used to add the NH_2-PEG-DBCO conjugate at LNCs surface.
(B) The azide moiety was added on Ab using the Thermofisher® Site-Click kit. The modification was made on the carbohydrate chains of the Fc region of the Ab specifically. The DBCO alkyne reacted with the Ab azide to form a triazole bond, linking the Ab covalently to the LNC.

II.2.4. Grafting of anti-PDGFRa on LNC

For LNC-PEG-Maleimide (Approach 1 and 2)

The primary amines on the anti-PDGFRα (Ab) were thiolated with 2-iminothiolane•HCl (IMT) in PBS (Fig. 1). A mixture of Ab and IMT was made using a molar ratio Ab:IMT of 10:1, with a concentration of IMT of 13.7 µg/ml. Ab and IMT were kept under agitation for 1h during which the solution was vortexed every 15 min [223]. Then, 200 µl of LNC were mixed with 100 µl of the Ab : IMT solution and incubated under agitation for 2h (vortexed every 30 min). To block the remaining free maleimide at the LNC surface, cysteine•HCl was added to the suspension and was further incubated for 30 min. The resulting suspension was dialyzed for 48 h (cut-off 300 kDa) to remove unbound Ab.

For LNC-PEG-DBCO (Approach 3)

According to supplier instructions, Ab and anti-IgG2a were azido-modified using the Thermofisher® Site-Click kit (Fig. 2). Briefly, a β-galactosidase enzyme was used to remove the terminal galactose residues of the carbohydrate chains localized on the Fc region of the antibody.

Those terminal residues were replaced by an azide-containing sugar (GalNAz) using a β-1,4-galactosyltransferase. Then 200 µl of LNC were incubated overnight with 100 µl of a solution containing 280 µg/ml of azido modified antibody diluted in PBS. According to the manufacturer, the average number of DBCO moieties per antibody was 3 to3.5. The resulting suspension was dialyzed for 48h (cut-off 300 kDa) to remove unbound Ab.

II.3. CHARACTERIZATION OF LNC-AB

Size, polydispersity index and zeta potential of LNC-Ab were measured in milliQ water using a ZetasizerUltra® (Malvern, United Kingdom).

To determine the antibody grafting yield, following removal by dialysis of the unbound Ab from the LNC preparation (see above), primary amines of the Ab were quantified with a fluorescamine assay [224, 225]. Briefly, 50 µl of LNC-Ab were mixed with 50 µl of HCl 12 M and incubated for 12 hours at 120 °C to hydrolyze the peptidic bonds. After heating, 100 µl of NaOH 6M were added to the mixture. Five hundred µl of a fluorescamine solution (30mg/100ml of dioxane), 1,5 ml of borate buffer (pH = 9, 45 mM of boric acid and 76 mM of borate) and 40 µl of sample were mixed in a quartz cuvette extemporaneously and resulting fluorescence was read at λex=400 nm and λem=480 nm (Spectramax® reader, Molecular Device®, United Kingdom). The calibration curve was made using increasing amounts of Ab (2.25 to 27.5 µg/ml) in the presence of LNC as a matrix. A representative calibration curve can be found in the supplementary data (Fig 1.S). The detection limit and the quantification limit of the method are 2.83 µg/ml and 9.83 µg/ml, respectively. The intraday day precision was 8.2% and 5.4%, and the interday precision was 6.8% and 4.5 %, when using 13.7 µg/ml and 27.5 µg/ml, respectively. The calculated accuracy is of 8.7%, and 3.5 % for 13.7µg/ml and 27.5 µg/ml, respectively.

To determine the amount of antibody, present in the LNC-Ab, the samples were prepared similarly to the calibration curve, where an increasing quantity of sample was reacted with fluorescamine, resulting in a sample curve that follows the equation $Y = ax$. Grafting efficiency was then calculated with the following equation:

$$Grafting\ efficiency\ (\%) = \frac{Slope\ of\ Sample\ curve}{Slope\ of\ Calibration\ curve} * 100$$

To obtain an estimation of the number of antibodies per LNC, the quantity of antibody was divided by the number of LNC in the sample (Table 1.S; measured by nanoparticle tracking analysis (NTA) (Zetaview®, Particle Metrix®, Germany)) using the following equations:

$$Quantity\ of\ Ab\ (g) = Amount\ of\ Ab\ introduced\ in\ LNC\ (g)\ \times Grafting\ efficiency$$

$$Total\ number\ of\ Ab\ in\ the\ formulation = \frac{quantity\ of Ab\ \times Na}{Molecular\ weight\ of\ Ab}$$

$$Number\ of\ Ab\ per\ LNC = \frac{Amount\ of\ Ab\ per\ L}{Number\ of\ particles\ per\ L}$$

Na: Avogadro number = 6.022×10^{23} mol^{-1}

Molecular weight of Ab = 150 000 $g.mol^{-1}$

II.4. IMPACT OF THE GRAFTING ON THE INTERACTION OF ANTI-PDGFRA WITH ITS TARGET

The impact of the grafting on the Ab ability to interact with its target has been assessed by an ELISA optimized in our lab. A 96-well plate was coated with 100 µl of soluble PDGFRα (rmPDGFRα) diluted at different concentrations (from 0.3 to 20 nM) in PBS and incubated overnight at 4°C. Then, the plate was washed 3 times and blocked with 300 µl of a 1% BSA solution in PBS during 1 h. Then, LNC-Ab and all other conditions were diluted in a 0,1% BSA solution at 1 nM of Ab. Following 4h of incubation at room temperature and 3 washes, 100 µl of anti-rat-HRP antibody (1:2000 dilution) were added to the wells and incubated for 1h at RT. TMB (3,3',5, 5'- tetramethylbenzidine) was used as HRP substrate, and the optical density was read at 450 nm. The Ab / rmPDGFRα association was appreciated by calculating the percentage of Ab response rate using the following equation:

$$\%\ response\ rate = \frac{OD_{450}\ of\ modified\ Ab\ at\ 20\ nM}{OD_{450}\ of\ unmodified\ Ab\ at\ 20\ nM} * 100$$

where a response rate of 100% would correspond to a similar recognition of the rmPDGFRα by the modified Ab and the commercial Ab.

To evaluate PEG chain impact on Ab activity, the Ab was pegylated according to the protocols used for Approach 1 and 3.

Pegylation of Ab with NH_2-PEG-Maleimide

The primary amines on the anti-PDGFRα (Ab) were thiolated with 2-Iminothiolane•HCl (IMT) in PBS (Fig. 1). A mixture of Ab and IMT was made using a molar ratio Ab:IMT of 10:1, with a concentration of IMT of 13.7 µg/ml. Ab and IMT were incubated under agitation for 1h during which the solution was vortexed every 15 min [223]. Then, 200 µl of a NH_2-PEG-Maleimide solution (1.25 mg/ml in MilliQ water) were mixed with 100 µl of the Ab: IMT solution and incubated under agitation for 2h (vortexed every 30 min).

Pegylation of Ab with NH_2-PEG-DBCO

According to supplier instructions, Ab and anti-IgG2a were azido-modified using the Thermofisher® Site-Click kit (Fig. 2). Briefly, a β-galactosidase enzyme was used to remove the terminal galactose residues of the carbohydrate chains localized on the Fc region of the antibody. Those terminal residues were replaced by an azide-containing sugar (GalNAz) using a β-1,4-galactosyltransferase. Then 200 µl of a NH_2-PEG-DBCO solution (1,25 mg/ml in MilliQ water) was incubated with 100 µl of a solution containing 280 µg/ml of azido modified antibody diluted in PBS.

II.5. OPC PRIMARY CULTURE

Cortical mixed glial cultures were generated from Sprague-Dawley rat pups (postnatal day 0-2), according to Directive 2010/63/EU, to guidelines of the Belgian Government following the approval by the ethical committee for animal care of the faculty of medicine of UCLouvain (2017/UCL/MD/030), as described previously by Miron et al [43]. Briefly, brains were dissected and the cerebellum, olfactory bulbs, and meninges were removed. Brains were then digested using papain (40 µg/ml) and platted in T75 flasks, for 10 days, in DMEM containing 4.5 g l^{-1} glucose, L-glutamine, pyruvate, 10% fetal calf serum (vol/vol) and 1% penicillin/streptomycin (vol/vol). To remove microglia, flasks were shaken on a rotary shaker at 230 rpm (1h, 37°C). After addition of 10 ml of fresh media, OPC were retrieved after further agitation (16 hours on a rotary shaker at 37°C at 220 rpm). OPC were then pelleted (250xg for 5 min) and plated at 1×10^4 cells/well in poly-D-Lysine coated (4µg/ml) 96 well plates Tc treated (BD Falcon) or 12 well plates. The medium consisted in DMEM containing 4.5 g/L glucose, L-glutamine, pyruvate, SATO (16 µg/ml putrescine, 400 ng/ml L-thyroxine, 400 ng/ml tri-iodothyroxine, 60 ng/ml progesterone, 5 ng/ml sodium selenite, 100 µg/ml bovine serum albumin fraction V, 10 µg/ml insulin, 5.5 µg/ml halo-transferrin (all from Sigma-Aldrich)), 0.5% fetal calf serum 1% penicillin/streptomycin, 10 ng/ml PDGFAA, and 10 ng/ml FGF. For experiments with depleted PDGFAA media, PDGFAA was removed 18h prior to LNC treatment.

II.6. LNC CYTOTOXICITY ON OPC

LNC were diluted at different concentrations (0.63 mg/ml to 0.15 mg/ml) in OPC medium and were incubated for 1h, 4h and 24h with OPC 2 days post-seeding. The media was then removed and replaced with fresh OPC medium containing 10% of PrestoBlue® Cell Viability Reagent. After 18h of incubation, the fluorescence was read at λex = 530 nm and λem = 580 nm. Untreated OPC were used as positive control (100 % viability).

II.7. LNC-AB ASSOCIATION WITH OPC

II.7.1. Confocal microscopy

Cells were seeded in 96 well plates and were treated 2 days after seeding with LNC (DiD)-Ab for 30 min, at the concentration of 0.42 mg/ml. Then they were washed once before fixation (15 min, PFA 4%). Cells were then washed 3 times with PBS, blocked and permeabilized using PBS containing 5% normal goat serum and 100 µg/ml digitonin. Cells were then washed gently 3 times with PBS and were incubated 30 min with Phalloidine-488 (1:100) diluted in PBS 1% Normal goat serum for 30 min. Cells were then washed 3 times and kept in PBS. Images were taken using a Cell Observer Spinning Disk Confocal microscope (ZEISS) and a 40x oil objective.

II.7.2. Fluorescence associated cell sorting (FACS)

Cells were seeded and treated in 12-well plates, with either LNC (DiD)-Ab or LNC (DiD)-IgG2a isotype or LNC (DiD). The nanoparticles were diluted at a concentration of 0.15 mg/ml in complete DMEM media and incubated with OPC for 30min. After incubation, the media was removed, and cells were rinsed with Dulbecco's phosphate-buffered saline. To detach the cells, 500 µl of DMEM 0,05% trypsin-EDTA were added into each well and incubated at 37°C for 8 min. Cells were then pelleted (300xg for 5min) and washed in FACS buffer (0.1% BSA and 1 mM EDTA in PBS). Dead cells were excluded from the analysis based on Propidium iodide staining. To differentiate DiD^+ cells from DiD^- ones, cells that were not incubated with LNC were used as control. Samples were analyzed with a BD FACSverse™. Flow cytometry data were treated with the Flowjo© software.

II.8. STATISTICAL ANALYSIS

T-tests, one-way ANOVA and two-way ANOVA were performed using PRISM version 9 (GraphPad Software, United-States) to determine statistical significance. Results were considered significant if $p < 0.05$. N indicates the number of independent experiments and n the number of replicates. Detailed information about the number of replicates and the statistical test applied can be found in figure captions.

III. RESULTS

III.1. CHARACTERIZATION OF LNC-AB OBTAINED WITH THE MALEIMIDE COUPLING STRATEGY

LNCs had a size of 58 nm, a PDI of 0.04 and a zeta potential of -3 mV (Fig. 3). The addition of maleimide moieties on LNCs surface with approach 1 significantly increased their size (+9 nm) and decreased their zeta potential (from -3 to -24 mV). The second approach increased LNC size (+13 nm), although it did not significantly impact the zeta potential (-3 to -8 mV). The PDI was < 0.2 for all these formulations. Grafting the Ab on LNC-Maleimide had no impact on their size and PDI, while it impacted LNC zeta potential for approach 2 (-8 mV vs -24 mV).

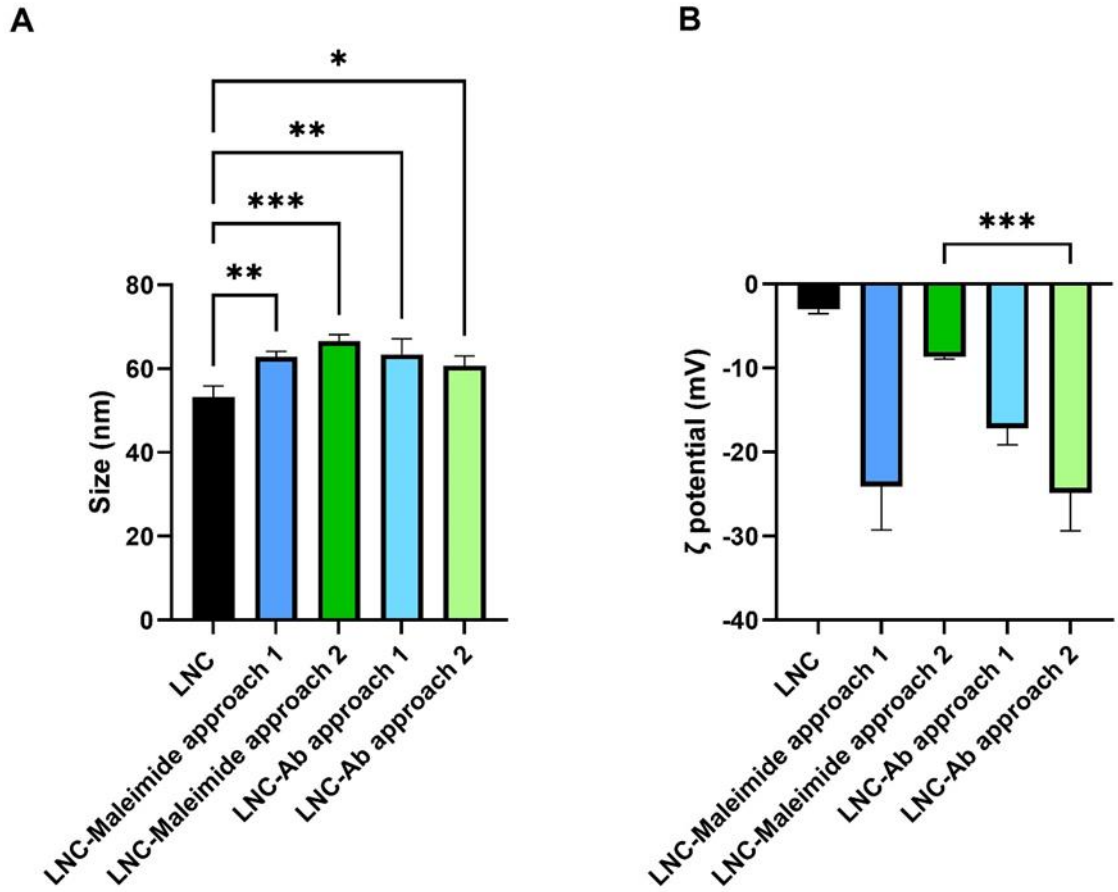

Figure 3. Impact of transacylation and post-insertion of PEG-Maleimide on the physicochemical properties of LNC

Following transacylation with NH_2-PEG-Maleimide (approach 1) or post-insertion of DSPE-PEG-Maleimide (approach 2) of the LNC, the Ab was linked to the LNC-Maleimides. LNC size (A) and Zeta potential (B) were measured, in water, using a Nanosizer. The values were presented as mean±SD (N=3, n=3). Statistical significance was determined by a one-way ANOVA test, *p < 0.05.

III.2. IMPACT OF PEG-MALEIMIDE INSERTION METHOD ON AB GRAFTING EFFICIENCY

The average number of Ab grafted at LNC surface was quantified using a primary amine quantification assay developed by Schelté et al. [224]. Approach 1 resulted in a higher number of antibodies at the nanoparticle's surface, with an estimate of 49 Ab per LNC, than approach 2 where an average of 7 Ab per LNC was detected (Table 1). Since approach 1 provided the highest grafting efficiency, it was selected for the next step.

Formulations	Molar Ratio of Maleimide / Kolliphor HS®	Quantity of antibody added at the beginning of the reaction (µg)	Grafting efficiency (%)	Number of antibodies per LNC
LNC-Ab approach 1	1:100	28	66 ± 9	49 ± 1
LNC-Ab approach 2	1:100	28	38 ± 7	7 ± 4

Table 1. Impact of PEG-Maleimide insertion method on Ab grafting efficiency. The values are presented as mean±SD *(N=3)*

III.3. IMPACT OF GRAFTING ON THE INTERACTION BETWEEN ANTI-PDGFRA AND PDGFRA

As grafting could modify Ab interaction with its receptor, the objective of this part was to evaluate if LNC-Ab had the same degree of interaction with its receptor than the unmodified Ab. We also evaluated if LNC would interfere with the ELISA signal by using the same concentration of Ab diluted in LNCs (Ab+LNC) but there was no significant change on the biding curve, meaning that LNC did not interfere with the assay (Fig. 4).

While mixing LNC with Ab and Ab thiolation (Ab-SH) did not impact their interaction with the rmPDGFRα, covalently grafting the Ab on LNC surface (with approach 1) impaired its ability to recognize its antigen (Fig. 4). We also wanted to assess impact the impact of PEGylation on Ab. It appeared that the addition of PEG-Maleimide on the Ab (Ab-PEG-Maleimide) prevented its interaction with its target.

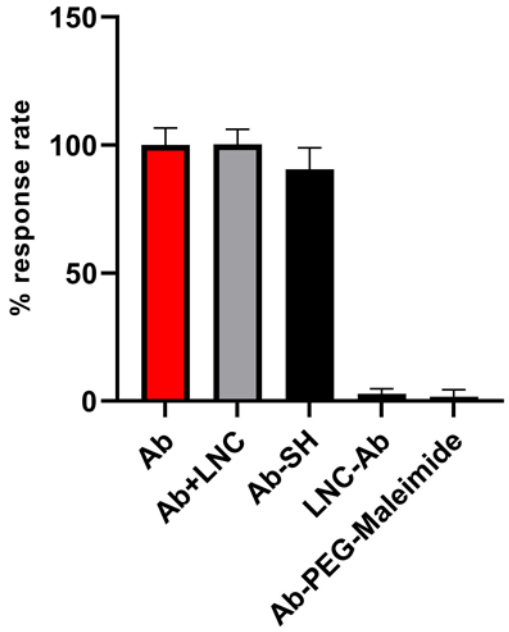

Figure 4. Impact of Ab grafting to the surface of the LNC (approach 1) on its interaction with PDGFRα.
An ELISA was used to determine the interaction between the Ab and its target protein (PDGFRα). Data are shown as a percentage of 1nM Ab response to 20 nM of PDGFRα. All percentages were calculated relatively to unmodified anti-PDGFRα. In all conditions, Ab was at 1nM. The values were presented as mean±SD (N=3, with 3 different batches of LNC-Ab, Ab-PEG-Maleimide, and Ab-SH).

We reasoned that if the unspecific multi-pegylation of the Ab was responsible for the loss of response of the Ab-PEG-Maleimide, then decreasing the number of thiols on the Ab could overcome the inactivation of Ab. The hypothesis was that if less PEG-Maleimide chains were grafted on the Ab, its activity might be less affected. Thus, different concentrations of IMT were used for the Ab thiolation but the interaction between the modified Ab and its target remained poor, regardless of the concentration of IMT used (supplementary data Fig 2.S).

While these approaches are primarily used and reported in the literature for other types of nanoparticles [226-228], our data showed that they were poorly efficient as far as Ab grafting on LNC surface was concerned. An alternative strategy was thus used to graft the Ab at LNC surface using click chemistry.

III.4. IMPACT OF THE CLICK CHEMISTRY METHOD ON AB ACTIVITY

A third strategy, based on click chemistry, was explored as an alternative to the maleimide-thiol coupling (approach 3) [229].

Grafting of the PEG-DBCO polymer at LNC surface increased LNC size and decreased its zeta potential, similarly to what was observed following the addition of the maleimide conjugate with

Approach 1 (Table 2). Adding the azido-modified Ab did not modify LNC size, but significantly ($p< 0,05$) increased LNC zeta potential from -28 mV to -19 mV.

Formulations	Size (nm)	PDI	Zeta-Potential (mV)
LNC	58 ± 3	0.04 ± 0.03	-3 ± 0.6
LNC-DBCO	66 ± 2	0.11 ±0.09	-28 ± 3
LNC-Ab (approach 3)	67 ± 1	0.11 ± 0.10	-19 ± 2

Table 2. Impact of Ab grafting using Approach 3 on LNC physicochemical properties.
Size, PDI and Zeta potential were measured by Nanosizer in water. The values were presented as mean±SD (N=3, n=3). Statistical significance was determined by a one-way ANOVA test, *$p < 0.05$.

When using a 1:100 molar ratio of PEG-DBCO: Kolliphor HS®, no Ab was detected using primary amine quantification. As it is selective, click-chemistry offers less linkage sites. Thus, to compensate the lower amount of linking sites, the ratio of PEG-DBCO: Kolliphor HS® was increased to 1:50. Using this molar ratio, an average of 5±3 Ab per LNC was obtained (23±7 % of grafting efficiency).

Ab azido-modification (Ab-N_3) and PEGylation using PEG-DBCO (Ab-PEG-DBCO) did not affect Ab interaction with the PDGFRα (Fig. 5A). When Ab-PEG-DBCO was grafted on LNC surface, the Ab was still able to recognize its target, albeit to a lesser extent than the unmodified Ab (Fig. 5B). This grafting strategy was consequently used for the following experiments.

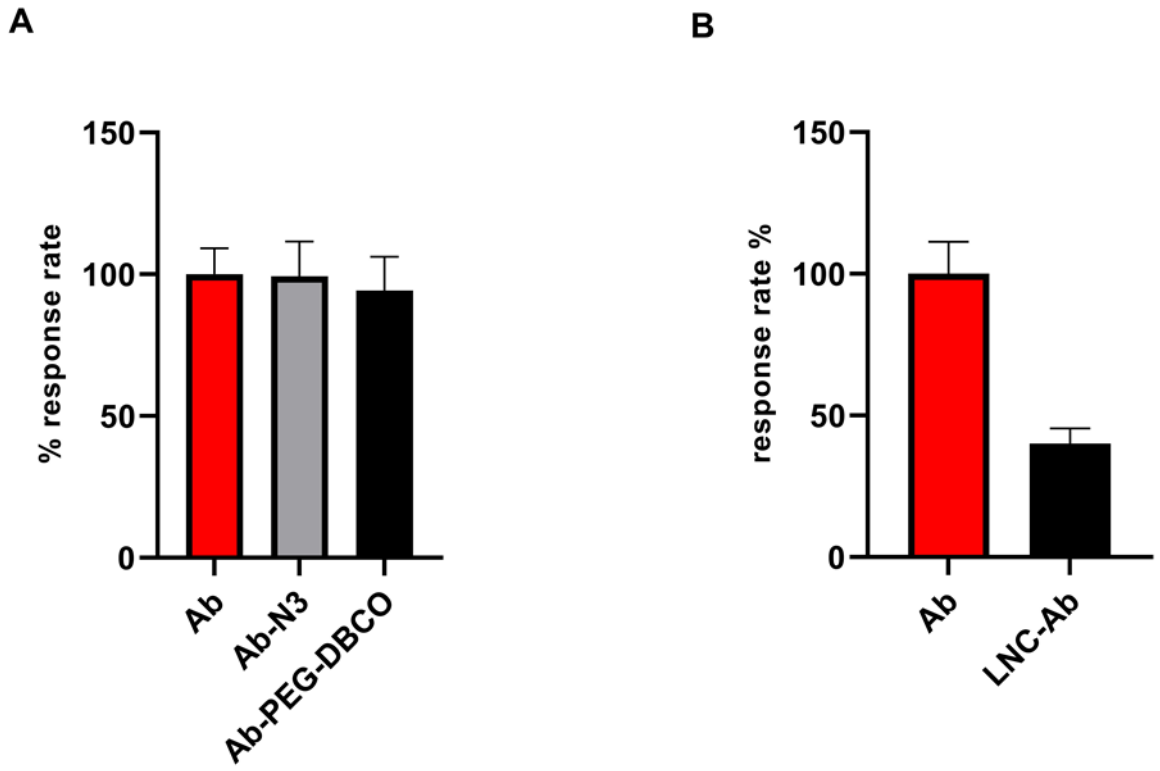

Figure 5. Impact of Ab grafting with approach 3 on its interaction with PDGFRα.
An ELISA was used to determine the interaction between the Ab and its target protein (PDGFRα) for (A) modified Ab and (B) Ab grafted on the LNC. Data are shown as a percentage of 1nM Ab response to 20 nM of PDGFRα. All percentage were calculated relatively to Ab (unmodified anti-PDGFRα). The values were presented as mean±SD (N=3, with 3 different batches of LNC-Ab, Ab-N3 and Ab-PEG-DBCO).

III.5. IMPACT OF AB GRAFTING AT LNC SURFACE ON LNC INTERACTIONS WITH OPC

This part of the study aimed to characterize the interactions between LNC-Ab obtained with Approach 3 and OPC *in vitro*.

First, LNC impact on OPC viability was evaluated. The highest nontoxic concentration was 0.31 mg/ml of LNC for 1 and 4h of incubation (Fig.6). However, LNC were toxic (no metabolic activity) for OPC after 24h of incubation whatever the concentration (data not shown).

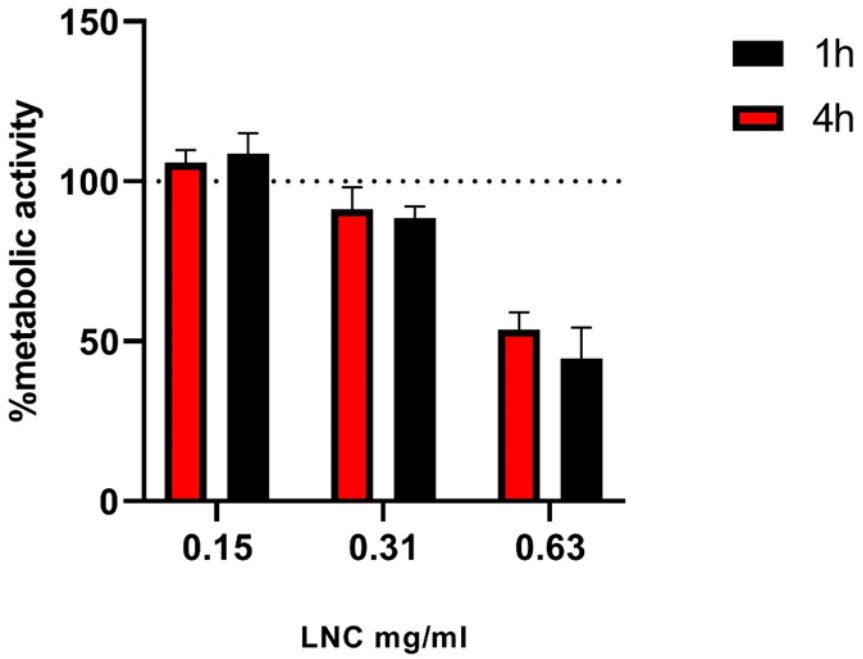

Figure 6. Effect of LNC on OPC viability.
OPC were incubated in the presence of LNC for 1 and 4h before assessment of their viability using PrestoBlue® Cell Viability Reagent. The dotted line represents 100% of living cell and corresponds to untreated OPC. The values were presented as mean±SD (N=3, n=4).

Then, DiD-loaded LNC-Ab, in conjunction with confocal microscopy and FACS, were used to assess whether LNC-Ab were able to interact with OPC. As illustrated by figure 7, LNC (DiD)-Ab were mainly visible in the cytoplasm of OPC, supporting their ability to enter these cells. Additional pictures of OPC treated with LNC (DiD)-Ab and negative control (untreated OPC) can be found in supplementary data (Fig 3.S).

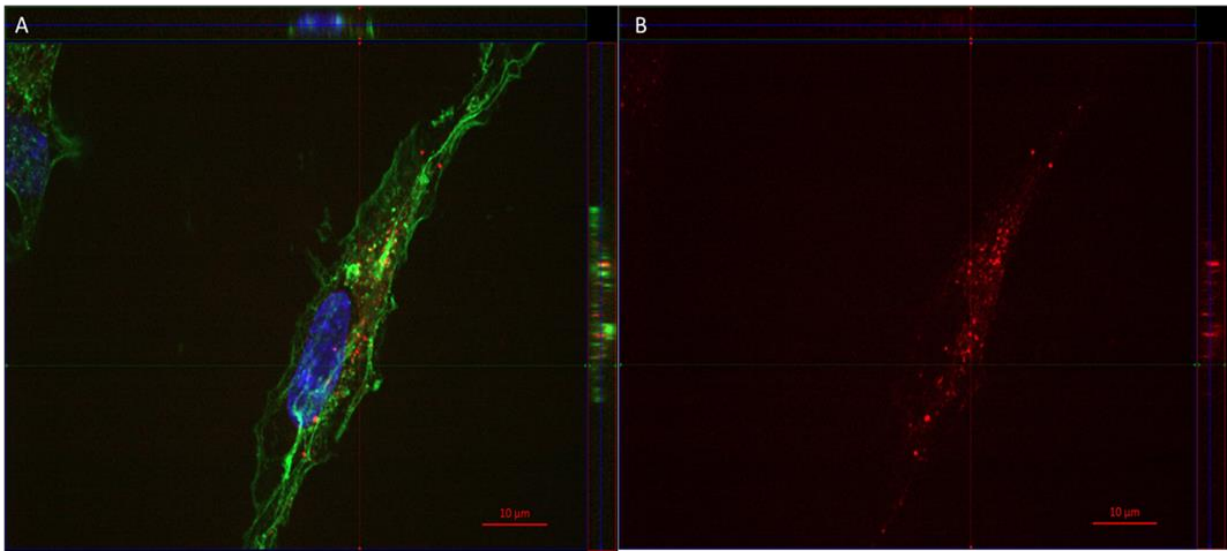

Figure 7. Visualization of LNC-Ab localization in OPC.

Representative picture of LNC localization in OPC. LNC-Ab were diluted to 0.42 mg/ml in OPC media and incubated 1 h with the cells. Blue is DAPI for cell nucleus; green is Alexa 488-Phalloidine, for F-actin, cytoskeleton; red is DiD for LNC.(A) Merged image of y−z, x−z, and z−y sections; (B) DiD-labeled LNC image of y−z, x−z, and z−y sections.

FACS was then used to quantify the amount of LNC associated with OPC and whether the Ab at LNC surface would increase LNC/OPC association compared to unmodified LNC. As shown in figure 8, grafting of the PDGFRα Ab at LNC surface allowed to increase by 1.5-fold their association with OPC.

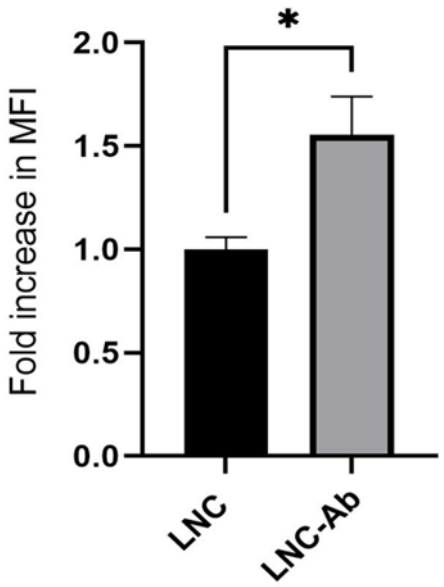

Figure 8. Impact of anti-PDGFRα grafting on LNC OPC-associated fluorescence. DiD-Loaded LNC were incubated for 30 min with OPC at a concentration of 0.15 mg/ml. The fold increase in Mean Fluorescence Intensity per cell (MFI) was calculated relatively to LNC's MFI. Statistical significance was calculated based on an unpaired t-test *$p < 0.05$. The values were presented as mean±SD (N=3, n=3).

As modifying the surface of a nanomedicine can strongly influence its interaction with cells [230, 231], this part aimed to determine whether the increased interaction of LNC-Ab with OPC was specific of the anti-PDGFRα or was linked to LNC surface modification due to Ab grafting. Thus, OPC association with LNC-Ab was compared with LNC grafted with an isotype control (LNC-IgG2a). It appeared that grafting the isotype control had the same effect than grafting the anti-PDGFRα (Fig. 9). Finally, to determine if LNC-Ab interactions with OPC could be affected by the presence of PDGFAA in the culture medium, the same experiment was repeated but without PDGFAA (i.e. the ligand of the receptor targeted by the Ab). However, the results were the same as the ones obtained in the presence of PDGFAA.

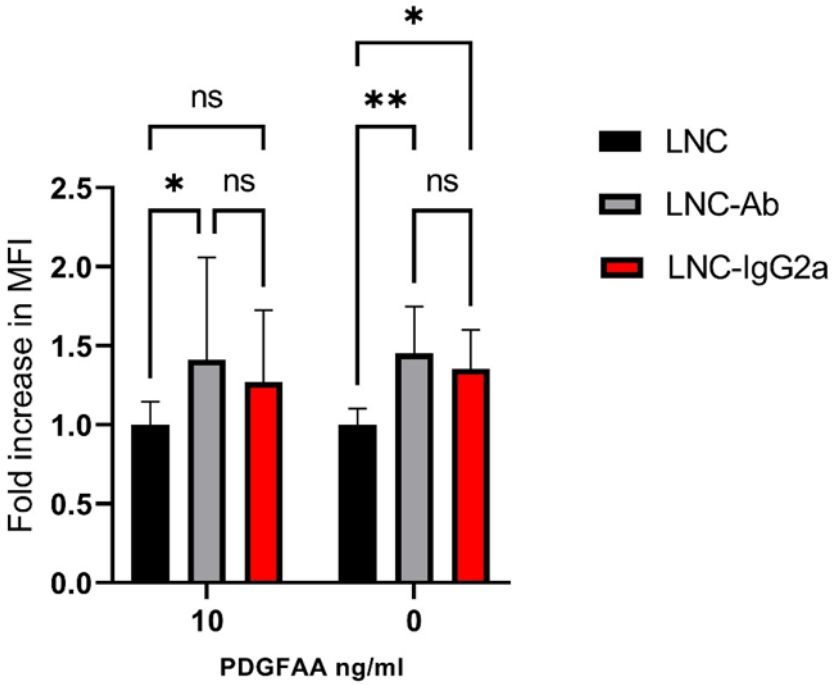

Figure 9. Impact of LNC-Ab and LNC-IgG2a uptake by OPCs in the presence of PDGFAA in the media. Statistical significance was calculated based on a two-way ANOVA*p < 0.05, **p<0,01. The values were presented as mean±SD (N=3, n=3).

IV. DISCUSSION

Nowadays, the only treatments available for multiple sclerosis are immunomodulatory therapies with mostly a peripheral action. Although they limit the burden of the symptoms, none of them stimulate the remyelination process [232]. This is why, for the last decades, researchers have developed strategies to promote remyelination, notably by inducing OPC differentiation into myelinating oligodendrocytes. Nevertheless, these therapies need to be efficiently delivered to OPC to be effective, and this aspect remains challenging. Hence, our goal was to improve the efficiency of pro-remyelinating therapies by improving their delivery and selectivity towards OPC. To do so, we selected lipid-based nanocarriers and we grafted an anti-PDGFRα at their surface to specifically target OPC. In the present work, for the first time, we successfully grafted an anti-PDGFRα at LNC surface, comparing two strategies: thiol-maleimide interaction and copper less click-chemistry. We were also able to quantify Ab at LNC surface, and for the first time, to demonstrate that modification of LNC surface by an antibody affected their uptake by OPC.

The thiol-maleimide chemistry is a classic technique widely used to modify nanoparticle surface [233]. To attach the maleimide moiety, we used two approaches already described in the literature, transacylation (approach 1) and post-insertion (approach 2). The transacylation of NH_2-PEG-Maleimide has never been used to graft an antibody at LNC surface. However, transacylation itself has been used to functionalize LNC surface with chitosan by Messaouidi et al. [221]. We observed an increase of LNC size and a decrease of zeta potential after post-insertion of DSPE-PEG-Maleimide. Perrier et al. reported similar observations [222] after the post-insertion of DPSE-PEG-OCH_3. However, in the work of Béduneau et al., after post-insertion of DPSE-PEG-Maleimide, the size of LNC increased to a lesser extent than in our case (+24 nm vs. +7 nm in our study) [124]. This might be explained by the smaller amount of maleimide moiety used in our work (50-fold lower).

To compare the different approaches regarding grafting efficiency, a reliable method to quantify the Ab at LNC surface was essential. Unfortunately, LNC interacted with most of the classical used methods for proteic ligand quantification or detection at a nanoparticle surface (i.e., Bradford, RMN, SDS PAGE…) [35, 234, 235], inducing a strong background signal (data not shown). Only the method developed by Schelte et al., based on primary amine quantification, allowed the direct quantification of the Ab at LNC surface without interferences [224]. To our knowledge, this is the first time that this methodology has been used to quantify an antibody at LNC surface and represent a real asset for surface modification characterization of LNC with a proteic moiety. We observed that transacylation provided the highest grafting efficiency compared to post-insertion.

As transacylation linked the maleimide moiety covalently to LNC surface when post-insertion only incorporated it in the LNC shell, we hypothesized that either more maleimide moieties were attached to LNC, as the whole LNC surface was accessible, or/and that the association was more stable in case of transacylation. To our knowledge, no other work has been published concerning the grafting of an antibody on LNC surface using the transacylation of NH_2-PEG-Maleimide, and no other study directly compared post-insertion and transacylation. Béduneau et al. successfully grafted an antibody at the surface of LNC using post-insertion and calculated that +/- 67 antibodies were incorporated in LNC, but they used an indirect quantification [124].

Chemical modification of antibodies occurring during grafting can hinder their ability to associate with their antigen. We found that thiolation of antibody's lysines with IMT did not decrease Ab response level. However, the subsequent PEGylation of the thiol residues resulted in the loss of Ab activity. Our results suggest that PEGylation very likely occurred at the Fv region of Ab upon thiolation by IMT of the lysines of the Fv region. Hence, the pegylation of the Ab most likely hindered its interaction with PDGFRα resulting in a loss of Ab activity. This could explain why LNC-Ab obtained using approaches 1 and 2 were not able to interact with PDGFRα. Of note, Béduneau et al. also demonstrated that a thiolated OX26 antibody could still interact with its target, but no investigation was made after grafting of the antibody on the nanoparticle [124]. Kitamura et al. reported that the unspecific coupling of PEG via active ester on an antibody led to a decrease of 90% of the antibody activity [236]. The decrease was linked to the number of PEG on the antibody and their molecular weight, reinforcing the hypothesis of a steric hindrance [236, 237]. This is why we finally used the more specific approach represented by the click-chemistry. While fewer Ab were grafted per LNC, nor its azido modification nor its PEGylation affected the Ab association with PDGFRα. Gai et al. modified an anti-CD11 Ab using the same strategy and observed no impact of the azido modification on the anti-CD11 functional integrity compared to the native antibody [238]. Taken together, our data and those reported by others put forth a site-specific modification strategy for Ab grafting.

Nonetheless, we found that once on LNC surface the Ab response level decreased of 40%. We hypothesized that this could be due to a steric hindrance created by the LNC, mainly via the PEG moieties at its surface, as they could prevent the Ab from reaching its target. Interestingly, Botosa et al. observed a similar phenomenon with PEGylated liposomes. They demonstrated, using surface plasmon resonance, that antibody-functionalized liposomes could interact with their antigen, whereas PEGylated antibody functionalized liposomes had a decreased interaction with the antigen. They showed that it was related to PEGylated lipid fraction and PEG molecular weight [239].

The association of LNC-Ab with primary OPC cultures was higher than LNC but the extent of this increase was more modest than we hoped for. As OPC uptook LNC quite quickly (87% of the cells were DiD positive after 30 min of incubation only) the advantage conferred by the Ab was more difficult to highlight. While the uptake of the lipid-based nanoparticles by OPC is not extensively studied, Osorio-Querejeta et al. found that primary OPC endocytosed liposomes to a greater extent than PLGA nanoparticles and exosomes (96%, 83 %, and 61%, respectively) [240]. This tropism for lipid-based nanoparticles is likely due to the involvement of several unspecific endocytosis pathways, as reported for other types of cells. For instance, it has been shown that vectorized LNC with the NFL-TBS.40–63 peptide use clathrin-, caveolin-, and micropinocytosis-mediated pathways to enter oligodendrocytes [241], whereas for monocytes they use mostly caveolae-mediated endocytosis and pinocytosis [242].

For the targeting to be efficient, LNC need to enter OPC primarily by specific receptor-mediated endocytosis rather than by unspecific pathways such as those mentioned above. The antibody addition only induced a slight increase in uptake. Probably because the uptake occurring through receptor-mediated endocytosis is negligible compared to the other pathways. It can be speculated that a nanoparticle with a lower tropism for OPC would have been more suitable to target OPC, as receptor-mediated endocytosis would have been the most significant route to penetrate the cell. As many studies have demonstrated that different types of nanoparticles have different uptake rates for the same cell line [223], this strategy could be considered for future experiments.

Lastly, we observed that grafting an isotype control produced the same increase in LNC/OPC association as grafting the anti-PDGFRα antibody. While this critical control is lacking in many papers, Walters et al. showed that the grafting of an isotype control on PLGA nanoparticle surface increased their cell association compared to the unmodified nanoparticle [243]. We can hypothesize that this could be due to the interaction of the Fc region with the immunoglobulin Fc receptors (FcR). These receptors are traditionally at the surface of immune cells, such as macrophages and monocytes, but are also present at OPC surface (especially the γ subunit) [244]. Hence, having an antibody at LNC surface may have unlocked receptor-mediated endocytosis via the FcR. The question remains on whether increasing the anti-PDGFRα at LNC surface is required to reach a threshold allowing to differentiate between Ab and control isotype as suggested by some studies [245].

V. CONCLUSION

In summary, we produced anti-PDGFRα functionalized LNC to target OPC to favor remyelination and reduce off-target effects by targeting OPC. To graft the antibody, we used three different approaches (transacylation, post-insertion of maleimide moiety and finally coperless click-chemistry). To evaluate the anti-PDGFRα grafting efficiency on LNC, we used primary amine quantification. This method can be considered a real asset to quantify the amount of functionalized protein moiety on LNC since these nanoparticles interfere with classical protein quantification techniques. We also developed an in-house ELISA to gauge the anti-PDGFRα activity after grafting on LNC. Our results demonstrated that site-selective antibody grafting on nanoparticles was the best way to maintain its activity. Nevertheless, *in vitro* uptake by primary OPC was only modestly increased by the Ab grafting and to the same extent as isotype control-grafted LNC. This observation highlights how crucial appropriate control is for uptake studies involving nanoparticle surface modification and how this modification impacts cell-nanoparticle interaction.

VI. SUPPLEMENTARY DATA

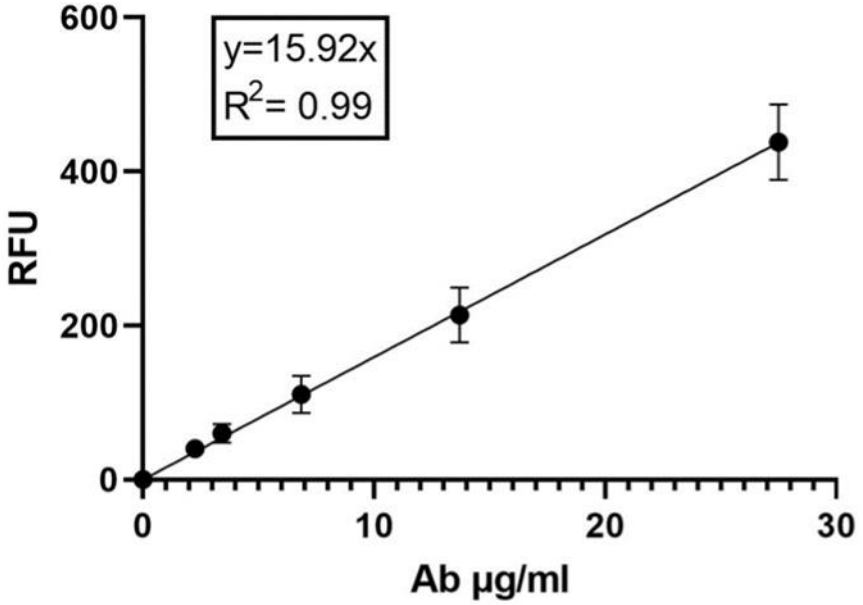

Figure 1.S. Calibration curve for the Ab quantification.
The calibration curve was built to quantify the PDGFRα Ab in presence of LNC used as matrix The values were presented as mean±SEM (N=3).

Formulation	Number of particles per L
LNC-Ab (Approach 1)	$4{,}3.10^{15} \pm 1{,}4.10^{15}$
LNC-Ab (Approach 2)	$3{,}2.10^{16} \pm 2.10^{16}$
LNC-Ab (Approach 3)	$3{,}8.10^{15} \pm 1{,}2.10^{15}$

Table 1.S. Measurement of LNC-Ab particles concentration using Nanoparticles Tracking Analysis. The values were presented as mean±SD (N=3)

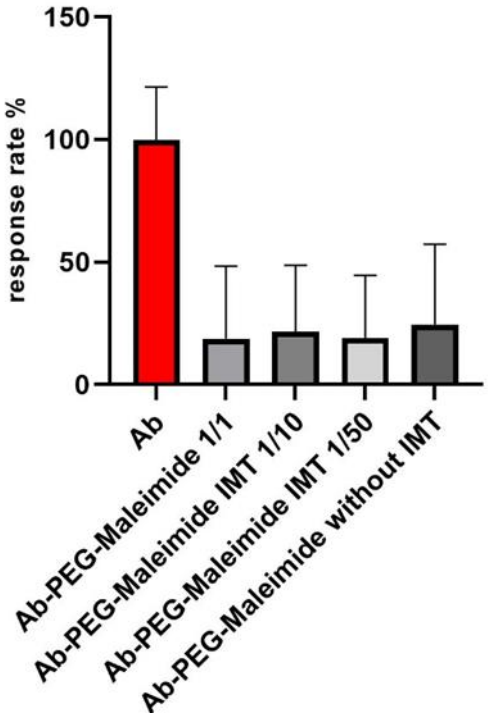

Figure 2.S. Impact of 2-Iminothiolane•HCl concentration on Ab interaction with PDGFRα.

An ELISA was used to determine the interaction between the Ab and its target protein (PDGFRα). Different concentrations of IMT were used to thiolate the antibody, going from the initial concentration used in the rest of the study (Ab-PEG-Maleimide 1/1) to 0 (Ab-PEG-Maleimide without IMT). Data are shown as a percentage of 1nM Ab response to 20 nM of PDGFRα. All rates were calculated relatively to Ab (i.e., unmodified anti-PDGFRα). The values were presented as mean±SD (N=3)

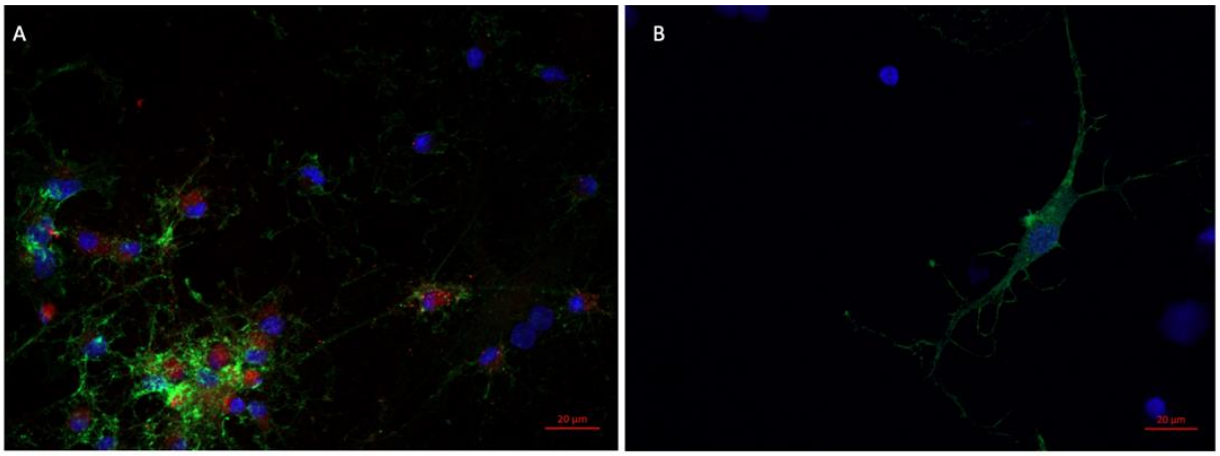

Figure 3.S. Additional visualization of LNC-Ab localization in OPC.

(A) Representative picture of LNC localization in OPC. LNC-Ab were diluted to 0,42 mg/ml in OPC media and incubated 1 h with the cells. (B) Untreated OPC (negative control). Blue is DAPI for cell nucleus; green is Alexa 488-Phalloidine, for F-actin, cytoskeleton; red is DiD for LNCpresented as mean±SD (N=3)

CHAPTER III

IMPACT OF RETINOIC ACID AND CALCITRIOL LOADED LNC ON REMYELINATION AFTER INTRANASAL DELIVERY IN A CUPRIZONE MODEL

Labrak Y., Al Houayek M., Mwema A., d'Auria L., Ucakar B., Muccioli G.G., Rieux A.

ABSTRACT

The blood-brain-barrier (BBB) is a formidable protective barrier that prevents toxic elements from penetrating the central nervous system (CNS); However, this barrier also limits the distribution of therapeutics in the brain and thus hinders the treatment of CNS diseases such as multiple sclerosis (MS). Intranasal administration can be an efficient strategy for bypassing the BBB, favoring drug accumulation in the brain, and improving efficacy. To engineer an optimal intranasal formulation, compounds need to be soluble in a physiological solution that can be easily administrated. Therefore, finding a way to solubilize lipophilic compounds to be administrated by this route is essential. Lipid nanocapsules (LNC) can be suitable nanocarriers for this matter; indeed, they have a lipophilic core that can favor lipophilic compound encapsulation, and drug-loaded LNC can be easily diluted in physiological solutions. Additionally, they are FDA-approved excipients, easily up-scalable. Oligodendrocyte progenitor cells (OPC) are at the heart of the myelin regeneration process that occurs after demyelination in MS. These cells can differentiate into myelinating oligodendrocytes that reform a new myelin sheath. Thus, we aimed to encapsulate in LNC two lipophilic compounds that can promote OPC differentiation, retinoic acid (RA) and calcitriol (Cal), to develop an intranasal solution that can be of use in the context of pro-remyelinating therapies. After encapsulation of RA (LNC-RA) and Cal (LNC-Cal), HPLC-UV analysis indicated stable molecules for at least 8 weeks. Our results show that RA and Cal maintained their ability to differentiate CG-4 cells (an OPC cell-line) after encapsulation in LNC. Finally, we evaluated our formulation *in vivo* in the cuprizone murine model of demyelination. After intranasal administration, LNC and LNC-CARA (i.e. LNC-RA + LNC-Cal) increased corpus callosum myelination and microglial infiltration. In conclusion, intranasal delivery of lipophilic drug encapsulated LNC is a potential route of administration for myelinating therapies.

KEYWORDS

Lipid nanocapsules, Intranasal delivery, Multiple sclerosis, Nanomedicine, Remyelination

TABLE OF CONTENTS

I. INTRODUCTION 101

II. MATERIALS AND METHOD 102

II.1. MATERIALS 102

II.2. RETINOIC ACID-LOADED LNC (LNC-RA) AND CALCITRIOL-LOADED LNC (LNC-CAL) 102

II.3. LNC-RA AND LNC-CAL CHARACTERIZATION 103

II.4. RA, LNC-RA, CAL AND LNC-CAL STABILITY OVER TIME 103

II.5. CG-4 CELL LINE CULTURE 104

II.6. MIXED GLIAL CELL CULTURE 104

II.7. BV-2 CELL LINE CULTURE 105

II.8. REAL-TIME QUANTITATIVE POLYMERASE CHAIN REACTION (QPCR) 105

II.9. RA-LNC AND CAL-LNC NOSE-TO-BRAIN ADMINISTRATION IN A MOUSE CUPRIZONE MODEL 106

II.10. HISTOLOGY 107

II.11. STATISTICAL ANALYSIS 107

III. RESULTS 108

III.1. IMPACT OF RA AND CAL ENCAPSULATION ON LNC PHYSICOCHEMICAL PROPERTIES 108

III.2. IMPACT OF LNC-RA AND LNC-CAL ON CG-4 DIFFERENTIATION 109

III.3. IMPACT OF CARA AND LNC-CARA ON REMYELINATION AND PRO-INFLAMMATORY MICROGLIA INFILTRATION AFTER NASAL ADMINISTRATION IN THE CUPRIZONE MODEL 114

IV. DISCUSSION 116

V. CONCLUSION 120

VI. SUPPLEMENTARY DATA 121

I. INTRODUCTION

The differentiation of oligodendrocyte progenitor cells (OPC) into oligodendrocytes is one of the fundamental mechanisms behind the remyelination process that follows myelin sheath damage in multiple sclerosis (MS) [25]. Nowadays, finding compounds to enhance myelin sheath regeneration is at the core of MS research. Among the compounds in clinical trials for remyelination, opacinumab and clemastine showed effective remyelination in animal models [105]. However, they were not effective in inducing remyelination in clinical trials. One of the reasons for this failure may be a low distribution of these drugs in the brain. Central nervous system (CNS) drug delivery is one of the most prominent challenges scientists must face due to the blood-brain barrier (BBB). The primary function of the BBB is to protect the CNS from harmful elements (i.e., toxins), and only drugs with a high logP and a molecular weight less than 400 Da can cross passively [246]. Intranasal delivery has the advantage of bypassing the BBB, making it an interesting administration route [203]. Indeed, the olfactive bulb and the trigeminal nerve give direct access to the brain through transcellular or paracellular pathways. In addition to offering privileged access to the CNS, intranasal delivery has the advantage of being non-invasive and patient friendly. This aspect is a considerable asset since MS patients are often subjected to invasive administration such as intravenous (IV) (i.e., natalizumab) subcutaneous (i.e., glatiramer acetate) or intramuscular administration (i.e., IFN-ß). Thus, having treatment for MS in the form of a nasal spray could be more convenient for patients.

All-trans-retinoic acid (RA) and calcitriol (Cal) are two lipophilic molecules known to promote remyelination in animal models of MS [100, 206]. RA binds to the RAR and Cal to VDR to form a heterodimer with RXR. The RAR/RXR or VDR/RXR complexes migrate to the nuclei and bind to RARE transcription factor (retinoic acid response element) for the former and the VDRE (Vitamin D Response Element) for the latter. These events will trigger the regulation of genes responsible for remyelination and OPC differentiation. Furthermore, these two compounds also have immunomodulatory properties that can be favorable in the scope of neuroinflammatory diseases such as MS [204, 247]. Therefore, they could be good candidates for MS treatment if their delivery to the CNS is selectively increased. However, nasal administration can be challenging when dealing with active lipophilic compounds. Indeed, these molecules are insoluble in physiological solution. Therefore, they can only be administrated as a nasal spray suspension composed of macroscopic particles that are strongly prone to elimination by ciliary cells in the nasal epithelium [203]. We hypothesized that the encapsulation of lipophilic molecules in LNC would improve their distribution in the CNS by allowing their solubilization and protection from enzymatic degradation in the nasal cavity. Moreover, recent studies have shown that LNC can cross the olfactive bulb and reach the brain (Mwema et al. in preparation). Therefore, we propose to encapsulate RA and Cal in LNC for optimal intranasal delivery of those molecules. [6, 7].

II. MATERIALS AND METHOD

II.1. MATERIALS

Labrafac® WL 1349 was provided by Gattefosse SA (France) and Lipoïd® S100 by Lipoid Gmbh (Germany). Solutol HS®15, poly-d-Lysine hydrobromide (70000–150000 Da), Sodium pyruvate, Insulin, Apo-transferrin, Biotin, Selenium, Holo-transferrin Bovine insulin, Fetal Bovine Serum (FBS), Lipopolysaccharides (LPS) from E. *coli* (serotype O55:B5,), Dapi, Charcoal, and all-trans retinoic acid were purchased from Sigma (Merck, Germany). Calcitriol was purchased from Win-Win Chemical CO., Limited (China). DMEM, HEPES, Pen/Strep, B27 supplements, Amphotericin B, DMEM 0.05% trypsin-EDTA (1x), Presto blue Cell Viability Reagent, Trizol reagent, Alexa-Fluor 568 goat anti-rat, Alexa-Fluor 647 goat anti-rabbit, and Green Fluoromyelin, were purchased from Thermo Fisher Scientific (Bleiswijk, The Netherlands). Myelin Basic Protein (MBP) rat monoclonal antibody was purchased from Biorad (United-States) and Ionized calcium-binding adaptor molecule-1 (Iba1) rabbit polyclonal antibody from Wako (Japan). Murine interleukin-6 (IL-6), Tumor Necrosis Factor α TNFα and monocytes chemoattractant protein-1 (MCP-1) ELISA kit, Platelet-derived growth factor A (PDGF-AA), fibroblast growth factor 2 (FGF), and Ciliary neurotrophic factor (CNTF) were purchased from Peprotech (United Kingdom). Amicon Ultra-0.5 mL 30 K filters were purchased from Merck Millipore (Germany). Rotilabo®-syringe sterile 0.22 µm, filters, RotiFix© Paraformaldehyde (PFA), Dimethyl sulfoxide, and trifluoroacetic acid were purchased from Carl Roth GmbH (Germany). Acetonitrile and SuperFrost plus slides were purchased from VWR (). Primers for RT-qPCR were purchased from Integrated D.N.A. technologies (Leuven, Belgium). Cuprizone (0,2% cuprizone) and control chow were purchased from SSNIFF (Germany). Reverse transcription kit was purchased from Promega Benelux BV (Leiden, The Netherlands)) and Tissue-Tek® Optimal cutting temperature compound (OCT) from Sakura Finetek (United-States)

II.2. RETINOIC ACID-LOADED LNC (LNC-RA) AND CALCITRIOL-LOADED LNC (LNC-CAL)

LNC were prepared following the protocol described in chapter 2. Briefly, 0.288 g of Solutol HS 15, 0.025 g of Lipoïd® S100, 0.029 g of NaCl, 400µL of Labrafac®WL 1349, and 0.9 mL of water were mixed under magnetic stirring for 5 min at 45 °C. Three temperature cycles of heating/cooling were done between 60 °C and 90 °C, also under magnetic stirring. During the cooling of the last cycle, at 77 °C, 3.7 ml of cold water were added under high-speed stirring. As for LNC-RA and LNC-Cal ([RA] = 1mM and [Cal]= 1mM), they were prepared by adding 37.5 µL of RA or Cal

stock solution (40 mg/mL and 55 mg/ml in DMSO, respectively) during the last cooling of LNC preparation (final volume of 5 mL). Similarly, blank LNC were prepared by adding 37.5 µL of DMSO at the last cooling cycle. LNC were filtered on 0.22 µm filter and stored at 4 °C until further use.

II.3. LNC-RA AND LNC-CAL CHARACTERIZATION

Size, zeta potential, and polydispersity index (PDI) of the formulations were measured in water using a ZetasizerUltra® (United Kingdom).

RA and Cal were extracted from RA-LNC and Cal-LNC by dissolution in methanol at a ratio of 1:20 (RA total). LNC structure disintegrates by dissolution in methanol at a ratio of 1:20 (*total amount of compound)*. In parallel, non-encapsulated RA and Cal were removed from LNC formulation by ultra-filtration using a 30-KDa molecular weight cut-off membrane. Both molecules were quantified by High Pressure Liquid Chromatography coupled to aUV detector (Shimadzu®). The separation was obtained using a Macherey-Nagel® 125/4 NUCLEODUR 100-5 C 18 column and an isocratic system (1mL/min). For RA, the mobile phase was composed of water and acetonitrile (15:85, vol/vol), containing 0.1% TFA while for Cal it was composed of water and acetonitrile (30:70, vol/vol). The volume of injection was 20 µL and the detection wavelength was set at 342 nm for RA and 269 nm for Cal. RA and Cal encapsulation efficiencies were calculated using the following formula:

$$Encapsulation\ Efficiency = \frac{Total\ amount\ of\ compound - non\ encapsulated\ compound}{Compound\ introduced\ in\ the\ formulation} \times 100$$

II.4. RA, LNC-RA, CAL AND LNC-CAL STABILITY OVER TIME

A solution of 1mM of RA in DMSO and a solution of 1mM of Cal in DMSO, as well as LNC-RA and LNC-Cal were stored at 4°C, protected from light. RA and Cal were quantified by HPLC-UV once a week for 8 weeks using the method mentioned above. The percentage of the remaining compound was calculated using the following formula:

$$Remaining\ compound\ (\%) = \frac{Compound\ at\ week\ n}{Compound\ at\ week\ 1} \times 100$$

Size, zeta potential, and PDI of LNC were also measured every week as described in 2.3.

II.5. CG-4 CELL LINE CULTURE

CG-4 cells were grown in proliferation medium (DMEM, 1% penicillin/streptomycin, apo-transferrin, Biotin, Selenium, insulin, B104 conditioned media) and were plated at 50 000 cell/well in 6 well plates in recovery medium (DMEM, 1% penicillin/streptomycin, insulin, sodium pyruvate, HEPES). After 30 minutes, the medium was replaced by a fresh proliferation medium. Cells were cultured overnight under standard conditions (37 °C in a humidified 5% CO_2 incubator). CG-4 cells were treated with RA-LNC, Cal-LNC and a combination of RA-LNC + Cal-LNC (LNC-CARA) for 24h in proliferation medium, followed by 5 days of culture in fresh proliferation medium. RA, Cal, a 1:1 combination of Cal and RA (CARA) and LNC were used as controls. Then, 500 µL of Trizol were added to each/well and the plates were then stored at − 80 °C for later assessment

II.6. MIXED GLIAL CELL CULTURE

Cortical mixed glial cultures were generated from Sprague-Dawley rat pups (postnatal day 0-2) as described previously by Miron et al. [43]. All the experiments involving animals were done in accordance with Directive 2010/63/E.U. and following the approval by the ethical committee for animal care of the faculty of medicine of UCLouvain (2017/UCL/MD/030). Briefly, brains were dissected, cerebellum, olfactory bulbs, and meninges were removed. Brains were then digested using papain (40 µg/mL) and slowly dissociated mechanically using a G18 and a G23 syringe. The cell suspension was diluted in DMEM medium (4.5 g/L glucose, L-glutamine, pyruvate, 10% FBS (vol/vol) and 1% penicillin/streptomycin (vol/vol)) then filtered through a 40 µm strainer. As FBS may contain RA and Cal, to avoid any interference with our treatments, FBS was treated with charcoal as described [207] to deplete it in RA, Cal, and steroids. FBS was incubated with 2.5% (w/vol) of activated charcoal for 18 h at 4°C and filtered before adding it to the mixed glial cell culture medium. Cells were then plated at 5×10^4 cells/well in poly-D-Lysine coated (1µg/mL) 24 well plates for 8 days. Mixed-glial cells culture were treated with RA-LNC, Cal-LNC and CARA-LNC for 24 hours. RA, Cal, CARA and LNC were used as controls. After treatment removal, cells were cultured for 5 days in DMEM medium. At the end of the process, 200 µL of Trizol were added to each well. Samples were then stored at − 80 °C for later assessment.

II.7. BV-2 CELL LINE CULTURE

BV-2 cells (murine microglial cell line) were grown in high-glucose DMEM medium with 10% FBS and 1% penicillin/streptomycin (vol/vol) under standard conditions [248]. The cells were seeded into 24-well plates at 200 000/well and treated the following day with 100 ng/mL of LPS for one-hour. Then, BV2 cells were incubated with RA-LNC, Cal-LNC and CARA-LNC diluted at concentrations ranging from (0,03 μM to 3 μM) in fresh media containing LPS at 100 ng/mL. RA, Cal, CARA and LNC were used as controls. After 8 hours of incubation, supernatants were collected and stored at -20°C for IL-6, TNFα and MCP-1 quantification by ELISA.

II.8. REAL-TIME QUANTITATIVE POLYMERASE CHAIN REACTION (QPCR)

Total RNA was extracted using the Trizol reagent. cDNA was synthesized using the GoScript reverse transcription kit (Promega) from 1 μg of total RNA. qPCR was performed using the GoTaq qPCR Master Mix (Promega) and a STEPone PLUS instrument and software (Applied Biosystems). Products were analyzed by performing a melting curve at the end of the PCR reaction. Data were analyzed with the ΔΔCt method using the 60S ribosomal protein L13 (RPL13) as a reference gene. RPL13 mRNA expression was not affected by any of the treatments. Primer sequences used are given in Table 1.

Table 1 : Primer sequences

Gene/product	Forward primer (5' to 3')	Reverse primer (5' to 3')
Mbp/MBP	CACACACAAGAACTACCCACTAC	GGTGTACGAGGTGTCACAATG
Rpl13/RPL13	GGCTGAAGCCTACCAGAAAG	CTTTGCCTTTTCCTTCCGTT

MBP: Myelin Basic Protein

II.9. RA-LNC AND CAL-LNC NOSE-TO-BRAIN ADMINISTRATION IN A MOUSE CUPRIZONE MODEL

Fifty-six 7-week-old male C57Bl/6 mice (Janvier©, France) were used for this experiment (n=6 per group). They were housed in filter-top cages under conditions of controlled temperature (20°C-22°C) and artificial light (12 hours dark/12 hours light) and supplied with water and food ad libitum. All experiments were performed in accordance with the guidelines of the local ethics committee 2018/UCL/MD/024 and in accordance with European Directive 2010/63/E.U. To induce demyelination, mice were given chow (Ssniff©, S8899-E040) containing 0.2% cuprizone for six weeks [101]. Control mice received the same chow but without cuprizone. LNC-CARA (1mM) or CARA (1mM) was diluted in saline and administrated by nasal instillation (5 µL/nostril x 4, 20 µL in total/mouse) under isoflurane anesthesia every day for 6 days (Fig.1). Saline (vehicle) and LNC were used as controls. Mice were euthanized and perfused with PFA 4% the day following the last administration. Brains were stored for 24h in PFA 4% at RT followed by 24h in a 30% sucrose solution. Tissues were embedded in OCT and kept at − 80 °C.

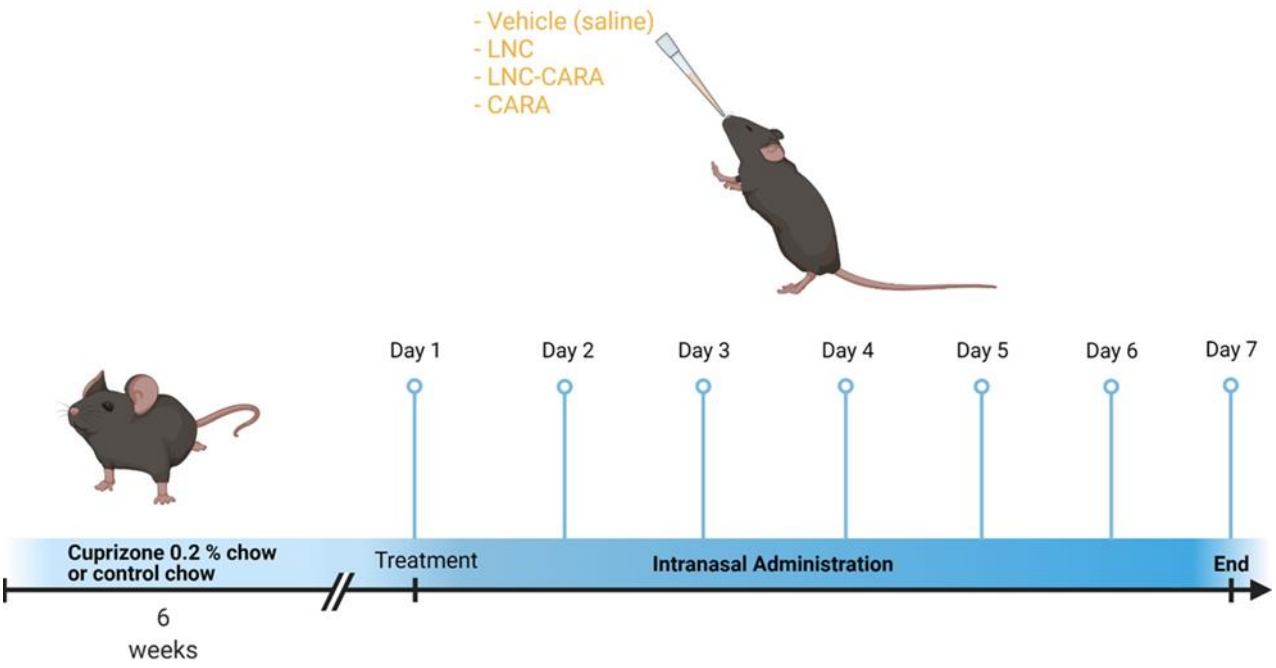

Figure 1. Study design to evaluate the impact of treatments on remyelination in a cuprizone model

II.10. HISTOLOGY

Brain rostral cryosections were serial sliced using a cryostat at a thickness of 10 µm (n=6). Each slide contained three to four brain slices. For immunofluorescence staining, cryosections were incubated in block solution (0.3% triton and 5% normal goat serum (NGS) in PBS) for 1h. Next, sections were incubated with primary antibodies (Iba1 1/1000 and Myelin Basic Protein (MBP) 1/300 in block solution) overnight at 4 °C. Detection was performed after incubation with relevant fluorescent secondary antibodies (Alexa-Fluor 568 conjugated goat anti-rat (1/500) and Alexa-Fluor 647 conjugated goat anti-rabbit (1/500), respectively), FluoroMyelin (1/300) and Dapi (1/1000) in block solution for 4h at RT. Image acquisition was performed using a Panoramic P250 Flash III slide scanner (3DHISTECH). Image analysis was performed with Visiopharm© software to quantify the surface of positive staining per analyzed area. Manual thresholding was applied using the control brain section (healthy mice without cuprizone). Three to four brain slices were analyzed per animal, and the mean of the values obtained for each slice was then calculated to generate a single value per animal.

II.11. STATISTICAL ANALYSIS

T-tests, one-way ANOVA and two-way ANOVA were performed using PRISM version 9 (GraphPad Software, United-States) to determine statistical significance. Results were considered significant if $p < 0.05$. N indicates the number of independent experiments and n the number of replicates. Detailed information about the number of replicates and the statistical tests applied can be found in figure captions.

III. RESULTS

III.1. IMPACT OF RA AND CAL ENCAPSULATION ON LNC PHYSICOCHEMICAL PROPERTIES

We first wanted to verify that RA and Cal encapsulation in LNC did not alter the main nanoparticle properties (size, polydispersity index (PDI), zeta potential). Upon RA and Cal encapsulation, LNC size decreased by 6 nm for the latter and increased by 4 nm for the former. However, these size variations were not significant, nor were the changes in PDI and zeta potential measurements (Table 2). Regarding RA and Cal encapsulation efficiency in LNC, it was superior to 80 % (83% for RA and 87 % for Cal), allowing us to reach an average concentration of 830 μM for RA and 860 μM for Cal in LNC formulations, respectively.

Table 2. Characterization of LNC-RA and LNC-CAL

Size, PDI, and zeta-potential were measured in milliQ water using a Nanosizer©. The values are presented as mean±SD (N=3)

Formulation	Size	PDI	Zeta Potential	Encapsulation efficiency (%)	Compound concentration in LNC
LNC	63 ± 2 nm	0,06 ± 0,03	-2,3 ± 0,05 mV	/	/
LNC-RA	67 ± 4 nm	0,01 ± 0,01	-3,5 ± 0,04 mV	83 ± 10 %	830 ± 101 μM
LNC-Cal	57 ± 6 nm	0,07 ± 0,02	-2,7 ± 0,03 mV	86 ± 2 %	860 ± 20 μM

To assess whether encapsulation in LNC would preserve RA and Cal from potential degradation and evaluate our formulations' shelf-life, RA-LNC and Cal-LNC were stored at 4°C for 8 weeks. As a control, RA and Cal in solution in DMSO were stored in the same condition. After 8 weeks, more than 85 % of RA and Cal encapsulated in LNC were detected by HPLC-UV (Fig.2). RA solution in DMSO was less stable than Cal. By the end of week 8, only 72% of RA initial quantity was detected. Regarding the size and zeta-potential, no substantial variation was observed throughout these 8 weeks (Supplementary data Fig.1), and PDI was always below 0,1.

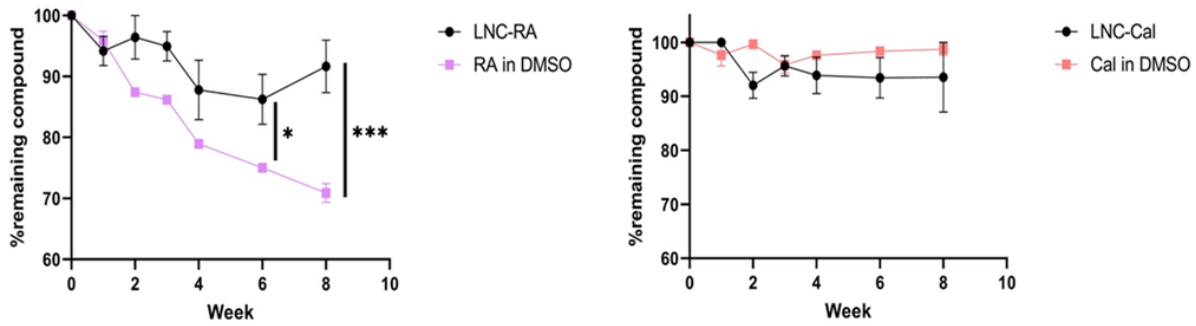

Figure 2. Comparison of RA and Cal stability in LNC and in DMSO.

RA and Cal were quantified by HPLC-UV at each time point in LNC and in DMSO solution. Percentages of the remaining compound were calculated relatively to the quantity of RA and Cal measured on the day they were produced. The values were presented as mean±SEM (N=3, with 3 different batches of LNC-RA and LNC-Cal and n=3 of RA and Cal in solution in DMSO). Statistical significance was calculated based on a two-way ANOVA *$p < 0.05$, ***$p<0,001$.

III.2. IMPACT OF LNC-RA AND LNC-CAL ON CG-4 DIFFERENTIATION

RA and Cal were shown to affect OPC differentiation [95, 207], therefore we wanted to assess their effects on the differentiation of an OPC cell line (CG-4 cells) and evaluate whether their encapsulation in LNC impacted this effect. CG-4 cells are an immortalized OPC cell-line that express OPC markers such as platelet-derived factor-receptor α [249] and differentiate into oligodendrocytes as OPC *in vitro* and *in vivo*. Thus, CG4-cells were first incubated with increasing concentrations of RA and Cal and MBP mRNA expression was used to assess cell differentiation. Indeed, MBP, MBP is one of the major proteins localized at the surface of myelinating oligodendrocytes [250] and has been used to highlight OPC differentiation in several studies [43, 100]

Only the highest RA concentration (200 nM) increased MBP expression in CG-4 cells, while even the lowest concentration of Cal (10 nM) induced the same level of MBP expression (Fig. 3).

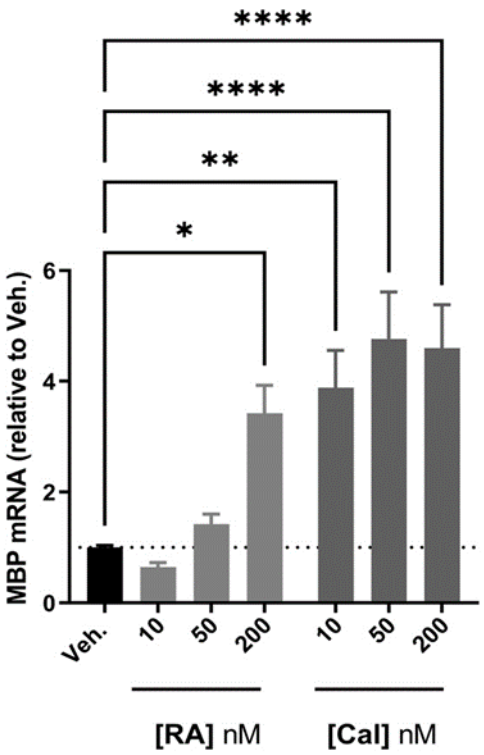

Figure 3. Impact of RA and Cal on CG-4 differentiation.

Treatments were incubated for 24h, and quantification of MBP mRNA by RT-qPCR was made 5 days after treatment removal. Statistical significance was calculated compared to Veh. based on a one-way ANOVA $p < 0.05$, **p<0,01, **** p< 0, 0001.The values were presented as mean±SEM (N=3, n=3).

Since 50 nM and 200 nM of Cal had a similar impact on MBP mRNA expression, the concentration of 50 nM was selected over 200 nM to limit the putative toxic effect that can be correlated with a higher concentration. Thus, based on our results (Fig.3) CG-4 cells were treated with LNC-RA at 200 nM and LNC-Cal at 50 nM, to assess the impact of encapsulation on their effect. Furthermore, CG-4 cells were treated with RA at 200 nM + Cal 50 nM (CARA) and LNC-RA (200 nM) + LNC-Cal (50 nM) (LNC-CARA) to investigate whether RA and Cal could have an additive effect on their differentiation. Treatment with CARA also increased MBP mRNA expression compared to vehicle-treated CG-4, and this to a greater extent than RA and Cal alone, suggesting an additive effect of those two molecules (Fig.4)

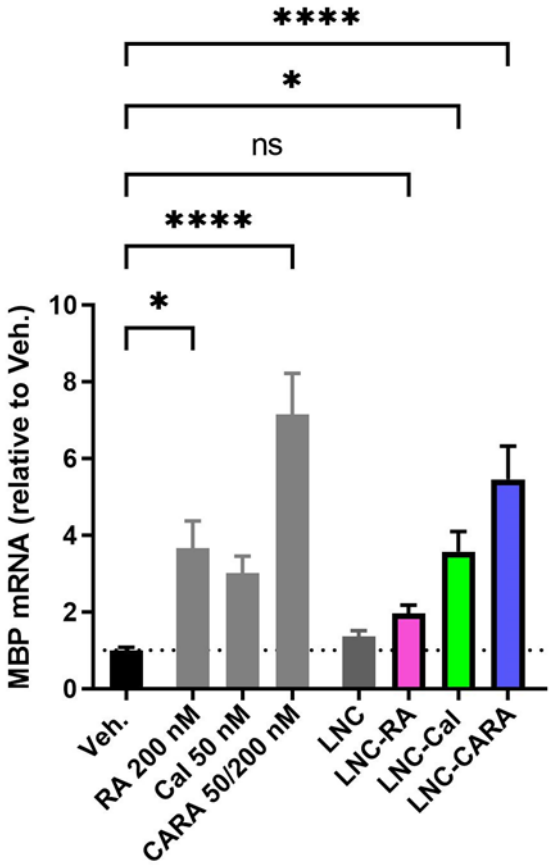

Figure 4. Impact of LNC-RA, LNC-Cal and LNC-CARA on CG-4 differentiation.

Molecules and drug-loaded formulations were incubated for 24 with CG-4 cells. Quantification of MBP mRNA by RTqPCR was made 5 days after treatment removal. Statistical significance was calculated compared to Veh. based on a one-way ANOVA $p < 0.05$, **** $p< 0, 0001$.The values were presented as mean±SEM (N=3, n=3).

While LNC-RA did not increase MBP mRNA expression of CG-4 cells, LNC-Cal significantly increased MBP mRNA expression (Fig.4). Moreover, CARA maintained its additive effect after encapsulation. As for LNC, they had no impact on CG-4 cells differentiation (Fig.4).

III.2.1. Impact of LNC-RA and LNC-Cal on OPC differentiation in a primary mixed glial culture

To confirm the effects of the drug-loaded formulations observed on CG-4 cells on primary OPC, a primary mixed glial cell culture was used. This complex mixed culture system, where astrocytes, microglia, oligodendrocytes, and OPC co-exist, is an interesting model to evaluate whether our formulations might induce OPC differentiation in the presence of other cells, hence mimicking an environment closer to *in vivo* settings. RA, Cal, and CARA in solution or encapsulated in LNC at the same concentrations as paragraph 3.2 were incubated with the co-culture. MBP mRNA expression was then evaluated seven days after.

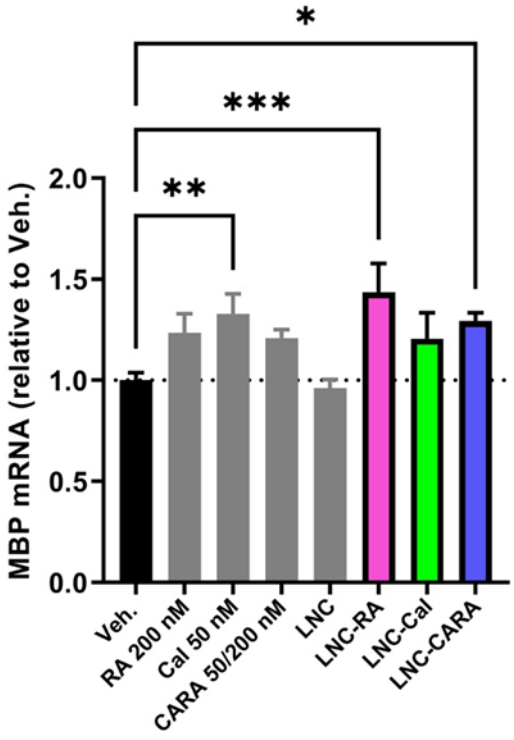

Figure 5. Impact of LNC-RA, LNC-Cal and LNC CARA on OPC differentiation in mixed glial culture.

Molecules and drug-loaded formulations were incubated for 24h with glial cells. Quantification of MBP mRNA by RTqPCR was made 7 days after treatment removal. Statistical significance was calculated compared to Veh. based on a one-way ANOVA $p < 0.05$, **** $p< 0, 0001$.The values were presented as mean±SEM (N=3, n=3).

In this model, LNC-RA, LNC-CARA and Cal significantly increased MBP mRNA expression compared to the vehicle. Nevertheless, this change was moderate compared to the observed effect on CG-4 cells for all treatments. For instance, LNC-CARA increased MBP mRNA expression 5,74-fold in CG-4 cell culture, and 1,29-fold in the mixed glial cell culture. In this model, LNC did not impact MBP mRNA expression either.

III.2.2. Impact of RA, Cal, and drug-loaded LNC on proinflammatory cytokine secretion of BV-2 cells

BV-2 cells are a microglial cell-line that can be activated with LPS to secrete pro-inflammatory cytokines such as tumor necrosis factor α (TNFα), interleukin-6 (IL-6), and monocyte chemoattractant protein-1 (MCP-1)[248].

Given that RA and Cal have immunomodulatory properties, we evaluated their impact on pro-inflammatory cytokines secretion by LPS-activated BV-2 cells. We also aimed to evaluate the impact of CARA (as an equimolar mix of RA and Cal) and drug-loaded formulations. Based on

previous studies [251, 252], we selected 3 concentrations of RA and Cal (0,03 µM, 0,3 µM and 3µM) to be incubated with LPS-activated BV-2 cells.

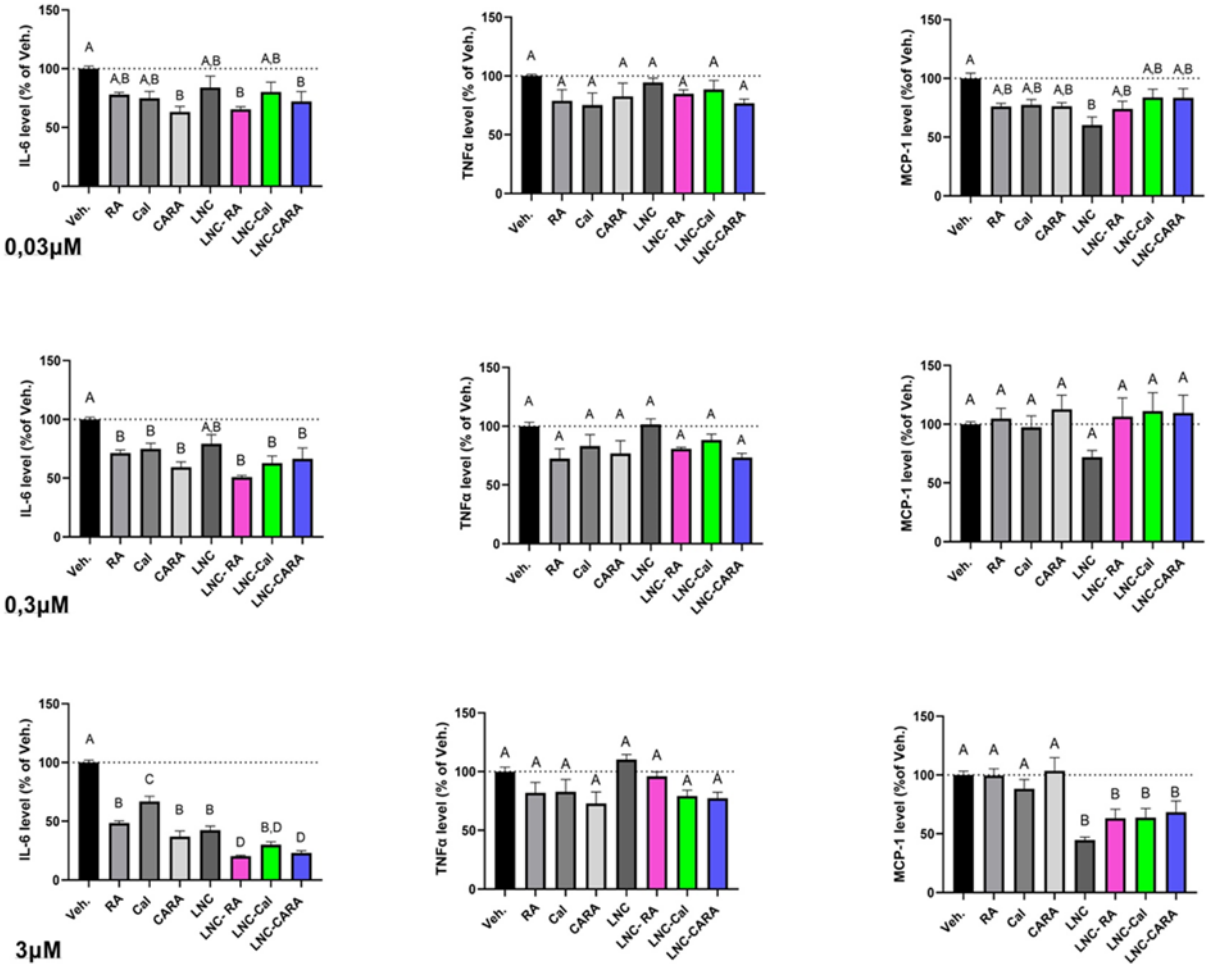

Figure 6. Impact of LNC-RA, LNC-Cal, LNC-CARA on TNFα, IL-6, and MCP-1 secretion by activated BV-2 cells.

BV-2 cells were stimulated, prior to treatment, with 100 ng/mL of LPS. After 8 h of treatment+ LPS, the supernatant was removed, and cytokine quantification was achieved by ELISA**.** The concentration of cytokines (pg/mL) was normalized compared to the vehicle (Veh.) Statistical significance was calculated with a Tukey multiple comparison test. The values were presented as mean±SEM (N=3, n=4). Conditions not related by the same letter are significantly different.

For IL-6, at 0,03 µM, only CARA, LNC-RA, and LNC-CARA significantly decreased the cytokine level compared to vehicle (Fig.6). While at 0,3 µM, IL-6 levels were substantially reduced for all treatments, the dose of 3 µM offered the most significant decrease with a reduction of -33.24% for Cal, -51.58% for RA, and -62.89 % for CARA. Like CG-4-cells differentiation, a combination of CARA offered an additive effect in reducing IL-6 secretion. At 0,3 µM, all drug-loaded formulations were more effective in decreasing IL-6 secretion from BV-2 cells than molecules in

solution (Fig.6). At 3 μM, LNC decreased up to 42% IL-6 compared to vehicle, implying the nanocarrier's pharmacological activity on cytokine production (Fig.6).

Similarly, at 0.03 and 3 μM LNC induced a significant decrease of MCP-1 level (-44% compared to vehicle for 3 μM). While RA, Cal and CARA had no impact on MCP-1 secretion at LNC-RA, LNC-Cal and LNC-CARA significantly decreased MCP-1 at 3 μM. Hence, encapsulation in LNC substantially increased the impact of the compounds on MCP-1 secretion (Fig.6)

Regarding TNFα levels, compared to vehicle, none of the selected concentrations significantly impacted its secretion by BV-2 cells (Fig.6)

III.3. IMPACT OF CARA AND LNC-CARA ON MYELINATION AND PRO-INFLAMMATORY MICROGLIA INFILTRATION AFTER NASAL ADMINISTRATION IN THE CUPRIZONE MODEL

The *in vitro* experiments aimed to evaluate whether, after encapsulation RA, Cal and CARA could still induce OPC and CG-4 cells differentiation and exert their reported anti-inflammatory properties on BV-2 cells. Our data showed that the encapsulation in LNC did not hinder their biological effect. Moreover, according to our data, LNC-CARA has shown the most promising pro-remyelinating effects and significantly impacted BV2 cytokine secretion among the drug-loaded formulations. Therefore, our next experiment was to evaluate *in vivo* whether nasal administration of LNC-CARA could induce remyelination and limit pro-inflammatory microglia infiltration in the corpus callosum of C57/BL6 mice after cuprizone-induced demyelination. The cuprizone regimen caused a reduction of 13% of the FluoroMyelin positive surface in the corpus callosum and increased $Iba1^+$ cell (microglia and macrophages) infiltration, in the corpus callosum (Fig.7).

Among the mice that received cuprizone, groups treated with LNC, and LNC-CARA had increased FluoroMyelin positive area in the corpus callosum. While these results suggest that LNC and LNC-CARA stimulated remyelination, CARA did not seem to impact myelination (Fig.7). Regarding microglia infiltration, LNC and LNC-CARA significantly increased the Iba1 positive surface in the corpus callosum to a greater extent than CARA that had a more discrete effect (not statistically significant).

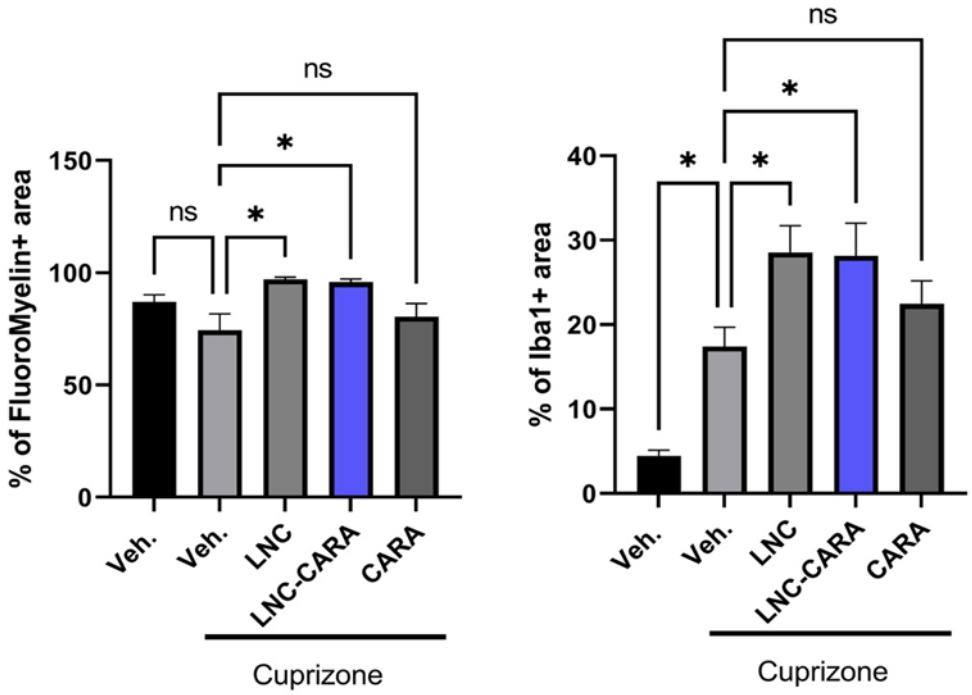

Figure 7. Impact of intranasal administration of LNC, LNC-CARA and LNC CARA on FluoroMyelin and Iba1 staining.

After 6 weeks of cuprizone-containing chow (or normal chow), mice received intranasally 4,1 μg of Cal + 3 μg of RA (CARA) or LNC-CARA for 6 days, then we assessed the corpus callosum of the mice at the histological level. The percentage of FluoroMyelin positive area (a marker of myelin) or Iba1 positive area (a market of microglia) was calculated with Visiopharm© software. Three brain slices were analyzed per animal (N=6 mice per group). The mean of the values obtained for each slice was then calculated to generate a single value per animal. Statistical significance was calculated compared to vehicle (Veh)+curpizone based on a one-way ANOVA * p< 0, 05. The values were presented as mean±SEM; ns = not significant

IV. DISCUSSION

The therapeutic arsenal against MS has known an incredible expansion since 1993 and the approval of IFN-ß by the FDA [253]. Several routes of administration have been used to deliver medicines to the patients, depending on the nature of the compound that must be administrated: IV for monoclonal antibody, *per os* for small molecules, and subcutaneous administration for peptides. However, all these administration routes face the BBB, a semi-permeable barrier protecting the CNS and limiting brain distribution. The nose-to-brain pathway is a delivery route that has been investigated for CNS delivery because of its unique ability to bypass the BBB [203]. Besides this important advantage, the intranasal route is also more patient-friendly. Thus, in the scope of MS, intranasal administration can be an interesting delivery route to investigate. Lipophilic compounds can be more challenging to administer as nasal spray due to their poor solubility in physiological solutions. A suspension can be made, but the aggregates formed by the compounds are more likely to form a deposit in the nasal epithelium than reach the olfactory bulb. Thus, we aimed to encapsulate two lipophilic compounds that can induce myelination (RA and Cal) in LNC to form a homogenous nanoemulsion that can be more easily administrated *via* the intranasal route.

Our first step was to encapsulate RA and Cal inside LNC. We achieved high encapsulation efficiency for both molecules (> 80%), which is in line with what has been described in the literature for other lipophilic molecules such as itraconazole [254].To our knowledge, our group was the first to encapsulate RA and Cal in LNC. However, other groups encapsulated these molecules in liposomes. For RA, Cristiano et al.[255] encapsulated 82% of RA in a liposome, which is similar to our data. But with Calcitriol, encapsulation in liposome was less efficient (58%-78% according to Rafique et al.[256]). LNC has the advantage of having an oily lipophilic core and a lipid shell. Therefore, a more considerable volume is available for the molecule to shelter from the hydrophilic part of the formulation, whereas liposomes have only their phospholipid bilayer to host the molecule, hence less volume.

For further characterization of LNC-RA and LNC-Cal formulation, we evaluated the stability of the drugs into the loaded-nanocapsules during eight weeks; stability of the free drugs has been monitored in DMSO as control. For RA, the remaining compound in the DMSO solution significantly decreased over time compared to LNC-RA. RA is indeed very unstable in solution and sensitive to oxidation, and our data suggest that encapsulation in LNC increased its stability. Indeed, after encapsulation, less than 15% of RA has been degraded in eight weeks (Fig.2). Our results are in accordance with what can be found in the literature. For instance, in an acetonitrile

solution containing other retinoids, only 37 % of RA was left in the solution [257]. These results highlight the utility of using LNC to store RA and maintain its stability. However, encapsulation in LNC was not a prerequisite for Cal to maintain its stability.

To our knowledge, we are the first to demonstrate that RA and Cal can increase MBP mRNA in CG-4 cells. These effects could be mediated via the RXR receptor. Indeed, RA binds to RAR, its nuclear receptor that forms a heterodimer with RXR [258]. Similarly, Cal binds to VDR, a cytoplasmic receptor that can form a heterodimer with RXR [259]. Even if they can form a complex with RXR, RAR/RXR binds to the RARE, and VDR/RXR binds to the VDRE. After binding, transcription factors and coactivators are recruited to modulate gene transcription. Our results show that CARA increased MBP mRNA to a greater extent than RA and Cal alone. This increased effect is likely due to RAR/RXR and VDR/RXR simultaneous action to enhance MBP transcription via their respective response element. This additive effect with LNC-Cal was maintained since LNC-CARA impact on MBP mRNA was superior to LNC-Cal and LNC-RA alone.

Conversely, after encapsulation, the impact of RA on CG-4 differentiation was lost. Two theories could potentially explain these results. The first is related to the quantity of RA that penetrated inside the cells. Since RA is a highly lipophilic small molecule, thus it can pass the cell membrane by diffusion. On the other hand, LNC enters the cell by active endocytosis and may be degraded by lysosomes [260]. Thus, when delivered by LNC, RA concentration in the cytoplasm may be lesser than RA alone.

Additionally, RA is a small molecule that can cross the cell member and be in the cytoplasm quicker than LNC that, likely relies on an active endocytosis pathway (slower than passive diffusion) to enter the cell. The second theory is that since RAR is a nuclear receptor, it may be possible that LNC does not favor a nuclear delivery but more of a cytoplasmic delivery. This latest theory can explain why its encapsulation did not impact a molecule such as Cal with a cytoplasmic receptor VDR in LNC.

When tested on mixed glial cell culture molecules and drug-loaded LNC had a minimal impact on MBP mRNA. Cal at 50 nM managed a significant increase of MBP mRNA but to a lesser extent than its impact on CG-4 cells (fold increase compared to the vehicle: 1,3 vs. 3). The same effect was observed for LNC-RA and LNC-CARA that had minimal influence on MBP mRNA compared to their effect on CG-4 cell culture. In Dietmer et al.'s work [261] using a similar mixed culture model, the impact of T-reg conditioned media on OPC differentiation was also lesser in the mixed culture than a pure OPC culture. As there are fewer OPC in the culture (10 % OPC vs.

70% of astrocytes), they could be sequestrated by astrocytes and microglia. Therefore, the concentration of RA and Cal used for CG-4 cell culture could be insufficient to influence OPC in this setting. We also hypothesized that MBP might not be the best marker to evaluate OPC differentiation in mixed glial culture in this setting. As MBP is expressed in mature myelinating oligodendrocytes, assessing the expression of an early differentiation marker such as the proteolipid protein (PLP) (expressed in pre-myelinating oligodendrocytes) might have shown more significant results [53]. In addition, as CG-4 cells are a modified cell-line and the mixed glial cell culture primary cells , there are also an intrasec difference between those two models that can explain why the impact of the drug-loaded formulation was limited in the setting of primary cells culture.

Being the resident immune cells of the CNS, microglia have a central role in perpetuating the neuroinflammation observed in MS [38]. Since RA [251] and Cal [247] are known in the literature for having immunomodulatory properties, we decided to treat LPS activated BV-2 cells (a microglia cell-line) with LNC-RA LNC-Cal, and LNC-CARA to see if RA and Cal could still exercise their reported effect after encapsulation. LPS activation of BV2- cells is an *in vitro* model used in several studies [262, 263]. Since these cytokines are involved in MS immunopathology, we assessed the impact of RA, Cal, CARA, and LNC on the secretion of IL-6, TNF α and MCP-1 at different doses.

Among the three cytokines, only IL-6 secretion significantly decreased when treated with the compounds in solution with a maximal effect at 3 μM (Fig.6). Surprisingly, when BV2 cells were treated with LNC, IL-6 and MCP-1 secretion significantly decreased, suggesting that LNC has a pharmacological effect on BV2 cytokine secretion, unlike their impacts on CG-4 differentiation. LNC's pharmacological impact has also been reported by Xu et al. [219] on glucagon-like peptide-1 (GLP-1) secretion by GLUTag cells, a murine L cells cell-line. In their study, the mere fact of changing LNC size impacted GLP-1 secretion. Drug-loaded formulation decreased to a greater extent IL-6 secretion than molecules in solution, suggesting an additive effect among LNC and molecule. However, in the case of MCP-1, LNC impacted its secretion. Since RA, Cal and CARA had no impact on MCP-1 secretion, the observed effect of LNC-RA, LNC-Cal, and LNC-CARA is very likely due to LNC. In this setting, it is challenging to decipher if LNC as a whole are responsible for this effect or a specific component of LNC. As for TNFα, no substantial impact has been witnessed in our experimental setting. Cytokine secretion after LPS stimulation follows a certain kinetic. In Lee et al.'s study [264], TNFα alpha secretion peaked 4 hours after LPS stimulation, whereas IL-6 peaked at 16 hours. This gap between the two cytokines can explain why we could not appreciate the impact of the formulation and the drug at 8h after treatment. At this time point, TNFα secretion was probably decreasing.

Our next goal was to confirm our formulations' pro-remyelinating and immunomodulatory effects in vivo using a cuprizone murine model. Indeed, this model is largely used to study remyelination [69]. Cuprizone is a copper-chelator that induces oligodendrocyte death in the corpus callosum, a rich myelinating area connecting the left and right brain hemispheres. Following oligodendrocyte apoptosis, inflammatory cues activate microglial cells that subsequently infiltrate the corpus callosum [265]. After 5 to 6 weeks of cuprizone diet, the corpus callosum is less than 25% myelinated. Upon removal of cuprizone, remyelination occurs spontaneously over 4 weeks, with a fast remyelination kinetic mostly observed in the first two weeks [71]. In the light of the above, after six weeks of being fed cuprizone chow, C57BL/6 male mice received intranasally LNC, LNC-CARA, and CARA. Our goal was to assess and compare the impact of the intranasal delivery of CARA suspension and the formulation of LNC-CARA on myelination and microglia.

To study the impact on myelination, we chose as marker FluoroMyelin, a dye that labels myelin; as for microglia, we selected to stain $Iba1^+$ cells, a marker of microglial cells [40]. One week after cuprizone withdrawal, in accordance with the literature, $Iba1^+$ cells infiltration of the corpus callosum was observed [265], but to our surprise, cuprizone only discreetly impacted the rostral corpus callosum myelination (Fig.7). In a recent study published by Toomey et al. [266], they demonstrated no significant differences in the level of myelination within the rostral corpus callosum after cuprizone diet. These results are also in accordance with Steelman et al.'s study [267]. However, a significant impact on myelination was observed in the caudal corpus callosum [266, 267]. In their hands, $Iba1^+$ cells infiltration also increased in the rostral corpus callosum, but this increase was more robust in the caudal orientation [266].

In our experiment, LNC and LNC-CARA similarly increased $Iba1^+$ infiltration in the corpus callosum with the same magnitude. On the other hand, CARA's impact was less significant. As LNC, significantly enhanced $Iba1^+$ as the same amplitude as LNC-CARA, our data suggest that the effect could be more mediated by LNC than CARA itself, mirroring the tendency observed with BV2-cells (Fig.6). Since LNC and LNC-CARA coincide with higher myelination, we hypothesized that LNC and LNC-CARA stimulated microglia/macrophage migration into the corpus callosum to clear myelin debris by phagocytosis and stimulate anti-inflammatory cytokine secretion that stimulates myelination [36, 265]. In this setting, it is difficult to decipher whether the increase in myelination observed is mediated by the pro-remyelinating properties of RA and Cal (as demonstrated in our *in vitro* experiments) or by stimulation of myelin debris clearance. Nonetheless, our results seem to indicate that intranasal administration of LNC-CARA can enhance remyelination of C57BL/6 mice corpus callosum after cuprizone diet, to a greater extent than CARA.

V. CONCLUSION

Our study demonstrated that RA and Cal could be encapsulated in LNC and that these nanocarriers can have protective properties against molecules degradation. Moreover, we showed that RA and Cal can promote differentiation of CG-4 cells after encapsulation and that an additive effect existed between those two compounds. Our work also highlights LNC's impact on pro-inflammatory cytokine secretion by LPS stimulated BV2-cells. Indeed, LNC and drug-loaded formulation decreased IL-6 and MCP-1 secretion to a higher extent than RA and Cal. Via intranasal administration in a murine cuprizone model, LNC and LNC-CARA promote myelination more efficiently than CARA suspension. In the light of the above, we can conclude with our study that LNC can be a suitable nanocarrier to deliver lipophilic pro-remyelinating therapies by intranasal delivery.

VI. SUPPLEMENTARY DATA

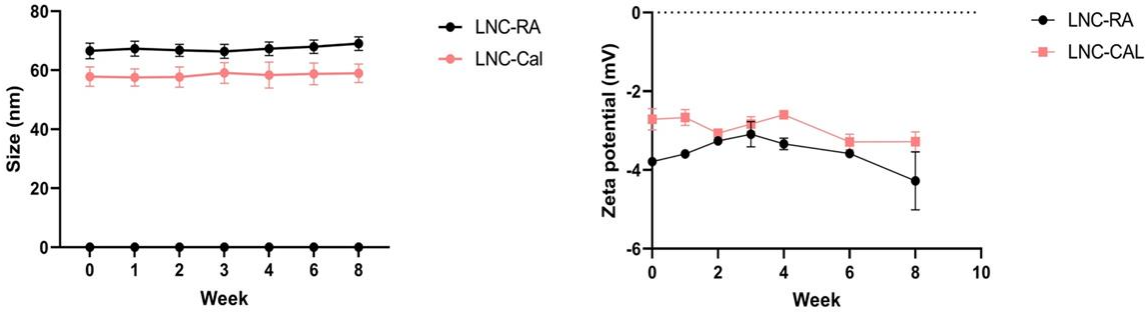

Figure 1.S Variation of size and zeta potential of LNC-RA and LNC-Cal.

The values were presented as mean±SEM (N=3, n=3 with 3 different batches of LNC-RA and LNC-Cal)

CHAPTER IV

DISCUSSION AND CONCLUSION

TABLE OF CONTENTS

I. MAIN ACHIEVEMENTS..... 127

II. DISCUSSION..... 130

III. PERSPECTIVES..... 139

IV. CONCLUSION 141

V. REFERENCES..... 142

As emphasized in **chapter 1**, OPC differentiation into myelinating oligodendrocytes is at the heart of future MS therapies [23]. Thus, stimulating OPC differentiation by using therapeutical compounds is of high interest. A few molecules have been tested, but none were efficient to promote remyelination during clinical trials; others are still in phase 2 clinical trials.

Our main objective was to enhance the delivery of pro-remyelinating therapies by using two different strategies:

- **Develop an OPC-targeted LNC to allow preferential accumulation of the molecules of interest to OPC.**
- **Bypass the BBB by using an intranasal administration of nanomedicines in order to increase the delivery of the molecules of interest and by extension remyelination**

These approaches were developed and applied to two molecules, namely retinoic acid (RA) and Calcitriol (Cal), which have reported OPC pro-differentiating effects.

I. MAIN ACHIEVEMENTS

The main achievements of this thesis are:

- **Production of a LNC formulation functionalized with an anti-PDGFRα (Ab) antibody in order to target OPC**

PDGFRα is a receptor predominantly expressed at the surface of OPC in the CNS. We reasoned that developing an LNC formulation with an anti-PDGFRα at its surface (LNC-Ab) could selectively deliver molecules of interest in OPC. To attach Ab at the surface of the LNC, we used different approaches (**chapter 1**). While the thiol/maleimide approach (approach 1) allowed a higher grafting yield, it hindered Ab interaction with PDGFRα. We reasoned that Ab might have been linked to the LNC via its Fv region (essential for epitope recognition), thus impeding its binding to the receptor with this technique. Hence, we used a site-selective click-chemistry that allowed the linkage of Ab to the LNC only via its Fc region (approach 3). Using this approach, we demonstrated that Ab recognition of PDGFRα was still maintained after grafting.

Although our study focused on Ab/PDGFRα binding, our observations suggest that when antibodies need to be grafted at the surface of nanoparticles, a site-selective approach needs to be considered at the risk of losing the antibody functionality.

- **Demonstration that the grafting of an antibody at the surface of LNC can impact their uptake by OPC**

Our research showed that LNC can be uptaken by OPC but adding an anti-PDGFRα at the LNC surface increased their uptake by OPC. Although it was less than Ab, the grafting an isotype control antibody at the surface of the LNC also modified their uptake. We hypothesized that this impact might be due to the presence of Fc receptor at OPC surface [268]. Our observation emphasized how important it is to use an appropriate control to demonstrate that a targeted drug delivery system can specifically target a given cell. Otherwise false conclusion on the targeting ability of the nanocarrier can be made.

- **Direct quantification of Ab at the surface of LNC**

As the number of antibodies per nanoparticle is an important parameter of nanoparticle characterization (**chapter 1 and chapter 2**), we needed to find a technique to quantify Ab at the surface of the LNC. Primary amine quantification using fluorescamine is a technique that has been developed to quantify peptides or antibodies [225]. In hour hands, contrary to other protein quantification assays like BCA, the primary amine quantification method did not interfere with LNC. To our knowledge, we were the first to use this technique to quantify the number of antibodies present at the surface of LNC. This protocol can be transposed to other kinds of LNC formulation to evaluate the grafting efficiency of antibodies or peptides.

- **Production of drug-loaded formulations for intranasal delivery**

In order to deliver RA and Cal to the CNS by intranasal delivery, they were encapsulated in LNC. Their encapsulation in LNC might prevent their degradation [113] by enzymes of the nasal cavity and favor their solubilization. Indeed, as described in **chapter 3,** RA and Cal are insoluble in physiological solution, but their encapsulation in LNC allowed them to be suspended in a physiological solution without forming aggregates (more prone to elimination by muco-ciliary clearance in the nasal pathway). In addition to succeeding in encapsulating RA and Cal in LNC with a satisfying encapsulation efficiency (> 80 %), we showed that LNC physicochemical properties (size, PDI, zeta potential) are stable over time. Moreover, for RA, we demonstrated that its encapsulation in LNC protected it from degradation over time and significantly increased their shelf-life.

Due to the versatility of this nanocarrier, LNC can deliver a wide range of molecules we used RA and Cal as proof of concept, but other drugs can be encapsulated in LNC.

- **OPC differentiation and decrease of pro-inflammatory cytokine secretion in microglial cells by LNC-RA and LNC-Cal**

LNC-RA, LNC-Cal and LNC-CARA favored CG-4 cell differentiation and LNC-CARA OPC differentiation in a mixed glial cell culture (**chapter 3)**. In addition, LNC-RA, LNC-Cal, LNC-CARA decreased IL-6 and MCP-1 secretion in BV-2 activated cells to a greater extent than the molecules in solution. LNC also decreased MCP-1 and IL-6 secretion. Thus, we reasoned that LNC might have immunomodulatory properties. Therefore, we think that LNC could have an additive effect with its cargo in decreasing inflammation. For this reason, we believe that LNC might be an ideal nanocarrier that can be of use in the management of inflammatory diseases such as MS.

- **Found that LNC and LNC-CARA could favor myelination *in vivo* after intranasal administration**

In **chapter 3**, our results suggest that LNC and LNC-CARA increased myelination in C57/BL6 mice to a greater extent than CARA after intranasal administration. Although these formulations were delivered intranasally, they could have passed through the nasopharynx and the intestinal tract. Hence the quantified effect can partly be mediated by systemic effect via intestinal absorption of the compounds. Nonetheless, our results are still very encouraging and show that there is a possibility to stimulate myelination using the nose-to-brain pathway and that LNC could be a real asset to deliver pro-remyelinating therapies to the CNS via intranasal administration.

II. DISCUSSION

Although our results have been discussed in their respective chapters, in this section, we aimed to discuss further the questions that arose from our data.

- **LNC-Ab characterization: a challenge?**

While characterizing the size and zeta potential of LNC is straightforward nowadays, characterizing LNC-Ab is a challenge. Indeed, besides the size, PDI and zeta potential, the number Ab at the surface of the LNC and the consequences of the grafting on Ab functionality are crucial information as they can impact the capacity of LNC-Ab to target OPC.

One of the main criteria to choose a grafting method was the yield of the reaction. We thus needed a reliable way to quantify Ab at LNC surface. While different technics are described in the literature, none were compatible with LNC, and quantifying Ab at LNC was complicated. Indeed, due to their lipid nature, when we used classical protein assays such as the Bradford assay [67] or the bicinchoninic acid assay [269], LNC induced a strong background signal. We explored indirect quantification methods (i.e., separation of the unbound Ab from the LNC), but we did not obtain reliable results. Indeed, the classical strategy [234] of ultra-centrifugation with the use of a membrane with a molecular weight cut-off to separate unbound Ab and LNC-Ab was incompatible with our system.

On the one hand (using a fluorescent antibody), we realized that ultracentrifugation with 300 kDa (molecular weight of Ab) cut-off membrane did not permit a 100% recovery of the Ab. On the other hand, when Ab recovery in the presence of LNC was assessed, only 70% of Ab was recovered, suggesting that LNC were clogging the filter pores. Therefore, an alternative strategy needed to be found. We finally collaborated with Prof. Frish's team (University of Strasbourg) that applied a primary amine quantification assay (developed by Udenfried et al. [225]) in his previous work. Thanks to this technique, we were able to perform a direct quantification of Ab at LNC surface that was not affected by a high signal/noise ratio.

The second challenge regarding the characterization of LNC-Ab was to monitor Ab interaction with PDGFRα after grafting. As no standardized test existed, we had to develop an assay to assess the quality of the Ab/PDGFRα interaction. To do so, we developed an in-house ELISA based on the coating of various concentrations of a soluble PDGFRα that interacts with a constant concentration of Ab. Importantly, as we have shown, it is not affected by the presence of LNC.

Our data have shown how vital these characterizations were before *in vitro* experiences. For instance, approach 1 provided the highest number of grafted Ab, but Ab interaction with its receptor was hindered, potentially due to changes in the Fv region. Hence, we used LNC-Ab obtained with approach 3 that maintained Ab interaction with PDGFRα after grafting even if the grafting efficiency of Ab was lower than approach 1. The advantage of the ELISA assay we developed is that it can be tunable and thus transposed to evaluate the interaction of a given antibody, other than Ab, after its grafting at LNC surface.

Of note, other techniques can be used to characterize the grafting of an antibody at the surface of LNC. Indeed, although not discussed in this manuscript, we had the opportunity to initiate the study of our formulations by nano-differential scanning fluorimetry (nanoDSF) [270]. NanoDSF allowed us to have in a few minutes the proof of the presence of Ab in the LNC-Ab formulation surface with approaches 1 and 2 (Fig.1). Briefly, in nanoDSF, tryptophan and tyrosine residues are detected at 350 nm and 330 nm as the fluorescence of the sample changes during heat-induced denaturation.

For both approaches, the fluorescence ratio profiles indicate the presence of tyrosine and tryptophan residues in the LNC-Ab samples (Fig.1) as their profiles are different from their respective LNC-Maleimide profile (negative control).

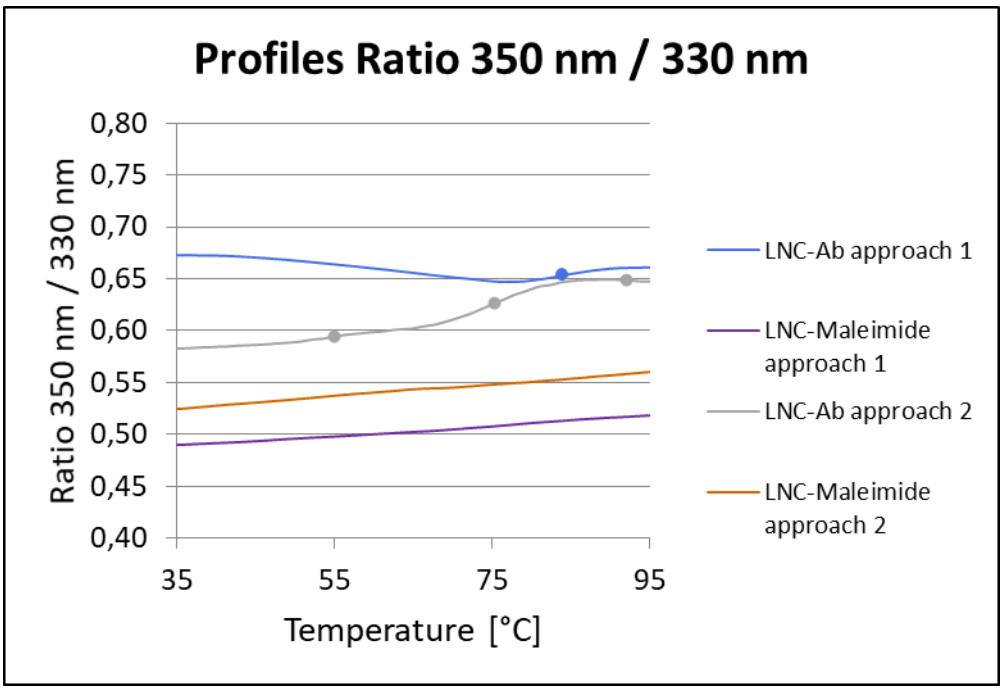

Figure 1. Fluorescence shift in LNC-Ab profile using nanoDSF.

These data show that as the samples are gradually heated, Ab is unfolded, revealing tyrosine and tryptophan residues that impact the fluorescence profile. The dotted point in the LNC-Ab profile indicates the temperature of inflection where a significant spike in fluorescence occurs due to tyrosine and/or tryptophan presence.

Gai et al. [271] also used nanoDSF but for another application. Their study evaluated the integrity of the antibody after azido modification (before grafting it on liposomes). Even if nanoDSF is an exciting technique to confirm the presence of the Ab in the LNC formulation (due to its quick sample analysis), it cannot quantify the number of antibodies present in the sample and has a high detection limit. In our hands, when we tried to analyze LNC-Ab obtained with approach 3, we could not detect any proteins in the sample. In contrast, with ELISA and primary amine quantification, we observed the presence of the Ab in LNC-Ab sample. Therefore, we assumed that the number of antibodies in the sample obtained with approach 3 (5 Ab per LNC vs. 49 Ab per LNC with approach 1) was too low to be detected.

Other approaches as microscale thermophoresis (MST) to calculate the affinity constant of ligand for its receptor could also be used to evaluate the interaction Ab/PDGFRα. We also had the opportunity to use this technology by collaborating with Dr. Léopold Thabault in our institute (CMFA/LDRI). With MST, we found that that LNC-Ab obtained with approach 1 could bind with the same soluble PDGFRα used for our in-house ELISA. Unfortunately, we were unable to reproduce our results. Although using MST would have been an innovative technology to evaluate how the grafting of an antibody could impact its interaction with its antigen, we choose not to pursue the optimization of our MST protocol since the ELISA already allowed us to assess Ab/PDGFRα interaction with reproducible results.

- **Impact of LNC surface modification on OPC cell uptake: Targeting or not targeting?**

We demonstrated that grafting an anti-PDGFRα at the surface of LNC increased their association with OPC. But we also established that an isotype control grafted on LNC had the same impact on OPC uptake**.** Nevertheless, we pushed our investigation further by evaluating LNC-Ab uptake by OPC in a mixed glial cell culture. We hypothesized that in a mixed glial culture, where OPC are the main cells expressing PDGFRα, the advantage of using an LNC-Ab would be more significant than in a pure OPC culture. Therefore, LNC-Ab were incubated with mixed glial culture, and uptake in OPC (A2B5 positive cells) was evaluated by FACS (Fig.2).

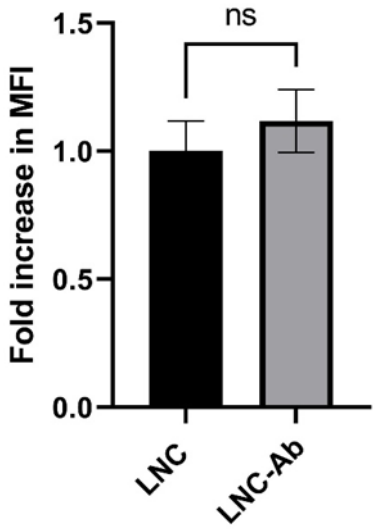

Figure 2. Impact of anti-PDGFRα grafting on LNC/OPC association in mixed glial cell culture.

DiD-Loaded LNC were incubated for 30 min with mixed glial culture at a concentration of 0.15 mg/ml. The fold increase in Mean Fluorescence Intensity (MFI) in $A2B5^{+}$cell was calculated relatively to LNC MFI. Statistical significance was calculated based on an unpaired t-test. The values were presented as mean±SEM (N=1, n=3).

Although more experiences need to be performed to confirm these preliminary observations, grafting Ab at the surface of LNC did not increase their uptake in OPC in this experimental setting. As LNC-Ab association with OPC was similar to LNC, we reasoned that using LNC-Ab as a nanocarrier would not bring any advantage in delivering bioactive compounds to OPC compared to LNC. Moreover, as previously discussed, LNC-Ab is more challenging to produce and characterize. This is why we chose not to pursue the targeting strategy and evaluated the impact of untargeted LNC-RA and LNC-Cal on remyelination in chapter 3.

Of note, LNC targeting capacities can be putatively mediated by other characteristics. Indeed, it has been demonstrated that certain types of cells are more prone to uptake nanoparticles than others (i.e., macrophages, microglia). Nanoparticles uptake by cells varies from one cell type to another and depends on the nanoparticle type. On this same principle, Doxil© (a liposome-doxorubicin-loaded formulation) decreased doxorubicin cardiotoxicity by sequestering the drug away from organs such as the heart increased accumulation in liver, spleen, and tumors [272].

As described in our introduction, our goal by targeting OPC was to increase remyelination and limit hypothetical side effects that could stem from off-target cell uptake. For instance, bexarotene, an RXRγ agonist used in clinics to treat lymphomas, has an exciting potential to stimulate remyelination. Nevertheless, the absence of cell selectivity makes it a last therapeutic choice for chronic diseases like MS [97]. Indeed, in addition to OPC, bexarotene can bind into RXR γ in

thyrotrope cells, responsible for thyroid-stimulating hormone (TSH) secretion. Upon RXR activation, TSH secretion decreases, inducing hypothyroidism [98]. Therefore, it would be interesting to assess if LNC can penetrate thyrotrope cells efficiently as OPC, as the mere fact of using LNC as a nanocarrier might have a targeting effect. As thoroughly discussed in **chapter 1,** nanocarrier cell endocytosis varies from one cell type to another, making this hypothesis worth investigating.

- **Is PDGFRα the right target for selective OPC delivery?**

The PDGFRα receptor is a tyrosine kinase receptor present at the surface of OPC. Upon activation by its ligands (PDGFA-B and -C), the homodimerization of the receptor is triggered [273]. The dimerized receptor is autophosphorylated on several domains, enabling downstream signaling cascades. Following activation, the receptor is internalized and degraded [273]. The blockade of PDGFRα by an anti-PDGFRα antibody is a therapeutical strategy used in cancer therapy. For instance, the anti-PDGFRα drug, olaratumab, blocks PDGF-AA, PDGF-BB, and PDGF-CC. Its binding prevents PDGFRα activation and its internalization and degradation [273, 274], thus inhibiting the proliferation of tumors. In OPC, PDGFRα activation by PDGFA leads to their increase, essential in remyelination [275]. Therefore, blockade of the receptor by an antibody might be problematic and may prevent OPC proliferation and differentiation. Furthermore, as discussed **in chapter 2**, targeting can only be achieved if LNC-Ab is mostly uptook by OPC via internalization of PDGFRα after binding to LNC-Ab. As olaratumab has been reported to induce PDGFRα internalization and its degradation, LNC-Ab, and by extension, the drug it may carry, could meet the same fate.

Other options, such as neural/glial antigen 2 (NG2), a proteoglycan at OPC surface, can be interesting to target. Rittchen et al. targeted OPC using polylactic-co-glycolic acid (PLGA) nanoparticles functionalized with an anti-NG2 antibody [276]. Their study showed that targeted PLGA nanoparticles loaded with Leukemia inhibitory factor (LIF) were more efficient in promoting OPC differentiation than LIF-loaded untargeted nanoparticles. *In vivo,* they demonstrated that brain organotypic cultures demyelinated with lysolecithin had thicker remyelinated myelin sheath when treated with LIF-loaded nanoparticles compared to LIF and LIF-loaded untargeted nanoparticles. Given that the association of LIF-loaded nanoparticles and untargeted LIF-loaded nanoparticles was not quantified by flow cytometry (as we did in **chapter 2**), it is impossible to know whether anti-NG2 antibody increased nanoparticles accumulation in OPC or not. Thus, the efficacy of the targeted formulation may be due to a higher accumulation

of LIF in the cells or linked to other effects related to endocytosis. Indeed, as thoroughly discussed in chapter **1**, modifying the surface of a nanoparticle may favor an endocytosis pathway more favorable for drug delivery, as for instance the caveolin-dependent pathway, where drug-loaded nanoparticles are less prone to degradation.

- **Are Cal and RA future MS therapies?**

Cal and RA have interesting properties in the context of MS. Indeed, RA and Cal have immunomodulatory properties and promote remyelination in animal models [101, 206, 207, 277]. We demonstrated that these molecules and their combination (CARA) favored CG-4 differentiation and that CARA was more effective than RA and Cal. In BV-2 cell experiments, CARA impact was more robust in decreasing IL-6 and MCP-1 secretion. *In vivo*, Parastouei et al. found in an EAE mouse model that Cal reduced the clinical score of the mice to a more considerable extent than RA, and than the combination of the two molecules [278].

Vitamin D, the precursor of Cal, has been administrated to MS patients at several doses to assess its immunomodulatory properties (see **chapter 1** for more details). A few studies have reported an impact on inflammation in MS patients. However, as mentioned in **chapter 1,** most clinical studies failed to demonstrate any benefits of using Vitamin D in MS but there are still other ongoing trials to evaluate different doses regimen, A thorough meta-analysis of Vitamin D impact on the immune system in MS would be needed to draw any conclusion. Some authors have reasoned that the dose of Vitamin D might be too low to impact remyelination or neuroinflammation positively. Unfortunately, high doses of Vitamin D lead to increased calcium absorption and decreased calcium kidney clearance, leading to hypercalcemia. Generally, Vitamin D-mediated hypercalcemia occurs only when substantial quantities are ingested (several hundred-fold the recommended intake; >10 000 UI/day) and can result in life-threatening side effects such as kidney failure and heart arrhythmias, to cite a few [279]. Regarding RA, it also has been tested in clinical trials but to a lesser extent than Cal. Qu et al. reported that, in combination with IFN-ß, RA restored the number of regulatory T-cells in patients [280]. As a stand-alone therapy, RA seemed inefficient in improving EDSS and did not impact T-cells or B-cells subsets [281]. Similarly to Cal, these disappointing effects might be due to a low dose of RA. However, increasing RA doses will lead to side effects such as hypercalcemia, hypothyroidism, and hypertriglyceridemia. These side effects may seem acceptable for life-threatening conditions, but for a chronic illness such as MS, RA may not be the best suitable choice because of its side effects.

Overall, even if several *in vitro* and *in vivo* preclinical studies seem to support a potential RA efficacy in halting MS progression [282], more clinical studies are needed to conclude RA efficacy and its benefice/risk balance.

- **Are LNC bioactive nanocarriers?**

As we demonstrated in **chapter 3**, LNC can decrease IL-6 and MCP-1 secretion in BV2- activated cells and increase corpus callosum remyelination *in vivo*. Our data suggest that LNC may have immunomodulatory properties on their own. On the other hand, LNC had no impact on OPC/CG-4 cells *in vitro*. With our data, it is difficult to elucidate whether LNC *per se* have biological properties or if the effects we observed are due to one of their components (or the combinations of all of them). Previous reports are in line with our observations regarding LNC bioactivity. For instance, Chauvet et al. [283] demonstrated *in vitro* that calcium channels in cortical neurons are inhibited by LNC, mainly via Kolliphor© HS15, a surfactant used in LNC formulation. Further, Xu et al. [219] showed that LNC of 100-200 nm can induce GLP-1 secretion by GLUT cells. Very few studies evaluated the impact of LNC (of the same composition as ours) on biological parameters (i.e., cell differentiation, cytokine secretion). Thus, it is difficult to conclude whether LNC can be considered bioactive entities, but pieces of evidence seem to point out that their effect might be cell-dependent. Aside from their role as a nanocarrier, if LNC immunomodulatory properties are confirmed in models other than BV-2 cells, they could be useful in neuroinflammatory diseases such as MS. Indeed, if LNC were to carry an immunomodulatory drug, drug-loaded LNC immunomodulatory properties could be stronger than the drug itself due to an additive effect between LNC and the compound, which can be a real asset from a therapeutical perspective.

- **Can LNC-RA and LNC-Cal be produced without organic solvent and up-scalable?**

The answer is yes. In **Chapter 3**, RA and Cal were added as a highly concentrated solution in DMSO (0.075 % v/v) to facilitate their incorporation in LNC and make the production process more manageable. However, in parallel, we also explored the possibility of encapsulating those molecules without using DMSO by solubilizing them in Labrafac© before formulating LNC. Briefly, RA or Cal were solubilized in Labrafac© by heating and steering at 50 C° for 5 min in an amber glass tube. The encapsulation efficiency of RA and Cal, whether solubilized in DMSO and added at the end of the process or solubilized in Labrafac© at the first step of the formulation, was similar and superior to 80%.

This organic-solvent-free formulation is a step further towards drug-loaded LNC translation into human use. Still, before that, LNC need to be scaled up for industrial production to have a larger batch that can allow their commercialization as human medicine. Urimi et al. performed a scale-up study to produce 10 L of LNC [284]. Scale-up batches of ibuprofen loaded-LNC and free-drug LNC were compared to lab-scale batches. Their result showed no difference in physicochemical characteristics (size, PDI, zeta potential) [284].

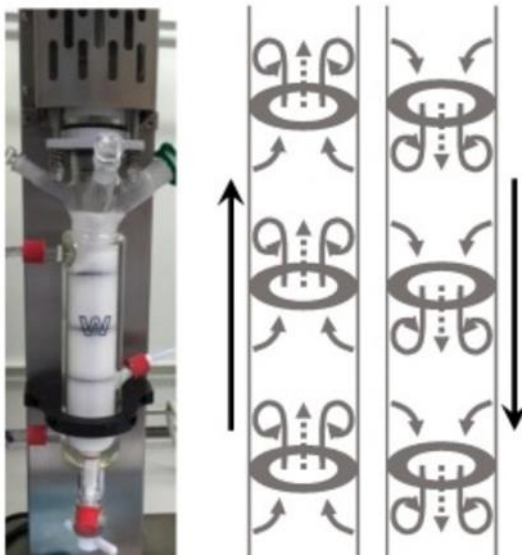

Figure 3. Production of LNC at a large scale [284].

Oscillating baffles cause agitation in the oscillatory baffled reactor to achieve improved heat transfer and better mixing of the excipient mixture. In the oscillatory baffled reactor, the liquid flow is indicated by dashed arrows and the solid arrows outside the drawing indicate the movement of the baffles.

To manufacture LNC, they used a vertical oscillatory baffled reactor vessel to have an optimal production time (Fig.3). The vertical reactor was connected to either one cold water bath (25 °C) or a warm water bath (95°C) to allow the 3 cycles of temperature needed for LNC production (see **chapter 1** for more details). The connection with the reactor was changed through the process, and the mixture was agitated in the reactor thanks to the oscillating baffles [284]. Thus Urimi et al.'s process showed that LNC are nanocarriers that can be produced on a large scale to fit the demand linked to the market.

- **Intranasal delivery: optimal CNS for remyelinating therapies?**

As summarized in **chapter 1**, CNS penetration remains a challenge for a significant number of drugs. Hence, to reach a therapeutic concentration in the CNS, a high dose must be administrated in the periphery (i.e. per os, i.m., i.v.), leading to side effects. Thus, finding a way to increase brain penetration is of primary interest for CNS therapies, including future remyelinating treatments for

MS [199]. Intranasal administration is a particularly interesting pathway for CNS since it can bypass the BBB, as discussed in **chapter 1.** The results of several studies support the effectiveness of this approach. For instance, insulin was delivered to the CNS by nasal administration in the scope of Alzheimer's diseases, improving memory and mood in patients without significant alteration of insulin and glucose level in the blood [199]. As promising as this pathway can be, it comes with challenges: 1) mucociliary clearance can remove foreign substances towards the nasopharynx, 2) efflux transport proteins, such as p-glycoprotein (P-gp), can decrease drug concentration in cells, and 3) enzymes can cause molecules degradation. LNC as nanocarriers can address some of these problems. They can protect the compound from enzymatic degradation, likely due to Kolliphor HS15©, which can inhibit P-glycoprotein efflux on its own [285, 286]. To highlight the advantage of intranasal administration over IV, Mohsen et al. [287] delivered nimodipine-loaded LNC (treating subarachnoid hemorrhage-induced vasospasm) intranasally and nimodipine intravenously. When comparing the pharmacokinetics of nimodipine after both administrations, IV achieved a higher nimodipine concentration in the brain than intranasal delivery (350 ng/g of brain vs. 200 ng/g, respectively). However, with intranasal delivery, nimodipine was detected into the brain up to 8h after administration compared to 4h for IV administration (Fig.5). Furthermore, the plasma concentration of nimodipine after intranasal administration was significantly lower

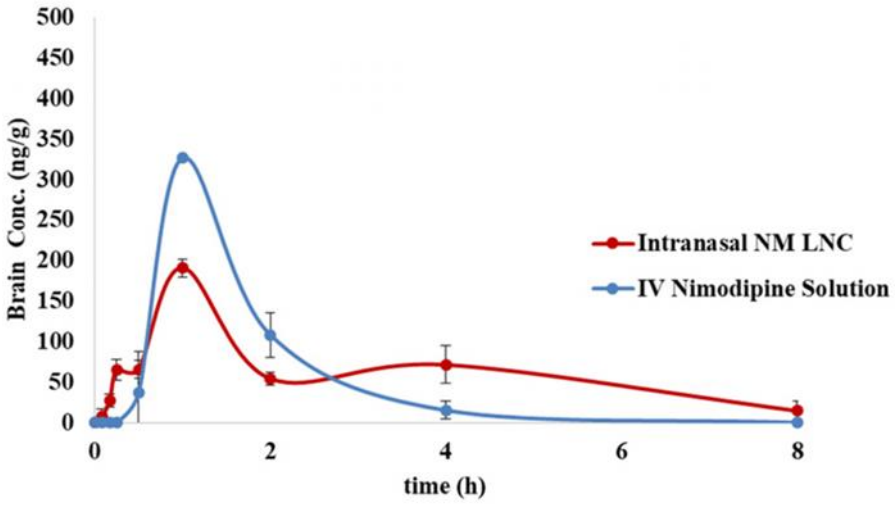

Figure 4. Nimodipine (NM) brain concentration profiles following intranasal administration of NM loaded-LNC and IV administration of NM solution [287].

The IV and nasal dose was 2 mg NM/kg. Data represent the mean ± SD (n = 16 for each time interval).

Even if the authors did not compare the biological effects following the two administration pathways, their results show that significant drug concentrations can be obtained in the brain without increasing the blood levels of the drug [287].

III. PERSPECTIVES

In this work, our primary aim was to engineer an **OPC-targeted LNC by grafting an anti-PDGFRα at its surface.** With this approach, we hoped to improve the delivery of lipophilic pro-remyelinating molecules by encapsulating them in LNC to 1) increase their solubility, 2) stimulate OPC differentiation into remyelinating oligodendrocytes, and finally 3) optimize pro-remyelinating therapies delivery in the CNS by using intranasal administration.

While these objectives have been reached to a certain extent, several **short-term perspectives** can be proposed:

- Explore *in vivo* the impact of the targeted LNC-CARA formulation

Our first step was to develop the OPC-targeted formulation, but anti-PDGFRα grafted at LNC surface modestly increased LNC uptake by OPC. While the admitted postulate is that the more drug-loaded nanoparticle accumulates in the cell of interest, the better the pharmacological effect, some studies demonstrated otherwise [185, 240]. In these studies, formulations with lesser cell uptake had a more significant pharmacological effect than those highly uptook by cells. The data, in **chapter 3** demonstrated that LNC-CARA could favor remyelination of the corpus callosum in a cuprizone model. In the light of the above, it will be interesting to compare targeted LNC-CARA to their untargeted counterpart impact. This way, we could evaluate the effect of Ab grafting on remyelination and assess if the strategy is worth investigating.

- Compare the impact of intranasal administration LNC-CARA vs. oral administration of CARA on remyelination

The added value of LNC was mostly to solubilize and protect the molecules of interest as RA and Cal are not soluble in physiological solutions. Suspensions are formed of macroparticles that are more prone to be cleared by the mucociliary mechanism of the nasal epithelium. Therefore, in a cuprizone model, we administrated LNC-CARA intranasally to mice. Compared to CARA, LNC-CARA increased remyelination to a greater extent than CARA. As most lipophilic drugs are administrated orally, it would be interesting to compare the impact of an intranasal administration of LNC-CARA vs. oral administration of a CARA suspension on remyelination using the cuprizone model. The data from these experiences would evaluate whether drug-loaded LNC intranasal administration can be an asset for pro-remyelinating lipophilic drug delivery.

Additionally, it will also be interesting to compare the pharmacokinetic and toxicologic profiles of both administration routes to evaluate whether intranasal administration can limit systemic distribution of RA and Cal and still be efficient. Overall, these experiments could determine if drug-loaded administration can propose a higher benefice/risk balance.

In addition to these short-term perspectives, the following **long-term perspectives** can also be considered**:**

- Encapsulation of other pro-remyelinating molecules to confirm LNC added value as a nanocarrier for intranasal delivery in multiple sclerosis

The data discussed in this thesis have shown that LNC-CARA favored remyelination *in vivo* after intranasal delivery putatively via the RXR receptor. Therefore, to assess if LNC can be a nanocarrier of choice in delivering pro-remyelinating therapies via the nose-to-brain pathway, it would be interesting to accumulate evidence that they can do so by encapsulating another molecule in LNC. The lipophilic (logP = 7.4) RXR agonist, IRX4204, can be candidate of choice [288]. In addition to having immunomodulatory properties (increasing the differentiation of CD4 + T cells into Treg cells *in vitro* and attenuating the severity of disease in the EAE model)[289], IRX4204 increased the density of myelinated axons in the corpus callosum in a cuprizone model after oral administration. These results have been shared by Io therapeutics© inc.

- LNC: a nanocarrier that can address other drug delivery issues in the scope of MS?

Although in this thesis we highlighted the challenge of working with lipophilic molecules, mainly regarding their administration and how LNC can address this issue, we also would like to enlighten the readers on other drug delivery strategies where LNC might be of use.

MicroRNA have reached high popularity in the latest years. In MS, they have been used to promote differentiation of OPC [240]. However, their high instability *in vivo* and storage conditions prevented their use as therapeutical entities. As they have already been used to deliver nucleic acids, we believe LNC could be a sustainable solution to increase their stability and facilitate their administration intranasally or by IV [290]. Alternatively, to the nose-to-brain pathways, other strategies can improve pro-remyelinating compound entrance in the CNS. Indeed, drug-loaded LNC surfaces can be tuned with peptides or antibodies to enhance their crossing of the BBB after IV administration[122]. In **chapter 1**, we have given numerous examples of the different entities that can be grafted at the surface nanoparticles to reach this goal.

IV. CONCLUSION

Albeit challenging, nanotechnology seems very promising on paper to enhance small molecule safety/efficacy profile and increase biodistribution of therapeutical compounds in the targeted organ. Several research groups focused on active targeting strategies for different applications (i.e., tumor targeting, BBB crossing); nevertheless, none of them have been approved. The latest failure is BIND-014, a polymeric nanoparticle made of polylactide polyethylene glycol (PLA-PEG) loaded with docetaxel and functionalized with a ligand targeting the extracellular domain of prostate-specific membrane antigen [291]. Even if pre-clinical studies showed a high accumulation of BIND-014 in tumors [292] and that phase 2 clinical study was promising, BIND-014 did not reduce docetaxel's toxicity profile [291]. The clinical translation of active targeting strategies is submitted to more profound evaluation is particularly challenging since every component of the targeted formulation needs to be evaluated: let it be from the targeting interaction with its ligand, the toxicity profile of each element, pharmacological evaluation, drug release studies, and physio-chemistry characterization similarly to what we did at each step.

Moreover, in **chapter 2,** we described several strategies to functionalize LNC. All the strategies we told were multistep processes that will be how expensive and difficult it will be to scale up such a system and achieve a reproducible formulation batch. Although in this thesis we didn't succeed in demonstrating that our formulation can target OPC, based on the results we shared in **chapter 2**; still we believe that drug-loaded LNC can be a real asset for non-invasive intranasal delivery in the scope of MS. Overall, we believe that nanomedicines, such as LNC, can centralize potential drug candidates into the market. As an example, for the last decades, some active compounds have been reformulated into a liposomal formulation, improving their toxicity/efficacy profile (more recently Vyxeox©, a liposomal formulation of cytarabine and daunorubicin). In a similar vein, we think that LNC could unravel the potential of biological compounds that could be used in MS. In conclusion, LNC can be a formidable tool to sublime the therapeutic effects of promising compounds that failed to go into development because of a drug delivery issues (Fig.5).

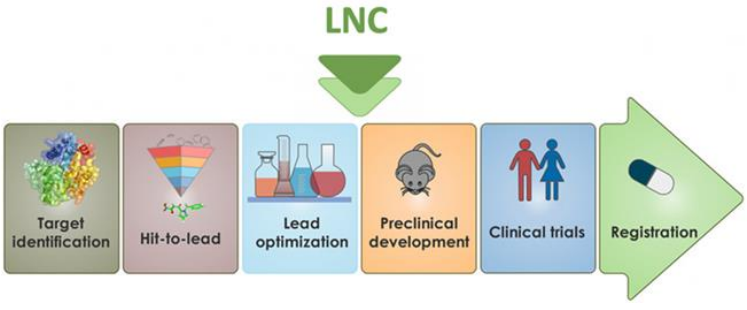

Figure 5. The place of LNC in the pipeline of drug development [293].

V. REFERENCES

1. Walton, C., et al., *Rising prevalence of multiple sclerosis worldwide: Insights from the Atlas of MS, third edition.* Mult Scler, 2020. **26**(14): p. 1816-1821.
2. Vaughn, C.B., et al., *Epidemiology and treatment of multiple sclerosis in elderly populations.* Nat Rev Neurol, 2019. **15**(6): p. 329-342.
3. Moghaddam, V.K., et al., *Socioeconomic determinants of global distribution of multiple sclerosis: an ecological investigation based on Global Burden of Disease data.* BMC Neurol, 2021. **21**(1): p. 145.
4. Chang, S.W. and H.C. Lee, *Vitamin D and health - The missing vitamin in humans.* Pediatr Neonatol, 2019. **60**(3): p. 237-244.
5. Khosravi-Largani, M., et al., *A review on potential roles of vitamins in incidence, progression, and improvement of multiple sclerosis.* eNeurologicalSci, 2018. **10**: p. 37-44.
6. Munger, K.L., T. Chitnis, and A. Ascherio, *Body size and risk of MS in two cohorts of US women.* Neurology, 2009. **73**(19): p. 1543-50.
7. Guillemot-Legris, O. and G.G. Muccioli, *Obesity-Induced Neuroinflammation: Beyond the Hypothalamus.* Trends Neurosci, 2017. **40**(4): p. 237-253.
8. Guerrero-Garcia, J.J., et al., *Multiple Sclerosis and Obesity: Possible Roles of Adipokines.* Mediators Inflamm, 2016. **2016**: p. 4036232.
9. Boziki, M.K., et al., *Microbiome in Multiple Sclerosis; Where Are We, What We Know and Do Not Know.* Brain Sci, 2020. **10**(4).
10. Arneth, B., *Multiple Sclerosis and Smoking.* Am J Med, 2020. **133**(7): p. 783-788.
11. Pittas, F., et al., *Smoking is associated with progressive disease course and increased progression in clinical disability in a prospective cohort of people with multiple sclerosis.* J Neurol, 2009. **256**(4): p. 577-85.
12. Healy, B.C., et al., *Smoking and disease progression in multiple sclerosis.* Arch Neurol, 2009. **66**(7): p. 858-64.
13. Rosso, M. and T. Chitnis, *Association Between Cigarette Smoking and Multiple Sclerosis: A Review.* JAMA Neurol, 2020. **77**(2): p. 245-253.
14. Seo, S.B., et al., *The effect of tobacco smoke exposure on the generation of reactive oxygen species and cellular membrane damage using co-culture model of blood brain barrier with astrocytes.* Toxicol Ind Health, 2017. **33**(6): p. 530-536.
15. Heldt, N.A., et al., *Electronic cigarette exposure disrupts blood-brain barrier integrity and promotes neuroinflammation.* Brain Behav Immun, 2020. **88**: p. 363-380.
16. Dobson, R., et al., *Epstein-Barr-negative MS: a true phenomenon?* Neurol Neuroimmunol Neuroinflamm, 2017. **4**(2): p. e318.
17. Bjornevik, K., et al., *Longitudinal analysis reveals high prevalence of Epstein-Barr virus associated with multiple sclerosis.* Science, 2022. **375**(6578): p. 296-301.
18. Bar-Or, A., et al., *Epstein-Barr Virus in Multiple Sclerosis: Theory and Emerging Immunotherapies.* Trends Mol Med, 2020. **26**(3): p. 296-310.
19. Robinson, W.H. and L. Steinman, *Epstein-Barr virus and multiple sclerosis.* Science, 2022. **375**(6578): p. 264-265.
20. Patsopoulos, N.A., *Genetics of Multiple Sclerosis: An Overview and New Directions.* Cold Spring Harb Perspect Med, 2018. **8**(7).
21. Hollenbach, J.A. and J.R. Oksenberg, *The immunogenetics of multiple sclerosis: A comprehensive review.* J Autoimmun, 2015. **64**: p. 13-25.

22. Waubant, E., et al., *Environmental and genetic risk factors for MS: an integrated review.* Ann Clin Transl Neurol, 2019. **6**(9): p. 1905-1922.

23. Lubetzki, C., et al., *Remyelination in multiple sclerosis: from basic science to clinical translation.* Lancet Neurol, 2020. **19**(8): p. 678-688.

24. Stadelmann, C., et al., *Myelin in the Central Nervous System: Structure, Function, and Pathology.* Physiol Rev, 2019. **99**(3): p. 1381-1431.

25. Franklin, R.J.M. and C. Ffrench-Constant, *Regenerating CNS myelin - from mechanisms to experimental medicines.* Nat Rev Neurosci, 2017. **18**(12): p. 753-769.

26. Lemus, H.N., A.E. Warrington, and M. Rodriguez, *Multiple Sclerosis: Mechanisms of Disease and Strategies for Myelin and Axonal Repair.* Neurol Clin, 2018. **36**(1): p. 1-11.

27. Barnett, M.H. and J.W. Prineas, *Relapsing and remitting multiple sclerosis: pathology of the newly forming lesion.* Ann Neurol, 2004. **55**(4): p. 458-68.

28. Dendrou, C.A., L. Fugger, and M.A. Friese, *Immunopathology of multiple sclerosis.* 2015.

29. van Langelaar, J., et al., *B and T Cells Driving Multiple Sclerosis: Identity, Mechanisms and Potential Triggers.* Front Immunol, 2020. **11**: p. 760.

30. Lubetzki, C. and B. Stankoff, *Demyelination in multiple sclerosis.* Handb Clin Neurol, 2014. **122**: p. 89-99.

31. Wynford-Thomas, R., A. Jacob, and V. Tomassini, *Neurological update: MOG antibody disease.* J Neurol, 2019. **266**(5): p. 1280-1286.

32. Srivastava, R., et al., *Potassium channel KIR4.1 as an immune target in multiple sclerosis.* N Engl J Med, 2012. **367**(2): p. 115-23.

33. Cencioni, M.T., et al., *B cells in multiple sclerosis - from targeted depletion to immune reconstitution therapies.* Nat Rev Neurol, 2021. **17**(7): p. 399-414.

34. Lisak, R.P., et al., *Secretory products of multiple sclerosis B cells are cytotoxic to oligodendroglia in vitro.* J Neuroimmunol, 2012. **246**(1-2): p. 85-95.

35. Perera, Y.R., et al., *Using NMR Spectroscopy To Measure Protein Binding Capacity on Gold Nanoparticles.* J Chem Educ, 2020. **97**(3): p. 820-824.

36. Lloyd, A.F. and V.E. Miron, *The pro-remyelination properties of microglia in the central nervous system.* Nat Rev Neurol, 2019. **15**(8): p. 447-458.

37. Zia, S., et al., *Microglia Diversity in Health and Multiple Sclerosis.* Front Immunol, 2020. **11**: p. 588021.

38. Lloyd, A.F., et al., *Central nervous system regeneration is driven by microglia necroptosis and repopulation.* Nat Neurosci, 2019. **22**(7): p. 1046-1052.

39. Guerrero, B.L. and N.L. Sicotte, *Microglia in Multiple Sclerosis: Friend or Foe?* Front Immunol, 2020. **11**: p. 374.

40. Stratoulias, V., et al., *Microglial subtypes: diversity within the microglial community.* EMBO J, 2019. **38**(17): p. e101997.

41. Accardo, A., et al., *Easy formulation of liposomal doxorubicin modified with a bombesin peptide analogue for selective targeting of GRP receptors overexpressed by cancer cells.* Drug Deliv Transl Res, 2019. **9**(1): p. 215-226.

42. Lloyd, A.F. and V.E. Miron, *The pro-remyelination properties of microglia in the central nervous system.* 2019.

43. Miron, V.E., et al., *M2 microglia and macrophages drive oligodendrocyte differentiation during CNS remyelination.* Nature Neuroscience, 2013.

44. Correale, J. and M.F. Farez, *The Role of Astrocytes in Multiple Sclerosis Progression.* Front Neurol, 2015. **6**: p. 180.

45. Guerrero-Garcia, J.J., *The role of astrocytes in multiple sclerosis pathogenesis.* Neurologia (Engl Ed), 2020. **35**(6): p. 400-408.

46. Ponath, G., C. Park, and D. Pitt, *The Role of Astrocytes in Multiple Sclerosis.* Front Immunol, 2018. **9**: p. 217.

47. Franklin, R.J.M. and C. Ffrench-Constant, *Regenerating CNS myelin - From mechanisms to experimental medicines*. 2017.

48. Nutma, E., et al., *Astrocyte and Oligodendrocyte Cross-Talk in the Central Nervous System.* Cells, 2020. **9**(3).

49. Boyd, A., H. Zhang, and A. Williams, *Insufficient OPC migration into demyelinated lesions is a cause of poor remyelination in MS and mouse models.* Acta Neuropathol, 2013. **125**(6): p. 841-59.

50. Adams, K.L., et al., *Intrinsic and extrinsic regulators of oligodendrocyte progenitor proliferation and differentiation.* Semin Cell Dev Biol, 2021. **116**: p. 16-24.

51. Traiffort, E., et al., *Astrocytes and Microglia as Major Players of Myelin Production in Normal and Pathological Conditions.* Front Cell Neurosci, 2020. **14**: p. 79.

52. Magri, L., et al., *E2F1 coregulates cell cycle genes and chromatin components during the transition of oligodendrocyte progenitors from proliferation to differentiation.* J Neurosci, 2014. **34**(4): p. 1481-93.

53. Kuhn, S., et al., *Oligodendrocytes in Development, Myelin Generation and Beyond.* Cells, 2019. **8**(11).

54. Marinelli, C., et al., *Systematic Review of Pharmacological Properties of the Oligodendrocyte Lineage.* Front Cell Neurosci, 2016. **10**: p. 27.

55. Blakemore, W.F., *Pattern of remyelination in the CNS*. Nature, 1974. **249**(457): p. 577-8.

56. Woodruff, R.H., et al., *Platelet-derived growth factor regulates oligodendrocyte progenitor numbers in adult CNS and their response following CNS demyelination.* Mol Cell Neurosci, 2004. **25**(2): p. 252-62.

57. Yeung, M.S.Y., et al., *Dynamics of oligodendrocyte generation in multiple sclerosis.* Nature, 2019. **566**(7745): p. 538-542.

58. Jakel, S., et al., *Altered human oligodendrocyte heterogeneity in multiple sclerosis.* Nature, 2019. **566**(7745): p. 543-547.

59. Franklin, R.J.M., J. Frisen, and D.A. Lyons, *Revisiting remyelination: Towards a consensus on the regeneration of CNS myelin.* Semin Cell Dev Biol, 2021. **116**: p. 3-9.

60. Bacmeister, C.M., et al., *Motor learning promotes remyelination via new and surviving oligodendrocytes.* Nat Neurosci, 2020. **23**(7): p. 819-831.

61. Duncan, I.D., et al., *The adult oligodendrocyte can participate in remyelination.* Proc Natl Acad Sci U S A, 2018. **115**(50): p. E11807-E11816.

62. Barzegar, M., et al., *Early predictors of conversion to secondary progressive multiple sclerosis.* Mult Scler Relat Disord, 2021. **54**: p. 103115.

63. Faissner, S., et al., *Progressive multiple sclerosis: from pathophysiology to therapeutic strategies.* Nat Rev Drug Discov, 2019. **18**(12): p. 905-922.

64. Filippi, M., et al., *Multiple sclerosis.* Nat Rev Dis Primers, 2018. **4**(1): p. 43.

65. Olek, M.J., *Multiple Sclerosis.* Ann Intern Med, 2021. **174**(6): p. ITC81-ITC96.

66. Thompson, A.J., et al., *Multiple sclerosis.* Lancet, 2018. **391**(10130): p. 1622-1636.

67. Barin, L., et al., *The disease burden of Multiple Sclerosis from the individual and population perspective: Which symptoms matter most?* Mult Scler Relat Disord, 2018. **25**: p. 112-121.

68. Roth, A.K., et al., *Cognition in older patients with multiple sclerosis compared to patients with amnestic mild cognitive impairment and healthy older adults.* Neuropsychology, 2018. **32**(6): p. 654-663.

69. Torre-Fuentes, L., et al., *Experimental models of demyelination and remyelination.* Neurologia (Engl Ed), 2020. **35**(1): p. 32-39.

70. Wiedrick, J., et al., *Sex differences in EAE reveal common and distinct cellular and molecular components.* Cell Immunol, 2021. **359**: p. 104242.

71. Zhan, J., et al., *The Cuprizone Model: Dos and Do Nots.* Cells, 2020. **9**(4).

72. Gudi, V., et al., *Glial response during cuprizone-induced de- and remyelination in the CNS: lessons learned.* Front Cell Neurosci, 2014. **8**: p. 73.

73. Denic, A., et al., *The relevance of animal models in multiple sclerosis research.* Pathophysiology, 2011. **18**(1): p. 21-9.

74. Sutiwisesak, R., et al., *Remyelination therapies for multiple sclerosis: optimizing translation from animal models into clinical trials.* Expert Opin Investig Drugs, 2021. **30**(8): p. 857-876.

75. Mozafari, S. and A. Baron-Van Evercooren, *Human stem cell-derived oligodendrocytes: From humanized animal models to cell therapy in myelin diseases.* Semin Cell Dev Biol, 2021. **116**: p. 53-61.

76. Hauser, S.L. and B.A.C. Cree, *Treatment of Multiple Sclerosis: A Review.* Am J Med, 2020. **133**(12): p. 1380-1390 e2.

77. Jakimovski, D., et al., *Interferon beta for Multiple Sclerosis.* Cold Spring Harb Perspect Med, 2018. **8**(11).

78. Aharoni, R., *The mechanism of action of glatiramer acetate in multiple sclerosis and beyond.* Autoimmun Rev, 2013. **12**(5): p. 543-53.

79. Syed, Y.Y., *Ocrelizumab: A Review in Multiple Sclerosis.* CNS Drugs, 2018. **32**(9): p. 883-890.

80. Brandstadter, R. and I. Katz Sand, *The use of natalizumab for multiple sclerosis.* Neuropsychiatr Dis Treat, 2017. **13**: p. 1691-1702.

81. Zhang, X., et al., *Differential reconstitution of T cell subsets following immunodepleting treatment with alemtuzumab (anti-CD52 monoclonal antibody) in patients with relapsing-remitting multiple sclerosis.* J Immunol, 2013. **191**(12): p. 5867-74.

82. Mi, S., R.B. Pepinsky, and D. Cadavid, *Blocking LINGO-1 as a therapy to promote CNS repair: from concept to the clinic.* CNS Drugs, 2013. **27**(7): p. 493-503.

83. Mi, S., A. Sandrock, and R.H. Miller, *LINGO-1 and its role in CNS repair.* Int J Biochem Cell Biol, 2008. **40**(10): p. 1971-8.

84. Mi, S., et al., *LINGO-1 antagonist promotes spinal cord remyelination and axonal integrity in MOG-induced experimental autoimmune encephalomyelitis.* Nat Med, 2007. **13**(10): p. 1228-33.

85. Moradbeygi, K., et al., *Anti-LINGO-1 improved remyelination and neurobehavioral deficit in cuprizone-induced demyelination.* Iran J Basic Med Sci, 2021. **24**(7): p. 900-907.

86. Cadavid, D., et al., *Safety and efficacy of opicinumab in acute optic neuritis (RENEW): a randomised, placebo-controlled, phase 2 trial.* Lancet Neurol, 2017. **16**(3): p. 189-199.

87. Cadavid, D., et al., *Safety and efficacy of opicinumab in patients with relapsing multiple sclerosis (SYNERGY): a randomised, placebo-controlled, phase 2 trial.* Lancet Neurol, 2019. **18**(9): p. 845-856.

88. Turner, R.B., et al., *Effectiveness of clemastine fumarate for treatment of rhinorrhea and sneezing associated with the common cold.* Clin Infect Dis, 1997. **25**(4): p. 824-30.

89. Mei, F., et al., *Micropillar arrays as a high-throughput screening platform for therapeutics in multiple sclerosis.* Nat Med, 2014. **20**(8): p. 954-960.

90. Green, A.J., et al., *Clemastine fumarate as a remyelinating therapy for multiple sclerosis (ReBUILD): a randomised, controlled, double-blind, crossover trial.* The Lancet, 2017.

91. Green, A.J., et al., *Clemastine fumarate as a remyelinating therapy for multiple sclerosis (ReBUILD): a randomised, controlled, double-blind, crossover trial.* Lancet, 2017. **390**(10111): p. 2481-2489.

92. Deshmukh, V.A., et al., *A regenerative approach to the treatment of multiple sclerosis.* Nature, 2013. **502**(7471): p. 327-332.

93. Huang, J.K., et al., *Retinoid X receptor gamma signaling accelerates CNS remyelination.* Nature Neuroscience, 2011.

94. Huang, J.K., et al., *Retinoid X receptor gamma signaling accelerates CNS remyelination.* Nat Neurosci, 2011. **14**(1): p. 45-53.

95. Carradori, D., et al., *Retinoic acid-loaded NFL-lipid nanocapsules promote oligodendrogenesis in focal white matter lesion.* Biomaterials, 2020.

96. Lefebvre, P., Y. Benomar, and B. Staels, *Retinoid X receptors: common heterodimerization partners with distinct functions.* Trends Endocrinol Metab, 2010. **21**(11): p. 676-83.

97. Brown, J.W.L., et al., *Safety and efficacy of bexarotene in patients with relapsing-remitting multiple sclerosis (CCMR One): a randomised, double-blind, placebo-controlled, parallel-group, phase 2a study.* Lancet Neurol, 2021. **20**(9): p. 709-720.

98. Haugen, B.R., *Drugs that suppress TSH or cause central hypothyroidism.* Best Pract Res Clin Endocrinol Metab, 2009. **23**(6): p. 793-800.

99. de Vries-van der Weij, J., et al., *Bexarotene induces dyslipidemia by increased very low-density lipoprotein production and cholesteryl ester transfer protein-mediated reduction of high-density lipoprotein.* Endocrinology, 2009. **150**(5): p. 2368-75.

100. De La Fuente, A.G., et al., *Vitamin D receptor-retinoid X receptor heterodimer signaling regulates oligodendrocyte progenitor cell differentiation.* Journal of Cell Biology, 2015.

101. Nystad, A.E., O. Torkildsen, and S. Wergeland, *Effects of vitamin D on axonal damage during de- and remyelination in the cuprizone model.* J Neuroimmunol, 2018. **321**: p. 61-65.

102. Wasnik, S., et al., *Vitamin D as a Potential Therapy for Multiple Sclerosis: Where Are We?* Int J Mol Sci, 2020. **21**(9).

103. Soilu-Hanninen, M., et al., *A randomised, double blind, placebo controlled trial with vitamin D3 as an add on treatment to interferon beta-1b in patients with multiple sclerosis.* J Neurol Neurosurg Psychiatry, 2012. **83**(5): p. 565-71.

104. Camu, W., et al., *Cholecalciferol in relapsing-remitting MS: A randomized clinical trial (CHOLINE).* Neurol Neuroimmunol Neuroinflamm, 2019. **6**(5).

105. Cunniffe, N. and A. Coles, *Promoting remyelination in multiple sclerosis.* J Neurol, 2021. **268**(1): p. 30-44.

106. Beloqui, A., et al., *Nanostructured lipid carriers as oral delivery systems for poorly soluble drugs.* Journal of Drug Delivery Science and Technology, 2017. **42**: p. 144-154.

107. Beloqui, A., et al., *Nanostructured lipid carriers: Promising drug delivery systems for future clinics.* Nanomedicine, 2016. **12**(1): p. 143-61.

108. Ashley, C.E., et al., *The targeted delivery of multicomponent cargos to cancer cells by nanoporous particle-supported lipid bilayers.* Nature Materials, 2011. **10**(5): p. 389-397.

109. Messerschmidt, S.K.E., et al., *Targeted lipid-coated nanoparticles: Delivery of tumor necrosis factor-functionalized particles to tumor cells.* Journal of Controlled Release, 2009. **137**(1): p. 69-77.

110. Rani, S., et al., *Self-Emulsifying Oral Lipid Drug Delivery Systems: Advances and Challenges.* AAPS PharmSciTech, 2019. **20**(3): p. 129.

111. Jesorka, A. and O. Orwar, *Liposomes: technologies and analytical applications.* Annu Rev Anal Chem (Palo Alto Calif), 2008. **1**: p. 801-32.

112. Uner, M. and G. Yener, *Importance of solid lipid nanoparticles (SLN) in various administration routes and future perspectives.* Int J Nanomedicine, 2007. **2**(3): p. 289-300.

113. Huynh, N.T., et al., *Lipid nanocapsules: a new platform for nanomedicine.* Int J Pharm, 2009. **379**(2): p. 201-9.

114. Dave, V., et al., *Lipid-polymer hybrid nanoparticles: Synthesis strategies and biomedical applications.* J Microbiol Methods, 2019. **160**: p. 130-142.

115. Mukherjee, A., et al., *Lipid-polymer hybrid nanoparticles as a next-generation drug delivery platform: state of the art, emerging technologies, and perspectives.* Int J Nanomedicine, 2019. **14**: p. 1937-1952.

116. Matougui, N., et al., *Lipid-based nanoformulations for peptide delivery.* Int J Pharm, 2016. **502**(1-2): p. 80-97.

117. Date, T., et al., *Lipid-polymer hybrid nanocarriers for delivering cancer therapeutics.* J Control Release, 2018. **271**: p. 60-73.

118. Hadinoto, K., A. Sundaresan, and W.S. Cheow, *Lipid-polymer hybrid nanoparticles as a new generation therapeutic delivery platform: a review.* Eur J Pharm Biopharm, 2013. **85**(3 Pt A): p. 427-43.

119. Jain, S., et al., *Gelatin coated hybrid lipid nanoparticles for oral delivery of amphotericin B.* Mol Pharm, 2012. **9**(9): p. 2542-53.

120. Battaglia, L. and M. Gallarate, *Lipid nanoparticles: state of the art, new preparation methods and challenges in drug delivery.* Expert Opin Drug Deliv, 2012. **9**(5): p. 497-508.

121. Soares, T.B., et al., *Lipid nanocarriers loaded with natural compounds: Potential new therapies for age related neurodegenerative diseases?* Prog Neurobiol, 2018. **168**: p. 21-41.

122. Moura, R.P., et al., *Lipid nanocapsules to enhance drug bioavailability to the central nervous system.* Journal of Controlled Release, 2020. **322**: p. 390-400.

123. Montigaud, Y., et al., *Optimized acriflavine-loaded lipid nanocapsules as a safe and effective delivery system to treat breast cancer.* Int J Pharm, 2018. **551**(1-2): p. 322-328.

124. Béduneau, A., et al., *Design of targeted lipid nanocapsules by conjugation of whole antibodies and antibody Fab' fragments.* Biomaterials, 2007. **28**(33): p. 4978-4990.

125. Heurtault, B., et al., *A novel phase inversion-based process for the preparation of lipid nanocarriers.* Pharmaceutical Research, 2002.

126. Thi, T.T.H., et al., *Lipid-Based Nanoparticles in the Clinic and Clinical Trials: From Cancer Nanomedicine to COVID-19 Vaccines.* Vaccines (Basel), 2021. **9**(4).

127. Lehner, R., et al., *Intelligent nanomaterials for medicine: Carrier platforms and targeting strategies in the context of clinical application.* Nanomedicine: Nanotechnology, Biology, and Medicine, 2013. **9**(6): p. 742-757.

128. Strebhardt, K. and A. Ullrich, *Paul Ehrlich's magic bullet concept: 100 Years of progress.* Nature Reviews Cancer, 2008. **8**(6): p. 473-480.

129. Nogueira, E., et al., *Design of liposomal formulations for cell targeting.* Colloids and Surfaces B: Biointerfaces, 2015. **136**: p. 514-526.

130. Zylberberg, C., et al., *Engineering liposomal nanoparticles for targeted gene therapy*. 2017, Nature Publishing Group. p. 441-452.

131. Singh, M.S., et al., *Therapeutic Gene Silencing Using Targeted Lipid Nanoparticles in Metastatic Ovarian Cancer.* Small, 2021. **17**(19): p. e2100287.

132. Konning, D. and H. Kolmar, *Beyond antibody engineering: directed evolution of alternative binding scaffolds and enzymes using yeast surface display.* Microb Cell Fact, 2018. **17**(1): p. 32.

133. Manjappa, A.S., et al., *Antibody derivatization and conjugation strategies: Application in preparation of stealth immunoliposome to target chemotherapeutics to tumor.* Journal of Controlled Release, 2011. **150**(1): p. 2-22.

134. Weisser, N.E. and J.C. Hall, *Applications of single-chain variable fragment antibodies in therapeutics and diagnostics.* Biotechnology Advances, 2009. **27**(4): p. 502-520.

135. Wang, Y., et al., *Nanobody-derived nanobiotechnology tool kits for diverse biomedical and biotechnology applications.* International Journal of Nanomedicine, 2016. **11**: p. 3287-3303.

136. Beuttler, J., et al., *Targeting of epidermal growth factor receptor (EGFR)-expressing tumor cells with sterically stabilized affibody liposomes (SAL).* Bioconjugate Chemistry, 2009. **20**(6): p. 1201-1208.

137. Danhier, F., et al., *Tumor Targeting by RGD-Grafted PLGA-Based Nanotheranostics Loaded with*

Paclitaxel and Superparamagnetic Iron Oxides, in *Methods in Pharmacology and Toxicology: Integrin Targeting Systems for Tumor Diagnosis and Therapy*, E. Patsenker, Editor. 2015, Springer. p. 1-17.

138. Jiang, T., et al., *Dual-functional liposomes based on pH-responsive cell-penetrating peptide and hyaluronic acid for tumor-targeted anticancer drug delivery.* Biomaterials, 2012. **33**(36): p. 9246-9258.

139. Qin, Y., et al., *Liposome formulated with TAT-modified cholesterol for improving brain delivery and therapeutic efficacy on brain glioma in animals.* International Journal of Pharmaceutics, 2011. **420**(2): p. 304-312.

140. Hong, S., et al., *Aptamer-integrated α-Gal liposomes as bispecific agents to trigger immune response for killing tumor cells.* Journal of Biomedical Materials Research Part A, 2019. **107**(6): p. 1176-1183.

141. Nascimento, T.L., et al., *Lipid-based nanosystems for CD44 targeting in cancer treatment: Recent significant advances, ongoing challenges and unmet needs.* Nanomedicine, 2016. **11**(14): p. 1865-1887.

142. Franzen, S., *A comparison of peptide and folate receptor targeting of cancer cells: from single agent to nanoparticle.* Expert Opinion on Drug Delivery, 2011. **8**(3): p. 281-298.

143. Nobs, L., et al., *Current methods for attaching targeting ligands to liposomes and nanoparticles.* Journal of Pharmaceutical Sciences, 2004. **93**(8): p. 1980-1992.

144. Marqués-Gallego, P. and A.I.P.M. de Kroon, *Ligation Strategies for Targeting Liposomal Nanocarriers.* BioMed Research International, 2014. **2014**: p. 1-12.

145. Dumont, N., et al., *Nanoliposome targeting in breast cancer is influenced by the tumor microenvironment.* Nanomedicine: Nanotechnology, Biology and Medicine, 2019. **17**: p. 71-81.

146. Vabbilisetty, P., et al., *Chemical Reactive Anchoring Lipids with Different Performance for Cell Surface Re-engineering Application.* ACS Omega, 2018. **3**(2): p. 1589-1599.

147. Baek, J.-S. and C.-W. Cho, *A multifunctional lipid nanoparticle for co-delivery of paclitaxel and curcumin for targeted delivery and enhanced cytotoxicity in multidrug resistant breast cancer cells.* Oncotarget, 2017. **8**(18): p. 30369-30382.

148. Toriyabe, N., et al., *Synthesis and Evaluation of Stearylated Hyaluronic Acid for the Active Delivery of Liposomes to Liver Endothelial Cells.* Biological & Pharmaceutical Bulletin, 2011. **34**(7): p. 1084-1089.

149. Allen, T.M., P. Sapra, and E. Moase, *Use of the post-insertion method for the formation of ligand-coupled liposomes.* Cell Mol Biol Lett, 2002. **7**(3): p. 889-94.

150. Tansi, F.L., et al., *Activatable bispecific liposomes bearing fibroblast activation protein directed single chain fragment/Trastuzumab deliver encapsulated cargo into the nuclei of tumor cells and the tumor microenvironment simultaneously.* Acta Biomater, 2017. **54**: p. 281-293.

151. Tansi, F.L., et al., *Activatable bispecific liposomes bearing fibroblast activation protein directed single chain fragment/Trastuzumab deliver encapsulated cargo into the nuclei of tumor cells and the tumor microenvironment simultaneously.* Acta Biomaterialia, 2017. **54**: p. 281-293.

152. He, Y., L. Zhang, and C. Song, *Luteinizing hormone-releasing hormone receptor-mediated delivery of mitoxantrone using LHRH analogs modified with PEGylated liposomes.* International Journal of Nanomedicine, 2010. **5**(1): p. 697-705.

153. Mitchell, M.J., et al., *E-selectin liposomal and nanotube-targeted delivery of doxorubicin to circulating tumor cells.* Journal of Controlled Release, 2012. **160**(3): p. 609-617.

154. Önyüksel, H., E. Jeon, and I. Rubinstein, *Nanomicellar paclitaxel increases cytotoxicity of multidrug resistant breast cancer cells.* Cancer Letters, 2009. **274**(2): p. 327-330.

155. Bourseau-Guilmain, E., et al., *Development and characterization of immuno-nanocarriers targeting the cancer stem cell marker AC133.* International Journal of Pharmaceutics, 2012. **423**(1): p. 93-101.

156. Kim, M.S., et al., *Engineering macrophage-derived exosomes for targeted paclitaxel delivery to pulmonary metastases: in vitro and in vivo evaluations.* Nanomedicine: Nanotechnology, Biology, and Medicine, 2018. **14**(1): p. 195-204.

157. Lin, Y.L., et al., *Specific drug delivery efficiently induced human breast tumor regression using a lipoplex by non-covalent association with anti-tumor antibodies.* Journal of Nanobiotechnology, 2019. **17**(1): p. 1-11.

158. Carradori, D., et al., *NFL-lipid nanocapsules for brain neural stem cell targeting in vitro and in vivo.* Journal of Controlled Release, 2016. **238**: p. 253-262.

159. Apaolaza, P.S., et al., *A novel gene therapy vector based on hyaluronic acid and solid lipid nanoparticles for ocular diseases.* International Journal of Pharmaceutics, 2014. **465**(1-2): p. 413-426.

160. Tiantian, Y., et al., *Study on intralymphatic-targeted hyaluronic acid-modified nanoliposome: Influence of formulation factors on the lymphatic targeting.* International Journal of Pharmaceutics, 2014. **471**(1-2): p. 245-257.

161. Fischer, D., et al., *In vitro cytotoxicity testing of polycations: influence of polymer structure on cell viability and hemolysis.* Biomaterials, 2003. **24**(7): p. 1121-31.

162. Platt, V., et al., *Influence of Multivalent Nitrilotriacetic Acid Lipid−Ligand Affinity on the Circulation Half-Life in Mice of a Liposome-Attached His 6 -Protein.* Bioconjugate Chemistry, 2010. **21**(5): p. 892-902.

163. Shao, S., et al., *Functionalization of cobalt porphyrin-phospholipid bilayers with his-tagged ligands and antigens.* Nature chemistry, 2015. **7**(5): p. 438-46.

164. Bak, M., et al., *Affinity Induced Surface Functionalization of Liposomes Using Cu-Free Click Chemistry.* Bioconjugate Chemistry, 2016. **27**(7): p. 1673-1680.

165. Alvarez-Erviti, L., et al., *Delivery of siRNA to the mouse brain by systemic injection of targeted exosomes.* Nature Biotechnology, 2011. **29**(4): p. 341-345.

166. Tian, Y., et al., *A doxorubicin delivery platform using engineered natural membrane vesicle exosomes for targeted tumor therapy.* Biomaterials, 2014. **35**(7): p. 2383-2390.

167. Hermanson, G.T., *Bioconjugate Techniques*. 2013: Elsevier.

168. Torchilin, V.P., et al., *p-nitrophenylcarbonyl-PEG-PE-liposomes: Fast and simple attachment of specific ligands, including monoclonal antibodies, to distal ends of PEG chains via p-nitrophenylcarbonyl groups.* Biochimica et Biophysica Acta - Biomembranes, 2001. **1511**(2): p. 397-411.

169. Khayrani, A.C., et al., *Targeting Ovarian Cancer Cells Overexpressing CD44 with Immunoliposomes Encapsulating Glycosylated Paclitaxel.* International Journal of Molecular Sciences, 2019. **20**(5): p. 1042-1042.

170. Sinhmar, G.K., et al., *Surface engineered lipid nanoparticle-mediated site-specific drug delivery system for the treatment of inflammatory bowel disease.* Artificial Cells, Nanomedicine and Biotechnology, 2018. **46**(sup2): p. 565-578.

171. Zhang, L., et al., *Targeted Codelivery of an Antigen and Dual Agonists by Hybrid Nanoparticles for Enhanced Cancer Immunotherapy.* Nano Letters, 2019. **19**(7): p. 4237-4249.

172. Noble, G.T., et al., *Ligand-targeted liposome design: Challenges and fundamental considerations.* Trends in Biotechnology, 2014. **32**(1): p. 32-45.

173. Varshosaz, J., et al., *Synthesis of octadecylamine-retinoic acid conjugate for enhanced cytotoxic effects of 5-FU using LDL targeted nanostructured lipid carriers.* European Journal of Medicinal Chemistry, 2012. **54**: p. 429-438.

174. Sobot, D., et al., *Conjugation of squalene to gemcitabine as unique approach exploiting endogenous lipoproteins for drug delivery.* Nature Communications, 2017. **8**(May): p. 1-9.

175. Song, H., et al., *Enhanced permeability of blood-brain barrier and targeting function of brain via borneol-modified chemically solid lipid nanoparticle.* International Journal of Nanomedicine, 2018.

176. Bunggulawa, E.J., et al., *Recent advancements in the use of exosomes as drug delivery systems.* J Nanobiotechnology, 2018. **16**(1): p. 81.

177. Gopalan, D., et al., *Receptor specific, stimuli responsive and subcellular targeted approaches for effective therapy of Alzheimer: Role of surface engineered nanocarriers*. 2020.

178. Aday, S., et al., *Stem Cell-Based Human Blood-Brain Barrier Models for Drug Discovery and Delivery.* Trends Biotechnol, 2016. **34**(5): p. 382-393.

179. Liu, Z., et al., *Preparation and evaluation of Baicalin-loaded cationic solid lipid nanoparticles conjugated with OX26 for improved delivery across the BBB.* Drug Development and Industrial Pharmacy, 2015.

180. McConnell, E.M., et al., *In Vivo Use of a Multi-DNA Aptamer-Based Payload/Targeting System to Study Dopamine Dysregulation in the Central Nervous System.* ACS Chemical Neuroscience, 2019.

181. Salvati, E., et al., *Liposomes functionalized to overcome the blood-brain barrier and to target amyloid-β peptide: The chemical design affects the permeability across an in vitro model.* International Journal of Nanomedicine, 2013. **8**: p. 1749-1758.

182. Loureiro, J.A., et al., *Resveratrol and Grape Extract-loaded Solid Lipid Nanoparticles for the Treatment of Alzheimer's Disease.* Molecules, 2017. **22**(2).

183. Neves, A.R., J.F. Queiroz, and S. Reis, *Brain-targeted delivery of resveratrol using solid lipid nanoparticles functionalized with apolipoprotein E.* Journal of Nanobiotechnology, 2016.

184. Papadia, K., et al., *Multifunctional LUV liposomes decorated for BBB and amyloid targeting - B. In vivo brain targeting potential in wild-type and APP/PS1 mice.* European Journal of Pharmaceutical Sciences, 2017. **102**: p. 180-187.

185. Malfanti, A., et al., *Oligo-guanidyl targeted bioconjugates forming rod shaped polyplexes as a new nanoplatform for oligonucleotide delivery.* J Control Release, 2019. **310**: p. 58-73.

186. Donahue, N.D., H. Acar, and S. Wilhelm, *Concepts of nanoparticle cellular uptake, intracellular trafficking, and kinetics in nanomedicine.* Adv Drug Deliv Rev, 2019. **143**: p. 68-96.

187. Zhang, P., et al., *Anti-PEG antibodies in the clinic: Current issues and beyond PEGylation.* J Control Release, 2016. **244**(Pt B): p. 184-193.

188. Sousa de Almeida, M., et al., *Understanding nanoparticle endocytosis to improve targeting strategies in nanomedicine.* Chem Soc Rev, 2021. **50**(9): p. 5397-5434.

189. Carradori, D., et al., *The origin of neural stem cells impacts their interactions with targeted-lipid nanocapsules: Potential role of plasma membrane lipid composition and fluidity.* J Control Release, 2018. **292**: p. 248-255.

190. Xie, X., et al., *The Effect of shape on Cellular Uptake of Gold Nanoparticles in the forms of Stars, Rods, and Triangles.* Sci Rep, 2017. **7**(1): p. 3827.

191. Chen, L., et al., *The role of surface charge on the uptake and biocompatibility of hydroxyapatite nanoparticles with osteoblast cells.* Nanotechnology, 2011. **22**(10): p. 105708.

192. Ngamcherdtrakul, W., et al., *Cationic Polymer Modified Mesoporous Silica Nanoparticles for Targeted SiRNA Delivery to HER2+ Breast Cancer.* Adv Funct Mater, 2015. **25**(18): p. 2646-2659.

193. Xie, Y., et al., *PEGylated carboxymethyl chitosan/calcium phosphate hybrid anionic nanoparticles mediated hTERT siRNA delivery for anticancer therapy.* Biomaterials, 2014. **35**(27): p. 7978-91.

194. Vigderman, L., P. Manna, and E.R. Zubarev, *Quantitative replacement of cetyl trimethylammonium bromide by cationic thiol ligands on the surface of gold nanorods and their extremely large uptake by cancer cells.* Angew Chem Int Ed Engl, 2012. **51**(3): p. 636-41.

195. Bhattacharjee, S., *DLS and zeta potential - What they are and what they are not?* J Control Release, 2016. **235**: p. 337-351.

196. McDaid, W.J., et al., *Repurposing of Cetuximab in antibody-directed chemotherapy-loaded nanoparticles in EGFR therapy-resistant pancreatic tumours.* Nanoscale, 2019. **11**(42): p. 20261-20273.

197. Lee, N.K., et al., *Impact of the conjugation of antibodies to the surfaces of polymer nanoparticles on the immune cell targeting abilities.* Nano Converg, 2021. **8**(1): p. 24.

198. Gratpain, V., et al., *Extracellular vesicles for the treatment of central nervous system diseases.* Adv Drug Deliv Rev, 2021. **174**: p. 535-552.

199. Dhuria, S.V., L.R. Hanson, and W.H. Frey, 2nd, *Intranasal delivery to the central nervous system: mechanisms and experimental considerations.* J Pharm Sci, 2010. **99**(4): p. 1654-73.

200. Pires, P.C. and A.O. Santos, *Nanosystems in nose-to-brain drug delivery: A review of non-clinical brain targeting studies.* J Control Release, 2018. **270**: p. 89-100.

201. Djupesland, P.G. and A. Skretting, *Nasal deposition and clearance in man: comparison of a bidirectional powder device and a traditional liquid spray pump.* J Aerosol Med Pulm Drug Deliv, 2012. **25**(5): p. 280-9.

202. Bharadwaj, V.N., et al., *Intranasal Administration for Pain: Oxytocin and Other Polypeptides.* Pharmaceutics, 2021. **13**(7).

203. Ganger, S. and K. Schindowski, *Tailoring Formulations for Intranasal Nose-to-Brain Delivery: A Review on Architecture, Physico-Chemical Characteristics and Mucociliary Clearance of the Nasal Olfactory Mucosa.* Pharmaceutics, 2018. **10**(3).

204. Machado-Pereira, M., et al., *Anti-Inflammatory Strategy for M2 Microglial Polarization Using Retinoic Acid-Loaded Nanoparticles.* Mediators of Inflammation, 2017.

205. Kim, S.y., et al., *The influence of retinoic acid on the human oligodendrocyte precursor cells by RNA-sequencing.* Biochemistry and Biophysics Reports, 2017. **9**: p. 166-172.

206. Carradori, D., et al., *Retinoic acid-loaded NFL-lipid nanocapsules promote oligodendrogenesis in focal white matter lesion.* Biomaterials, 2020. **230**: p. 119653.

207. de la Fuente, A.G., et al., *Vitamin D receptor-retinoid X receptor heterodimer signaling regulates oligodendrocyte progenitor cell differentiation.* J Cell Biol, 2015. **211**(5): p. 975-85.

208. Dobson, R. and G. Giovannoni, *Multiple sclerosis – a review.* 2019.

209. Göttle, P., et al., *An unmet clinical need: roads to remyelination in MS*. Neurological Research and Practice, 2019.

210. Roger, E., et al., *Lipid nanocapsules maintain full integrity after crossing a human intestinal epithelium model.* J Control Release, 2017. **253**: p. 11-18.

211. Hirsjarvi, S., et al., *Tumour targeting of lipid nanocapsules grafted with cRGD peptides.* Eur J Pharm Biopharm, 2014. **87**(1): p. 152-9.

212. Laine, A.L., et al., *Brain tumour targeting strategies via coated ferrociphenol lipid nanocapsules.* Eur J Pharm Biopharm, 2012. **81**(3): p. 690-3.

213. Morille, M., et al., *Galactosylated DNA lipid nanocapsules for efficient hepatocyte targeting.* Int J Pharm, 2009. **379**(2): p. 293-300.

214. Carradori, D., et al., *NFL-lipid nanocapsules for brain neural stem cell targeting in vitro and in vivo.* J Control Release, 2016. **238**: p. 253-262.

215. Gazaille, C., et al., *Characterization of Biological Material Adsorption to the Surface of Nanoparticles without a Prior Separation Step: a Case Study of Glioblastoma-Targeting Peptide and Lipid Nanocapsules.* Pharm Res, 2021. **38**(4): p. 681-691.

216. Umerska, A., et al., *Understanding the adsorption of salmon calcitonin, antimicrobial peptide AP114 and polymyxin B onto lipid nanocapsules.* Int J Pharm, 2016. **506**(1-2): p. 191-200.

217. Li, P., et al., *Expression of NG2 and platelet-derived growth factor receptor alpha in the developing neonatal rat brain.* Neural Regen Res, 2017. **12**(11): p. 1843-1852.

218. Zou, J., et al., *Distribution of lipid nanocapsules in different cochlear cell populations after round window membrane permeation.* Journal of Biomedical Materials Research - Part B Applied Biomaterials, 2008.

219. Xu, Y., et al., *Size Effect on Lipid Nanocapsule-Mediated GLP-1 Secretion from Enteroendocrine L Cells.* Mol Pharm, 2018. **15**(1): p. 108-115.

220. Bastiat, G., et al., *A new tool to ensure the fluorescent dye labeling stability of nanocarriers: a real challenge for fluorescence imaging.* J Control Release, 2013. **170**(3): p. 334-42.

221. Messaoudi, K., et al., *Anti-epidermal growth factor receptor siRNA carried by chitosan-transacylated lipid nanocapsules increases sensitivity of glioblastoma cells to temozolomide.* International Journal of Nanomedicine, 2014.

222. Perrier, T., et al., *Post-insertion into Lipid NanoCapsules (LNCs): From experimental aspects to mechanisms.* International Journal of Pharmaceutics, 2010.

223. Behzadi, S., et al., *Cellular uptake of nanoparticles: journey inside the cell.* Chem Soc Rev, 2017. **46**(14): p. 4218-4244.

224. Schelte, P., et al., *Differential reactivity of maleimide and bromoacetyl functions with thiols: application to the preparation of liposomal diepitope constructs.* Bioconjug Chem, 2000. **11**(1): p. 118-23.

225. Udenfriend, S., et al., *Fluorescamine: A reagent for assay of amino acids, peptides, proteins, and primary amines in the picomole range.* Science, 1972.

226. Altieri, F., et al., *Influence of Ellagitannins Extracted by Pomegranate Fruit on Disulfide Isomerase PDIA3 Activity.* Nutrients, 2019. **11**(1).

227. Khayrani, A.C., et al., *Targeting Ovarian Cancer Cells Overexpressing CD44 with Immunoliposomes Encapsulating Glycosylated Paclitaxel.* Int J Mol Sci, 2019. **20**(5).

228. Oh, E., et al., *Preparation of stable maleimide-functionalized au nanoparticles and their use in counting surface ligands.* Small, 2010. **6**(12): p. 1273-8.

229. van Geel, R., et al., *Chemoenzymatic Conjugation of Toxic Payloads to the Globally Conserved N-Glycan of Native mAbs Provides Homogeneous and Highly Efficacious Antibody-Drug Conjugates.* Bioconjug Chem, 2015. **26**(11): p. 2233-42.

230. Yu, S.S., et al., *Size- and charge-dependent non-specific uptake of PEGylated nanoparticles by macrophages.* Int J Nanomedicine, 2012. **7**: p. 799-813.

231. Lorenz, M.R., et al., *Uptake of functionalized, fluorescent-labeled polymeric particles in different cell lines and stem cells.* Biomaterials, 2006. **27**(14): p. 2820-8.

232. McGinley, M.P., C.H. Goldschmidt, and A.D. Rae-Grant, *Diagnosis and Treatment of Multiple Sclerosis: A Review.* JAMA, 2021. **325**(8): p. 765-779.

233. Martinez-Jothar, L., et al., *Insights into maleimide-thiol conjugation chemistry: Conditions for efficient surface functionalization of nanoparticles for receptor targeting.* J Control Release, 2018. **282**: p. 101-109.

234. Jahan, S.T. and A. Haddadi, *Investigation and optimization of formulation parameters on preparation of targeted anti-CD205 tailored PLGA nanoparticles.* Int J Nanomedicine, 2015. **10**: p. 7371-84.

235. Kirpotin, D.B., et al., *Building and characterizing antibody-targeted lipidic nanotherapeutics.* Methods Enzymol, 2012. **502**: p. 139-66.

236. Kitamura, K., et al., *Polyethylene glycol modification of the monoclonal antibody A7 enhances its tumor localization.* Biochem Biophys Res Commun, 1990. **171**(3): p. 1387-94.

237. Chapman, A.P., *PEGylated antibodies and antibody fragments for improved therapy: a review.* Adv Drug Deliv Rev, 2002. **54**(4): p. 531-45.

238. Gai, M., et al., *A bio-orthogonal functionalization strategy for site-specific coupling of antibodies on vesicle surfaces after self-assembly.* Polymer Chemistry, 2020.

239. Botosoa, E.P., et al., *Antibody-Hapten Recognition at the Surface of Functionalized Liposomes Studied by SPR: Steric Hindrance of Pegylated Phospholipids in Stealth Liposomes Prepared for Targeted Radionuclide Delivery.* J Drug Deliv, 2011. **2011**: p. 368535.

240. Osorio-Querejeta, I., et al., *MiR-219a-5p Enriched Extracellular Vesicles Induce OPC Differentiation and EAE Improvement More Efficiently Than Liposomes and Polymeric Nanoparticles.* Pharmaceutics, 2020. **12**(2).

241. Fressinaud, C., et al., *Lipid Nanoparticles Vectorized with NFL-TBS.40-63 Peptide Target Oligodendrocytes and Promote Neurotrophin-3 Effects After Demyelination In Vitro.* Neurochem Res, 2020. **45**(11): p. 2732-2748.

242. Pinton, L., et al., *Targeting of immunosuppressive myeloid cells from glioblastoma patients by modulation of size and surface charge of lipid nanocapsules.* J Nanobiotechnology, 2020. **18**(1): p. 31.

243. Walters, A.A., et al., *Assessment of the enhancement of PLGA nanoparticle uptake by dendritic cells through the addition of natural receptor ligands and monoclonal antibody.* Vaccine, 2015. **33**(48): p. 6588-95.

244. Nakahara, J., et al., *Signaling via immunoglobulin Fc receptors induces oligodendrocyte precursor cell differentiation.* Dev Cell, 2003. **4**(6): p. 841-52.

245. Bruckner, M., et al., *The conjugation strategy affects antibody orientation and targeting properties of nanocarriers.* Nanoscale, 2021. **13**(21): p. 9816-9824.

246. Banks, W.A., *Characteristics of compounds that cross the blood-brain barrier.* BMC Neurol, 2009. **9 Suppl 1**: p. S3.

247. Lee, P.W., et al., *Neuron-Specific Vitamin D Signaling Attenuates Microglia Activation and CNS Autoimmunity.* Front Neurol, 2020. **11**: p. 19.

248. Mutemberezi, V., et al., *Oxysterol levels and metabolism in the course of neuroinflammation: insights from in vitro and in vivo models.* J Neuroinflammation, 2018. **15**(1): p. 74.

249. De Vries, G.H. and A.I. Boullerne, *Glial cell lines: an overview.* Neurochem Res, 2010. **35**(12): p. 1978-2000.

250. Boggs, J.M., *Myelin basic protein: a multifunctional protein.* Cell Mol Life Sci, 2006. **63**(17): p. 1945-61.

251. Dheen, S.T., et al., *Retinoic acid inhibits expression of TNF-a and iNOS in activated rat microglia.* GLIA, 2005.

252. Hur, J., et al., *Regulatory effect of 25-hydroxyvitamin D3 on nitric oxide production in activated microglia.* Korean Journal of Physiology and Pharmacology, 2014.

253. Tintore, M., A. Vidal-Jordana, and J. Sastre-Garriga, *Treatment of multiple sclerosis - success from bench to bedside.* Nat Rev Neurol, 2019. **15**(1): p. 53-58.

254. El-Sheridy, N.A., et al., *Enhancing the in vitro and in vivo activity of itraconazole against breast cancer using miltefosine-modified lipid nanocapsules.* Drug Deliv, 2021. **28**(1): p. 906-919.

255. Cristiano, M.C., et al., *Anticancer activity of all-trans retinoic acid-loaded liposomes on human thyroid carcinoma cells.* Colloids Surf B Biointerfaces, 2017. **150**: p. 408-416.

256. Rafique, A., et al., *Targeted lipid nanoparticle delivery of calcitriol to human monocyte-derived macrophages in vitro and in vivo: investigation of the anti-inflammatory effects of calcitriol.* Int J Nanomedicine, 2019. **14**: p. 2829-2846.

257. Gatti, R., M.G. Gioia, and V. Cavrini, *Analysis and stability study of retinoids in pharmaceuticals by LC with fluorescence detection.* J Pharm Biomed Anal, 2000. **23**(1): p. 147-59.

258. Kouchmeshky, A., et al., *Tissue localization of retinoic acid receptor (RAR) active drugs.* Methods Enzymol, 2020. **637**: p. 513-538.

259. Kato, S., *The function of vitamin D receptor in vitamin D action.* J Biochem, 2000. **127**(5): p. 717-22.

260. Paillard, A., et al., *The importance of endo-lysosomal escape with lipid nanocapsules for drug subcellular bioavailability.* Biomaterials, 2010. **31**(29): p. 7542-54.

261. Dittmer, M., et al., *Characterization of a murine mixed neuron-glia model and cellular responses to regulatory T cell-derived factors.* Molecular Brain, 2018.

262. Dulla, Y.A.T., et al., *Regulatory Mechanisms of Vitamin D3 on Production of Nitric Oxide and Pro-inflammatory Cytokines in Microglial BV-2 Cells.* Neurochemical Research, 2016.

263. Nam, H.Y., et al., *Ibrutinib suppresses LPS-induced neuroinflammatory responses in BV2 microglial cells and wild-type mice.* J Neuroinflammation, 2018. **15**(1): p. 271.

264. Lee, S.C., et al., *Cytokine production by human fetal microglia and astrocytes. Differential induction by lipopolysaccharide and IL-1 beta.* J Immunol, 1993. **150**(7): p. 2659-67.

265. Gonsalvez, D.G., et al., *Imaging and Quantification of Myelin Integrity After Injury With Spectral Confocal Reflectance Microscopy.* Front Mol Neurosci, 2019. **12**: p. 275.

266. Toomey, L.M., et al., *Cuprizone feed formulation influences the extent of demyelinating disease pathology.* Sci Rep, 2021. **11**(1): p. 22594.

267. Steelman, A.J., J.P. Thompson, and J. Li, *Demyelination and remyelination in anatomically distinct regions of the corpus callosum following cuprizone intoxication.* Neurosci Res, 2012. **72**(1): p. 32-42.

268. Kirby, L., et al., *Oligodendrocyte precursor cells present antigen and are cytotoxic targets in inflammatory demyelination.* Nat Commun, 2019. **10**(1): p. 3887.

269. Quarta, A., et al., *Targeting FR-expressing cells in ovarian cancer with Fab-functionalized nanoparticles: a full study to provide the proof of principle from in vitro to in vivo.* Nanoscale, 2015. **7**(6): p. 2336-51.

270. Joshi, S., C. Maharana, and A.S. Rathore, *An application of Nano Differential Scanning Fluorimetry for Higher Order Structure assessment between mAb originator and biosimilars: Trastuzumab and Rituximab as case studies.* J Pharm Biomed Anal, 2020. **186**: p. 113270.

271. Gai, M., et al., *A bio-orthogonal functionalization strategy for site-specific coupling of antibodies on vesicle surfaces after self-assembly.* Polymer Chemistry, 2020. **11**(2): p. 527-540.

272. Waterhouse, D.N., et al., *A comparison of liposomal formulations of doxorubicin with drug administered in free form: changing toxicity profiles.* Drug Saf, 2001. **24**(12): p. 903-20.

273. Papadopoulos, N. and J. Lennartsson, *The PDGF/PDGFR pathway as a drug target.* Mol Aspects Med, 2018. **62**: p. 75-88.

274. Lowery, C.D., et al., *Olaratumab Exerts Antitumor Activity in Preclinical Models of Pediatric Bone and Soft Tissue Tumors through Inhibition of Platelet-Derived Growth Factor Receptor alpha.* Clin Cancer Res, 2018. **24**(4): p. 847-857.

275. McKinnon, R.D., S. Waldron, and M.E. Kiel, *PDGF alpha-receptor signal strength controls an RTK rheostat that integrates phosphoinositol 3'-kinase and phospholipase Cgamma pathways during oligodendrocyte maturation.* J Neurosci, 2005. **25**(14): p. 3499-508.

276. Rittchen, S., et al., *Myelin repair in vivo is increased by targeting oligodendrocyte precursor cells with nanoparticles encapsulating leukaemia inhibitory factor (LIF).* Biomaterials, 2015. **56**: p. 78-85.

277. Lovett-Racke, A.E. and M.K. Racke, *Retinoic acid promotes the development of Th2-like human myelin basic protein-reactive T cells.* Cell Immunol, 2002. **215**(1): p. 54-60.

278. Parastouei, K., et al., *The effect of 1, 25(OH)2 D3 (calcitriol) alone and in combination with all-trans retinoic acid on ROR-gammat, IL-17, TGF-beta, and FOXP3 gene expression in experimental autoimmune encephalomyelitis.* Nutr Neurosci, 2018. **21**(3): p. 210-218.

279. Hemachandar, R., et al., *Hyper Vitaminosis D: Are we Overprescribing Vitamin D?* J Family Med Prim Care, 2014. **3**(4): p. 464-6.

280. Qu, Z.X., et al., *All-trans retinoic acid potentiates the ability of interferon beta-1b to augment suppressor cell function in multiple sclerosis.* Arch Neurol, 1998. **55**(3): p. 315-21.

281. Ruschil, C., et al., *Treatment of progressive multiple sclerosis with high-dose all-trans retinoic acid - no clear evidence of positive disease modifying effects.* Neurol Res Pract, 2021. **3**(1): p. 25.

282. Abdelhamid, L. and X.M. Luo, *Retinoic Acid, Leaky Gut, and Autoimmune Diseases.* Nutrients, 2018. **10**(8).

283. Chauvet, S., et al., *Lipid nanocapsules containing the non-ionic surfactant Solutol HS15 inhibit the transport of calcium through hyperforin-activated channels in neuronal cells.* Neuropharmacology, 2015. **99**: p. 726-34.

284. Urimi, D., et al., *Formulation development and upscaling of lipid nanocapsules as a drug delivery system for a novel cyclic GMP analogue intended for retinal drug delivery.* Int J Pharm, 2021. **602**: p. 120640.

285. Lamprecht, A. and J.P. Benoit, *Etoposide nanocarriers suppress glioma cell growth by intracellular drug delivery and simultaneous P-glycoprotein inhibition.* J Control Release, 2006. **112**(2): p. 208-13.

286. Coon, J.S., et al., *Solutol HS 15, nontoxic polyoxyethylene esters of 12-hydroxystearic acid, reverses multidrug resistance.* Cancer Res, 1991. **51**(3): p. 897-902.

287. Mohsen, K., et al., *Intranasal lipid nanocapsules for systemic delivery of nimodipine into the brain: In vitro optimization and in vivo pharmacokinetic study.* Mater Sci Eng C Mater Biol Appl, 2020. **116**: p. 111236.

288. Sharma, S., et al., *Retinoid X Receptor: Cellular and Biochemical Roles of Nuclear Receptor with a Focus on Neuropathological Involvement.* Mol Neurobiol, 2022.

289. Chandraratna, R.A., R.J. Noelle, and E.C. Nowak, *Treatment with retinoid X receptor agonist IRX4204 ameliorates experimental autoimmune encephalomyelitis.* Am J Transl Res, 2016. **8**(2): p. 1016-26.

290. Bai, Z., et al., *Non-viral nanocarriers for intracellular delivery of microRNA therapeutics.* J Mater Chem B, 2019. **7**(8): p. 1209-1225.

291. Autio, K.A., et al., *Safety and Efficacy of BIND-014, a Docetaxel Nanoparticle Targeting Prostate-Specific Membrane Antigen for Patients With Metastatic Castration-Resistant Prostate Cancer: A Phase 2 Clinical Trial.* JAMA Oncol, 2018. **4**(10): p. 1344-1351.

292. Hrkach, J., et al., *Preclinical development and clinical translation of a PSMA-targeted docetaxel nanoparticle with a differentiated pharmacological profile.* Sci Transl Med, 2012. **4**(128): p. 128ra39.

293. Sanna, V. and M. Sechi, *Therapeutic Potential of Targeted Nanoparticles and Perspective on Nanotherapies.* ACS Med Chem Lett, 2020. **11**(6): p. 1069-1073.